ASTM

Designation: E 647 – 99

Standard Test Method for
Measurement of Fatigue Crack Growth Rates[1]

This standard is issued under the fixed designation E 647; the number immediately following the designation indicates the year of original adoption or, in the case of revision, the year of last revision. A number in parentheses indicates the year of last reapproval. A superscript epsilon (ϵ) indicates an editorial change since the last revision or reapproval.

1. Scope

1.1 This test method[2] covers the determination of steady-state fatigue crack growth rates from near-threshold to K_{max} controlled instability using either compact tension, C(T), (Fig. 1) middle-tension, M(T), (Fig. 2) or eccentrically loaded single edge crack tension, ESE(T), (Fig. A4.1) specimens. Results are expressed in terms of the crack-tip stress-intensity factor range (ΔK), defined by the theory of linear elasticity.

1.2 Several different test procedures are provided, the optimum test procedure being primarily dependent on the magnitude of the fatigue crack growth rate to be measured.

1.3 Materials that can be tested by this test method are not limited by thicknesses or by strength so long as specimens are of sufficient thickness to preclude buckling and of sufficient planar size to remain predominantly elastic during testing.

1.4 A range of specimen sizes with proportional planar dimensions is provided, but size is variable to be adjusted for yield strength and applied load. Specimen thickness may be varied independent of planar size.

1.5 Specimen configurations other than those contained in this method may be used provided that well-established stress-intensity factor calibrations are available and that specimens are of sufficient planar size to remain predominantly elastic during testing.

1.6 Residual stress/crack closure may significantly influence the fatigue crack growth rate data, particularly at low stress-intensity factors and low stress ratios, although such variables are not incorporated into the computation of ΔK.

1.7 Values stated in SI units are to be regarded as the standard. Values given in parentheses are for information only.

1.8 *This standard does not purport to address all of the safety concerns, if any, associated with its use. It is the responsibility of the user of this standard to establish appropriate safety and health practices and determine the applicability of regulatory limitations prior to use.*

2. Referenced Documents

2.1 *ASTM Standards:*

E 4 Practices for Force Verification of Testing Machines[3]

E 6 Terminology Relating to Methods of Mechanical Testing[3]

E 8 Test Methods for Tension Testing of Metallic Materials[3]

E 337 Test Method for Measuring Humidity with a Psychrometer (the Measurement of Wet- and Dry-Bulb Temperatures)[4]

E 338 Test Method for Sharp-Notch Tension Testing of High-Strength Sheet Materials[3]

E 399 Test Method for Plane-Strain Fracture Toughness of Metallic Materials[3]

E 467 Practice for Verification of Constant Amplitude Dynamic Loads on Displacements in an Axial Load Fatigue Testing System[3]

E 561 Practice for *R*-Curve Determination[3]

E 616 Terminology Relating to Fracture Testing[3]

E 813 Test Method for J_{Ic}, A Measure of Fracture Toughness[3]

E 1012 Practice for Verification of Specimen Alignment Under Tensile Loading[3]

E 1150 Definitions of Terms Relating to Fatigue[3]

3. Terminology

3.1 The terms used in this test method are given in Terminology E 6, Definitions E 1150, and Terminology E 616. Wherever these terms are not in agreement with one another, use the definitions given in Terminology E 616 which are applicable to this test method.

3.2 *Definitions:*

3.2.1 *crack length, a*[L], *n*—See *crack size.*

3.2.2 *crack size, a*[L], *n*—a linear measure of a principal planar dimension of a crack. This measure is commonly used in the calculation of quantities descriptive of the stress and displacement fields and is often also termed crack length or depth.

3.2.2.1 *Discussion*—In the C(T) specimen, *a* is measured from the line connecting the bearing points of load application; in the M(T) specimen, *a* is measured from the perpendicular bisector of the central crack; in the ESE(T) specimen, *a* is measured from the specimen front face.

3.2.2.2 *Discussion*—In fatigue testing, crack length is the physical crack size. See *physical crack size* in Terminology E 616.
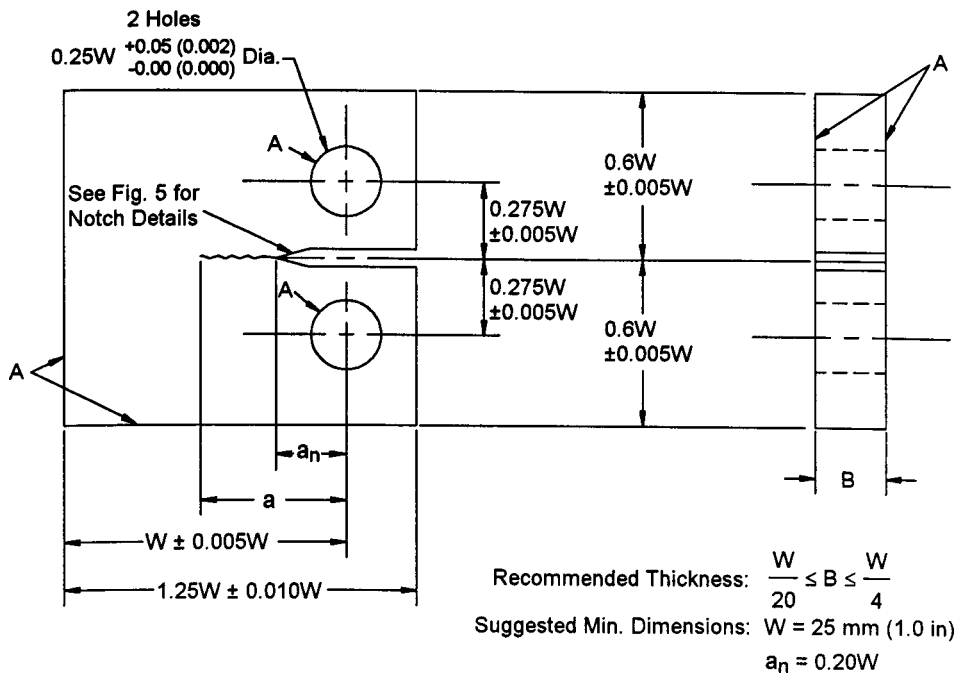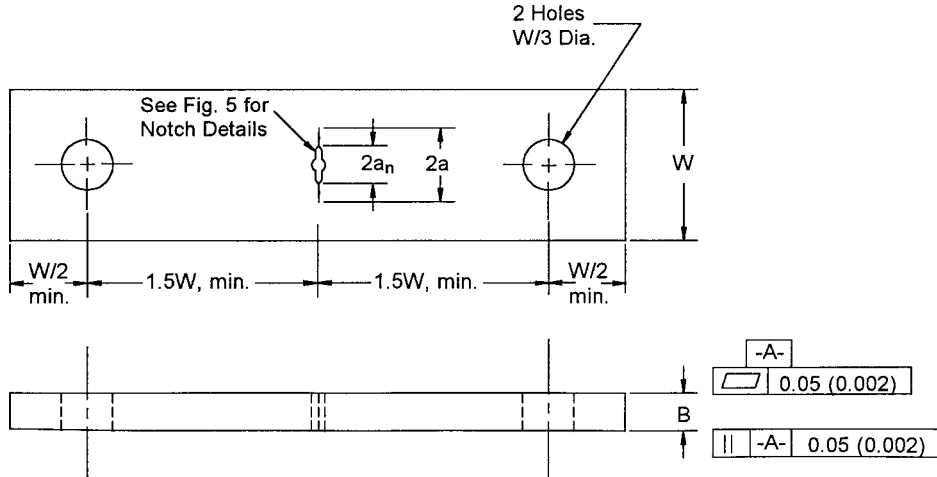
NOTE 1—Dimensions are in millimetres (inches).
NOTE 2—*A*-surfaces shall be perpendicular and parallel as applicable to within ±0.002 *W*, TIR.
NOTE 3—The intersection of the tips of the machined notch (a_n) with the specimen faces shall be equally distant from the top and bottom edges of the specimen to within 0.005 *W*.
NOTE 4—Surface finish, including holes, shall be 0.8 (32) or better.

FIG. 1 Standard Compact-Tension C(T) Specimen for Fatigue Crack Growth Rate Testing

NOTE 1—Dimensions are in millimetres (inches).
NOTE 2—The machined notch ($2a_n$) shall be centered to within ±0.001 *W*.
NOTE 3—For specimens with *W* > 75 mm (3 in.) a multiple pin gripping arrangement is recommended, similar to that described in Practice 561.
NOTE 4—Surface finish, including holes, shall be 0.8 (32) or better.

FIG. 2 Standard Middle-Tension M(T) Specimen for Fatigue Crack Growth Rate Testing when *W* ≤ 75 mm (3 in.)

3.2.3 *cycle—in fatigue,* under constant amplitude loading, the load variation from the minimum to the maximum and then to the minimum load.

3.2.3.1 *Discussion*—In spectrum loading, the definition of cycle varies with the counting method used.

3.2.3.2 *Discussion*—In this test method, the symbol *N* is used to represent the number of cycles.

3.2.4 *fatigue-crack-growth rate, da/dN, [L]*—crack exten-

sion per cycle of loading.

3.2.5 *fatigue cycle—*See *cycle*.

3.2.6 *load cycle—*See *cycle*.

3.2.7 *load range, ΔP [F]*—in fatigue, the algebraic difference between the maximum and minimum loads in a cycle expressed as:

$$\Delta P = P_{max} - P_{min} \qquad (1)$$

2

3.2.8 *load ratio (also called stress ratio), R—in fatigue*, the algebraic ratio of the minimum to maximum load (stress) in a cycle, that is, $R = P_{min}/P_{max}$.

3.2.9 *maximum load, P_{max}* [F]—*in fatigue*, the highest algebraic value of applied load in a cycle tensile loads are considered positive and compressive loads negative.

3.2.10 *maximum stress-intensity factor, K_{max}* [FL$^{-3/2}$]—*in fatigue*, the maximum value of the stress-intensity factor in a cycle. This value corresponds P_{max}.

3.2.11 *minimum load, P_{min}* [F]—*in fatigue*, the lowest algebraic value of applied load in a cycle. Tensile loads are considered positive and compressive loads negative.

3.2.12 *minimum stress-intensity factor, K_{min}* [FL$^{-3/2}$]—*in fatigue*, the minimum value of the stress-intensity factor in a cycle. This value corresponds to P_{min} when R > 0 and is taken to be zero when R ≤ 0.

3.2.13 *stress cycle*—See **cycle** in Terminology E 616.

3.2.14 *stress-intensity factor, K, K_1, K_2, K_3* [FL$^{-3/2}$]—See Terminology E 616.

3.2.14.1 *Discussion*—In this test method, mode 1 is assumed and the subscript 1 is everywhere implied.

3.2.15 *stress-intensity factor range, ΔK* [FL$^{-3/2}$]—*in fatigue*, the variation in the stress-intensity factor in a cycle, that is

$$\Delta K = K_{max} - K_{min} \qquad (2)$$

3.2.15.1 *Discussion*—The loading variables R, ΔK, and K_{max} are related in accordance with the following relationships:

$$\Delta K = (1 - R)K_{max} \text{ for } R \geq 0, \text{ and} \qquad (3)$$

$$\Delta K = K_{max} \text{ for } R \leq 0.$$

3.2.15.2 *Discussion*—These operational stress-intensity factor definitions do not include local crack-tip effects; for example, crack closure, residual stress, and blunting.

3.2.15.3 *Discussion*—While the operational definition of ΔK states that ΔK does not change for a constant value of K_{max} when R ≤ 0, increases in fatigue crack growth rates can be observed when R becomes more negative. Excluding the compressive loads in the calculation of ΔK does not influence the material's response since this response (da/dN) is independent of the operational definition of ΔK. For predicting crack-growth lives generated under various R conditions, the life prediction methodology must be consistent with the data reporting methodology.

3.2.16 *stress-intensity factor range*—See *range of stress-intensity factor*.

3.3 *Definitions of Terms Specific to This Standard:*

3.3.1 *applied-K curve*—a curve (a fixed-load or fixed-displacement crack-extension-force curve) obtained from a fracture mechanics analysis for a specific specimen configuration. The curve relates the stress-intensity factor to crack size and either applied load or displacement.

3.3.1.1 *Discussion*—The resulting analytical expression is sometimes called a *K* calibration and is frequently available in handbooks for stress-intensity factors.

3.3.2 *fatigue crack growth threshold, ΔK_{th}* [FL$^{-3/2}$]—that asymptotic value of ΔK at which da/dN approaches zero. For most materials an *operational*, though arbitrary, definition of

ΔK_{th} is given as that ΔK which corresponds to a fatigue crack growth rate of 10^{-10} m/cycle. The procedure for determining this *operational* ΔK_{th} is given in 9.4.

3.3.2.1 *Discussion*—The intent of this definition is not to define a true threshold, but rather to provide a practical means of characterizing a material's fatigue crack growth resistance in the near-threshold regime. Caution is required in extending this concept to design (see 5.1.5).

3.3.3 *fatigue crack growth rate, da/dN or $\Delta a/\Delta N$*, [L]—*in fatigue*, the rate of crack extension caused by fatigue loading and expressed in terms of average crack extension per cycle.

3.3.4 *K-decreasing test*—a test in which the value of *C* is nominally negative. In this test method *K*-decreasing tests are conducted by shedding load, either continuously or by a series of decremental steps, as the crack grows.

3.3.5 *K-increasing test*—a test in which the value of *C* is nominally positive. For the standard specimens in this method the constant-load-amplitude test will result in a *K*-increasing test where the *C* value increases but is always positive.

3.3.6 *normalized K-gradient, C = (1/K)*. d*K*/d*a*[L^{-1}]—the fractional rate of change of *K* with increasing crack length.

3.3.6.1 *Discussion*—When *C* is held constant the percentage change in *K* is constant for equal increments of crack length. The following identity is true for the normalized *K*-gradient in a constant load ratio test:

$$\frac{1}{K} \cdot \frac{dK}{da} = \frac{1}{K_{max}} \cdot \frac{dK_{max}}{da} = \frac{1}{K_{min}} \cdot \frac{dK_{min}}{da} = \frac{1}{\Delta K} \cdot \frac{d\Delta K}{da} \qquad (4)$$

4. Summary of Test Method

4.1 This test method involves cyclic loading of notched specimens which have been acceptably precracked in fatigue. Crack length is measured, either visually or by an equivalent method[5], as a function of elapsed fatigue cycles and these data are subjected to numerical analysis to establish the rate of crack growth. Crack growth rates are expressed as a function of the stress-intensity factor range, ΔK, which is calculated from expressions based on linear elastic stress analysis.

5. Significance and Use

5.1 Fatigue crack growth rate expressed as a function of crack-tip stress-intensity factor range, da/dN versus ΔK, characterizes a material's resistance to stable crack extension under cyclic loading. Background information on the ration-ale for employing linear elastic fracture mechanics to analyze fatigue crack growth rate data is given in Refs (**1**)[6] and (**2**).

5.1.1 In innocuous (inert) environments fatigue crack growth rates are primarily a function of ΔK and load ratio, R, or K_{max} and R (Note 1). Temperature and aggressive environments can significantly affect da/dN versus ΔK, and in many cases accentuate R-effects and introduce effects of other loading variables such as cycle frequency and waveform.

---

[5] Subcommittee E08.06 has initiated a task group activity (E08.06.06) on nonvisual methods for measuring crack growth. These measurement methods include compliance (near front face and back face), a-c potential, d-c potential, eddy current, ultrasonic, and acoustic emission. Refs (**1**) and (**3**) provide basic information on the current uses of these methods.

[6] The boldface numbers in parentheses refer to the list of references at the end of this standard.

Attention needs to be given to the proper selection and control of these variables in research studies and in the generation of design data.

NOTE 1—ΔK, $K_{\max}$, and R are not independent of each other. Specification of any two of these variables is sufficient to define the loading condition. It is customary to specify one of the stress-intensity parameters (ΔK or $K_{\max}$) along with the load ratio, R.

5.1.2 Expressing da/dN as a function of ΔK provides results that are independent of planar geometry, thus enabling exchange and comparison of data obtained from a variety of specimen configurations and loading conditions. Moreover, this feature enables da/dN versus ΔK data to be utilized in the design and evaluation of engineering structures. The concept of similitude is assumed, which implies that cracks of differing lengths subjected to the same nominal ΔK will advance by equal increments of crack extension per cycle.

5.1.3 Fatigue crack growth rate data are not always geometry-independent in the strict sense since thickness effects sometimes occur. However, data on the influence of thickness on fatigue crack growth rate are mixed. Fatigue crack growth rates over a wide range of ΔK have been reported to either increase, decrease, or remain unaffected as specimen thickness is increased. Thickness effects can also interact with other variables such as environment and heat treatment. For example, materials may exhibit thickness effects over the terminal range of da/dN versus ΔK, which are associated with either nominal yielding (Note 2) or as $K_{\max}$ approaches the material fracture toughness. The potential influence of specimen thickness should be considered when generating data for research or design.

NOTE 2—This condition should be avoided in tests that conform to the specimen size requirements of 7.2.

5.1.4 Residual stresses can have an influence on fatigue crack growth rate behavior. The effect can be significant when test specimens are removed from material in which complete stress relief is impractical, such as weldments, as-quenched materials, and complex forged or extruded shapes. Residual stresses superimposed on the applied stress can cause the localized crack-tip stress-intensity factor to be different than that computed solely from externally applied loads. Residual stresses may lead to partly compressive stress cycles, even when the nominal applied stress range is wholly tensile, or vice versa. Irregular crack growth, namely excessive crack front curvature or out-of-plane crack growth, generally indicates that residual stresses are affecting the measured da/dN versus ΔK relationship (4).

5.1.5 The growth rate of small fatigue cracks can differ noticeably from that of long cracks at given ΔK values. Use of long crack data to analyze small crack growth often results in non-conservative life estimates. The small crack effect may be accentuated by environmental factors. Cracks are defined as being small when 1) their length is small compared to relevant microstructural dimension (a continuum mechanics limitation), 2) their length is small compared to the scale of local plasticity (a linear elastic fracture mechanics limitation), and 3) they are merely physically small (<1 mm). Near-threshold data established according to this method should be considered as representing the materials' steady-state fatigue crack growth

rate response emanating from a long crack, one that is of sufficient length such that transition from the initiation to propagation stage of fatigue is complete. Steady-state near-threshold data, when applied to service load histories, may result in non-conservative lifetime estimates, particulary for small cracks (5-7).[7]

5.1.6 Crack closure can have a dominant influence on fatigue crack growth rate behavior, particularly in the near-threshold regime at low stress ratios. This implies that the conditions in the wake of the crack and prior loading history can have a bearing on the current propagation rates. The understanding of the role of the closure process is essential to such phenomena as the behavior of small cracks and the transient crack growth rate behavior during variable amplitude loading. Closure provides a mechanism whereby the cyclic stress intensity near the crack tip, ΔK_{eff}, differs from the nominally applied values, ΔK. This concept is of importance to the fracture mechanics interpretation of fatigue crack growth rate data since it implies a non-unique growth rate dependence in terms of ΔK, and R (8).[8]

NOTE 3—The characterization of small crack behavior may be more closely approximated in the near-threshold regime by testing at a high stress ratio where the anomalies due to crack closure are minimized.

5.2 This test method can serve the following purposes:

5.2.1 To establish the influence of fatigue crack growth on the life of components subjected to cyclic loading, provided data are generated under representative conditions and combined with appropriate fracture toughness data (for example, see Test Method E 399), defect characterization data, and stress analysis information (9, 10).

NOTE 4—Fatigue crack growth can be significantly influenced by load history. During variable amplitude loading, crack growth rates can be either enhanced or retarded (relative to steady-state, constant-amplitude growth rates at a given ΔK) depending on the specific loading sequence. This complicating factor needs to be considered in using constant-amplitude growth rate data to analyze variable amplitude fatigue problems (11).

5.2.2 To establish material selection criteria and inspection requirements for damage tolerant applications.

5.2.3 To establish, in quantitative terms, the individual and combined effects of metallurgical, fabrication, environmental, and loading variables on fatigue crack growth.

6. Apparatus

6.1 *Grips and Fixtures for C(T) Specimens*—A clevis and pin assembly (Fig. 3) is used at both the top and bottom of the specimen to allow in-plane rotation as the specimen is loaded. This specimen and loading arrangement is to be used for tension-tension loading only.

6.1.1 Suggested proportions and critical tolerances of the clevis and pin are given (Fig. 3) in terms of either the specimen width, W, or the specimen thickness, B, since these dimensions may be varied independently within certain limits.

6.1.2 The pin-to-hole clearances illustrated in Fig. 3 are designed to reduce nonlinear load vs. displacement behavior

---

[7] Subcommittee E08.06 has initiated a study group activity on crack closure measurement and analysis. Reference (8) provides basic information on this subject.

[8] Supporting data available from ASTM Headquarters. Request RR: E-24-1009.
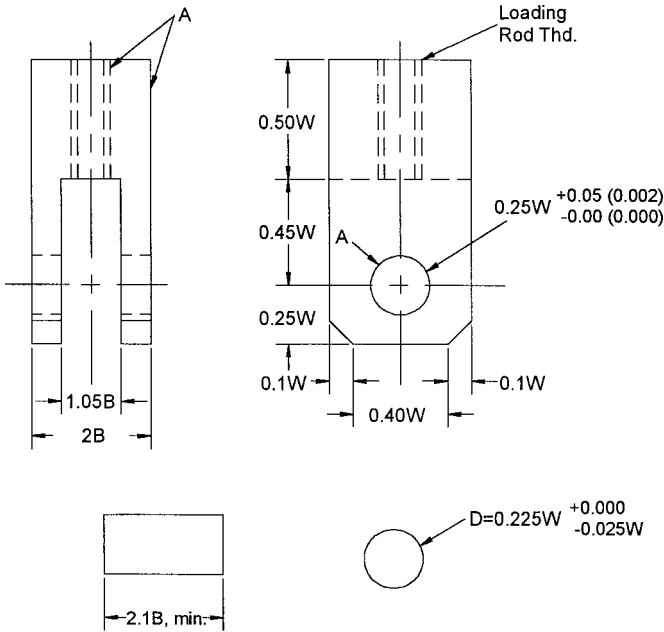
NOTE 1—Dimensions are in millimetres (inches).

NOTE 2—A-surfaces shall be perpendicular and parallel as applicable to within ±0.05 mm (0.002 in.), TIR.

NOTE 3—Surface finish of holes and loading pins shall be 0.8 (32) or better.

FIG. 3 Clevis and Pin Assembly for Gripping C(T) Specimens

caused by rotation of the specimen and pin (12). Using this arrangement to test materials with relatively low yield strength may cause plastic deformation of the specimen hole. Similarly, when testing high strength materials or when the clevis opening exceeds 1.05B (or both), a stiffer load pin (that is, >0.225W) may be required. In these cases, a flat bottom clevis hole or bearings may be used with the appropriate loading pins (D = 0.24W) as indicated in Annex A2. The use of high viscosity lubricants such as grease may introduce hysteresis in the load vs. displacement behavior and is not recommended.

6.1.3 Using a 1000-MPa (150-ksi) yield-strength alloy (for example, AISI 4340 steel) for the clevis and pins provides adequate strength and resistance to galling and fatigue.

6.2 *Grips and Fixtures for M(T) Specimens*—The types of grips and fixtures to be used with the M(T) specimens will depend on the specimen width, W, (defined in Fig. 2), and the loading conditions (that is, either tension-tension or tension-compression loading). The minimum required specimen gage length varies with the type of gripping and is specified so that a uniform stress distribution is developed in the specimen gage length during testing. For testing of thin sheets, constraining plates may be necessary to minimize specimen buckling (see Practice E 561 for recommendations on buckling constraints).

6.2.1 For tension-tension loading of specimens with $W \leq 75$ mm (3 in.) a clevis and single pin arrangement is suitable for gripping provided that the specimen gage length (that is, the distance between loading pins) is at least 3W (Fig. 2). For this arrangement it is also helpful to either use brass shims between the pin and specimen or to lubricate the pin to prevent fretting-fatigue cracks from initiating at the specimen loading hole. Additional measures which may be taken to prevent

cracking at the pinhole include attaching reinforcement plates to the specimen (for example, see Test Method E 338) or employing a "dog bone" type specimen design. In either case, the gage length shall be defined as the uniform section and shall be at least 1.7W.

6.2.2 For tension-tension loading of specimens with $W \geq 75$ mm (3 in.) a clevis with multiple bolts is recommended (for example, see Practice E 561). In this arrangement, the loads are applied more uniformly; thus, the minimum specimen gage length (that is, the distance between the innermost row of bolt holes) is relaxed to 1.5W.

6.2.3 The M(T) specimen may also be gripped using a clamping device instead of the above arrangements. This type of gripping is necessary for tension-compression loading. An example of a specific bolt and keyway design for clamping M(T) specimens is given in Fig. 4. In addition, various hydraulic and mechanical-wedge systems which supply adequate clamping force are commercially available and may be used. The minimum gage length requirement for clamped specimens is relaxed to 1.2W.

6.3 *Alignment of Grips*—It is important that attention be given to achieving good alignment in the load train through careful machining of all gripping fixtures. Misalignment can cause non-symmetric cracking, particularly for critical applications such as near-threshold testing, which in turn may lead to invalid data (see Sec. 8.3.4, 8.8.3). If non-symmetric cracking occurs, the use of a strain-gaged specimen to identify and minimize misalignment might prove useful. One method to identify bending under tensile loading conditions is described in Practice E 1012. Another method which specifically addresses measurement of bending in pin-loaded specimen configurations is described in Ref (13). For tension-compression loading the length of the load train (including the hydraulic
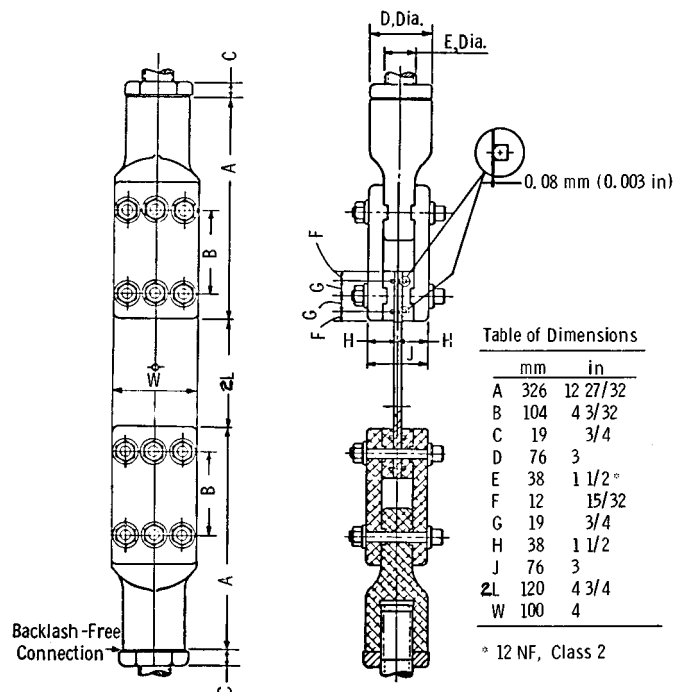

Table of Dimensions		
	mm	in
A	326	12 27/32
B	104	4 3/32
C	19	3/4
D	76	3
E	38	1 1/2 [a]
F	12	15/32
G	19	3/4
H	38	1 1/2
J	76	3
2L	120	4 3/4
W	100	4

[a] 12 NF, Class 2

FIG. 4 Example of Bolt and Keyway Assembly for Gripping 100-mm (4-in.) wide M(T) Specimen

actuator) should be minimized, and rigid, non-rotating joints should be employed to reduce lateral motion in the load train.

7. Specimen Configuration, Size, and Preparation

7.1 *Standard Specimens*—The geometry of standard C(T) and M(T) specimens is given in Figs. 1 and 2, respectively. The geometry of the standard ESE(T) specimen is given in Fig. A4.1. The specific geometry of M(T) specimens depends on the method of gripping as specified in 6.2. Notch and precracking details for the specimens are given in Fig. 5. The C(T) and ESE(T) specimen are not recommended for tension-compression testing because of uncertainties introduced into the loading experienced at the crack tip.

NOTE 5—In the near threshold regime (below 10^{-8} m/cycle), one can experience difficulty in meeting the crack symmetry requirements of 8.8.3 when using the M(T) specimen; the C(T) or ESE(T) specimen may be an appropriate alternative.

7.1.1 It is required that the machined notch, a_n, in the C(T) specimen be at least $0.2W$ in length so that the K-calibration is not influenced by small variations in the location and dimensions of the loading-pin holes.

7.1.2 The machined notch, $2a_n$, in the M(T) specimen shall be centered with respect to the specimen centerline to within $\pm 0.001W$. The length of the machined notch in the M(T) specimen will be determined by practical machining considerations and is not restricted by limitations in the K-calibration.

NOTE 6—It is recommended that $2a_n$ be at least $0.2W$ when using the

FIG. 5 Notch Details and Minimum Fatigue Precracking Requirements

compliance method to monitor crack extension in the M(T) specimen so that accurate crack length determinations can be obtained.

7.1.3 For the specimens described in this method, the thickness, B, and width, W, may be varied independently within the following limits, which are based on specimen buckling and through-thickness crack-curvature considerations:

7.1.3.1 For C(T) and ESE(T) specimens it is recommended that thickness be within the range $W/20 \leq B \leq W/4$. Specimens having thicknesses up to and including $W/2$ may also be employed; however, data from these specimens will often require through-thickness crack curvature corrections (see 9.1). In addition, difficulties may be encountered in meeting the through-thickness crack straightness requirements of 8.3.4 and 8.8.3.

7.1.3.2 Using the above rationale, the recommended upper limit on thickness in M(T) specimens is $W/8$, although $W/4$ may also be employed. The minimum thickness necessary to avoid excessive lateral deflections or buckling in M(T) specimens is sensitive to specimen gage length, grip alignment, and load ratio, R. It is recommended that strain gage information be obtained for the particular specimen geometry and loading condition of interest and that bending strains not exceed 5 % of the nominal strain.

7.1.3.3 For specimens removed from material for which complete stress relief is impractical (see 5.1.4), the effect of residual stresses on the crack propagation behavior can be minimized through the careful selection of specimen shape and size. By selecting a small ratio of specimen dimensions, b/w the effect of a through-the-thickness distribution of residual stresses acting perpendicular to the direction of crack growth can be reduced. This choice of specimen shape minimizes crack curvature or other crack front irregularities which confuse the calculation of both da/dN and ΔK. Residual stresses acting parallel to the direction of crack growth can produce moments about the cracktip which also confound test results. These residual stresses can be minimized by selecting symmetrical specimen configurations, that is, the M(T) specimen, for the evaluation of the material's crack growth behavior.

7.2 *Specimen Size*—In order for results to be valid according to this test method it is required that the specimen be predominantly elastic at all values of applied load. The minimum in-plane specimen sizes to meet this requirement are based primarily on empirical results and are specific to specimen configuration (**10**).

7.2.1 For the C(T) and ESE(T) specimen the following is required:

$$(W - a) \geq (4/\pi)(K_{max}/\sigma_{YS})^2 \qquad (5)$$

where:
$(W - a)$ = specimen's uncracked ligament (Fig. 1), and
σ_{YS} = 0.2 % offset yield strength determined at the same temperature as used when measuring the fatigue crack growth rate data.

7.2.2 For the M(T) specimen the following is required:

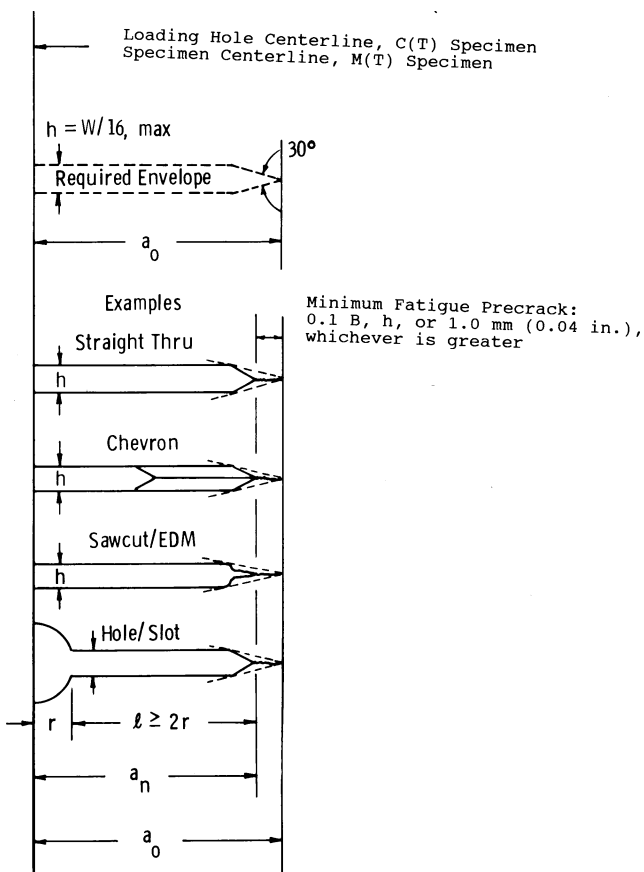$$(W - 2a) \geq 1.25\, P_{max}/(B\sigma_{YS}) \qquad (6)$$

where:

(W – 2a) = specimen's uncracked ligament (Fig. 2), and
B = specimen thickness.

NOTE 7—The size requirements in 7.2 are appropriate for low-strain hardening materials ($\sigma_{ULT}/\sigma_{YS} \leq 1.3$) (14) and for high-strain hardening materials ($\sigma_{ULT}/\sigma_{YS} \geq 1.3$) under certain conditions of load ratio and temperature (15, 16) (where σ_{ULT} is the ultimate tensile strength of the material). However, under other conditions of load ratio and temperature, these same requirements appear to be overly restrictive—that is, they require specimen sizes which are larger than necessary (17, 18). Currently, the conditions giving rise to each of these two regimes of behavior are not clearly defined.

7.2.2.1 An alternative size requirement may be employed for high-strain hardening materials as follows. The uncracked ligament requirement may be relaxed by replacing σ_{YS} with a higher, effective yield strength which accounts for the material strain hardening capacity. For purposes of this test method, this *effective* yield strength, termed flow strength, is defined as follows:

$$\sigma_{FS} = (\sigma_{YS} + \sigma_{ULT})/2 \qquad (7)$$

However, it should be noted that the use of this alternative size requirement allows mean plastic deflections to occur in the specimen. These mean deflections under certain conditions, as noted previously, can accelerate growth rates by as much as a factor of two. Although these data will generally add conservatism to design or structural reliability computations, they can also confound the effects of primary variables such as specimen thickness (if B/W is maintained constant), load ratio, and possibly environmental effects. Thus, when the alternative size requirement is utilized, it is important to clearly distinguish between data that meet the yield strength or flow strength criteria. In this way, data will be generated that can be used to formulate a specimen size requirement of general utility.

7.3 *Notch Preparation*—The machined notch for either of the standard specimens may be made by electrical-discharge machining (EDM), milling, broaching, or sawcutting. The following notch preparation procedures are suggested to facilitate fatigue precracking in various materials:

7.3.1 *Electric Discharge Machining*—ρ < 0.25 mm (0.010 in.) (ρ = notch root radius), high-strength steels ($\sigma_{YS} \geq 1175$ MPa/170 ksi), titanium and aluminum alloys.

7.3.2 *Mill or Broach*—$\rho \leq 0.075$ mm (0.003 in.), low or medium-strength steels ($\sigma_{YS} \leq 1175$ MPa/170 ksi), aluminum alloys.

7.3.3 *Grind*—$\rho \leq 0.25$ mm (0.010 in.), low or medium-strength steels.

7.3.4 *Mill or Broach*—$\rho \leq 0.25$ mm (0.010 in.), aluminum alloys.

7.3.5 *Sawcut*—Recommended only for aluminum alloys.

7.3.6 Examples of various machined-notch geometries and associated precracking requirements are given in Fig. 5 (see 8.3).

7.3.7 When residual stresses are suspected of being present (see 5.1.4), local displacement measurements made before and after machining the crack starter slot are useful for detecting the potential magnitude of the effect. A simple mechanical displacement gage can be used to measure distance between two hardness indentations at the mouth of the notch (4). Limited data show that for aluminum alloys when these

mechanical displacement measurements change by more than 0.05 mm (0.002 in.), fatigue crack growth rates can be changed significantly.

8. Procedure

8.1 *Number of Tests*—At crack growth rates greater than 10^{-8} m/cycle, the within-lot variability (neighboring specimens) of da/dN at a given ΔK typically can cover about a factor of two (19). At rates below 10^{-8} m/cycle, the variability in da/dN may increase to about a factor of five or more due to increased sensitivity of da/dN to small variations in ΔK. This scatter may be increased further by variables such as microstructural differences, residual stresses, changes in crack tip geometry (crack branching) or near tip stresses as influenced for example by crack roughness or product wedging, load precision, environmental control, and data processing techniques. These variables can take on added significance in the low crack growth rate regime (da/dN < 10^{-8} m/cycle). In view of the operational definition of the threshold stress-intensity (see 3.3.2 and 9.4), at or near threshold it is more meaningful to express variability in terms of ΔK rather than da/dN. It is good practice to conduct replicate tests; when this is impractical, multiple tests should be planned such that regions of overlapping da/dN versus ΔK data are obtained, particularly under both K-increasing and K-decreasing conditions. Since confidence in inferences drawn from the data increases with number of tests, the desired number of tests will depend on the end use of the data.

8.2 *Specimen Measurements*—The specimen dimensions shall be within the tolerances given in Figs. 1 and 2.

8.3 *Fatigue Precracking*—The importance of precracking is to provide a sharpened fatigue crack of adequate size and straightness (also symmetry for the M(T) specimen) which ensures that *1*) the effect of the machined starter notch is removed from the specimen K-calibration, and *2*) the effects on subsequent crack growth rate data caused by changing crack front shape or precrack load history are eliminated.

8.3.1 Conduct fatigue precracking with the specimen fully heat treated to the condition in which it is to be tested. The precracking equipment shall be such that the load distribution is symmetrical with respect to the machined notch and K_{max}-during precracking is controlled to within ±5 %. Any convenient loading frequency that enables the required load accuracy to be achieved can be used for precracking. The machined notch plus the precrack must lie within the envelope, shown in Fig. 5, that has as its apex the end of the fatigue precrack. In addition the fatigue precrack shall not be less than 0.10B, h, or 1.0 mm (0.040 in.), whichever is greater (Fig. 5).

8.3.2 The final K_{max} during precracking shall not exceed the initial K_{max} for which test data are to be obtained. If necessary, loads corresponding to higher K_{max} values may be used to initiate cracking at the machined notch. In this event, the load range shall be stepped-down to meet the above requirement. Furthermore, it is suggested that reduction in P_{max} for any of these steps be no greater than 20 % and that measurable crack extension occur before proceeding to the next step. To avert transient effects in the test data, apply the load range in each step over a crack length increment of at least $(3/\pi) (K'_{max}/\sigma_{YS})^2$, where K'_{max} is the terminal value of K_{max} from the

previous loadstep. If P_{min}/P_{max} during precracking differs from that used during testing, see the precautions described in 8.5.1.

8.3.3 For the K-decreasing test procedure, prior loading history may influence near-threshold growth rates despite the precautions of 8.3.2. It is good practice to initiate fatigue cracks at the lowest stress intensity possible. Precracking growth rates less than 10^{-8} m/cycle are suggested. A compressive load, less than or equal to the precracking load, may facilitate fatigue precracking and may diminish the influence of the K-decreasing test procedure on subsequent fatigue crack growth rate behavior.

8.3.4 Measure the crack lengths on the front and back surfaces of the specimen to within 0.10 mm (0.004 in.) or 0.002W, whichever is greater. For specimens where W > 127 mm (5 in.), measure crack length to within 0.25 mm (0.01 in.). If crack lengths measured on front and back surfaces differ by more than 0.25B, the pre-cracking operation is not suitable and subsequent testing would be invalid under this test method. In addition for the M(T) specimen, measurements referenced from the specimen centerline to the two cracks (for each crack use the average of measurements on front and back surfaces) shall not differ by more than 0.025W. If the fatigue crack departs more than the allowable limit from the plane of symmetry (see 8.8.3) the specimen is not suitable for subsequent testing. If the above requirements cannot be satisfied, check for potential problems in alignment of the loading system and details of the machined notch.

8.4 *Test Equipment*—The equipment for fatigue testing shall be such that the load distribution is symmetrical to the specimen notch.

8.4.1 Verify the load cell in the test machine in accordance with Practices E 4 and Practice E 467. Conduct testing such that both ΔP and P_{max} are controlled to within ±2 % throughout the test.

8.4.2 An accurate digital device is required for counting elapsed cycles. A timer is a desirable supplement to the counter and provides a check on the counter. Multiplication factors (for example, ×10 or ×100) should not be used on counting devices when obtaining data at growth rates above 10^{-5} m/cycle since they can introduce significant errors in the growth rate determination.

8.5 *Constant-Load-Amplitude Test Procedure for da/dN > 10^{-8} m/cycle*—This test procedure is well suited for fatigue crack growth rates above 10^{-8} m/cycle. However, it becomes increasingly difficult to use as growth rates decrease below 10^{-8} m/cycle because of precracking considerations (see 8.3.3). (A K-decreasing test procedure which is better suited for rates below 10^{-8} m/cycle is provided in 8.6.) When using the constant-load-amplitude procedure it is preferred that each specimen be tested at a constant load range (ΔP) and a fixed set of loading variables (stress ratio and frequency). However, this may not be feasible when it is necessary to generate a wide range of information with a limited number of specimens. When loading variables are changed during a test, potential problems arise from several types of transient phenomenon (20). The following test procedures should be followed to minimize or eliminate transient effects while using this K-increasing test procedure.

8.5.1 If load range is to be incrementally varied it should be done such that P_{max} is increased rather than decreased to preclude retardation of growth rates caused by overload effects; retardation being a more pronounced effect than accelerated crack growth associated with incremental increase in P_{max}. Transient growth rates are also known to result from changes in P_{min} or R. Sufficient crack extension should be allowed following changes in load to enable the growth rate to establish a steady-state value. The amount of crack growth that is required depends on the magnitude of load change and on the material. An incremental increase of 10 % or less will minimize these transient growth rates.

8.5.2 When environmental effects are present, changes in load level, test frequency, or waveform can result in transient growth rates. Sufficient crack extension should be allowed between changes in these loading variables to enable the growth rate to achieve a steady-state value.

8.5.3 Transient growth rates can also occur, in the absence of loading variable changes, due to long-duration test interruptions, for example, during work stoppages. In this case, data should be discarded if the growth rates following an interruption are less than those before the interruption.

8.6 *K-Decreasing Procedure for da/dN < 10^{-8} m/cycle*— This procedure is started by cycling at a ΔK and K_{max} level equal to or greater than the terminal precracking values. Subsequently, loads are decreased (shed) as the crack grows, and test data are recorded until the lowest ΔK or crack growth rate of interest is achieved. The test may then be continued at constant load limits to obtain comparison data under K-increasing conditions. The K-decreasing procedure is not recommended at fatigue crack growth rates above 10^{-8} m/cycle since prior loading history at such associated ΔK levels may influence the near-threshold fatigue crack growth rate behavior.

8.6.1 Load shedding during the K-decreasing test may be conducted as decreasing load steps at selected crack length intervals, as shown in Fig. 6. Alternatively, the load may be shed in a continuous manner by an automated technique (for example, by use of an analog computer or digital computer, or both) (21).

8.6.2 The rate of load shedding with increasing crack length shall be gradual enough to 1) preclude anomalous data resulting from reductions in the stress-intensity factor and concomitant transient growth rates, and 2) allow the establishment of about five da/dN, ΔK data points of approximately equal spacing per decade of crack growth rate. The above requirements can be met by limiting the normalized K-gradient, $C = 1/K \cdot dK/da$, to a value algebraically equal to or greater than –0.08 mm^{-1}(–2 in.$^{-1}$). That is:

$$C = \left(\frac{1}{K}\right) \cdot \left(\frac{dK}{da}\right) > -\ 0.08 \text{ mm}^{-1}\ (-2 \text{ in.}^{-1}) \qquad (8)$$

When loads are incrementally shed, the requirements on C correspond to the nominal K-gradient depicted in Fig. 6.

Note 8—Acceptable values of C may depend on load ratio, test material, and environment. Values of C algebraically greater than that indicated above have been demonstrated as acceptable for use in decreasing K tests of several steel alloys and aluminum alloys tested in laboratory air over a wide range of load ratios (14, 21).

8.6.3 If the normalized K-gradient C is algebraically less
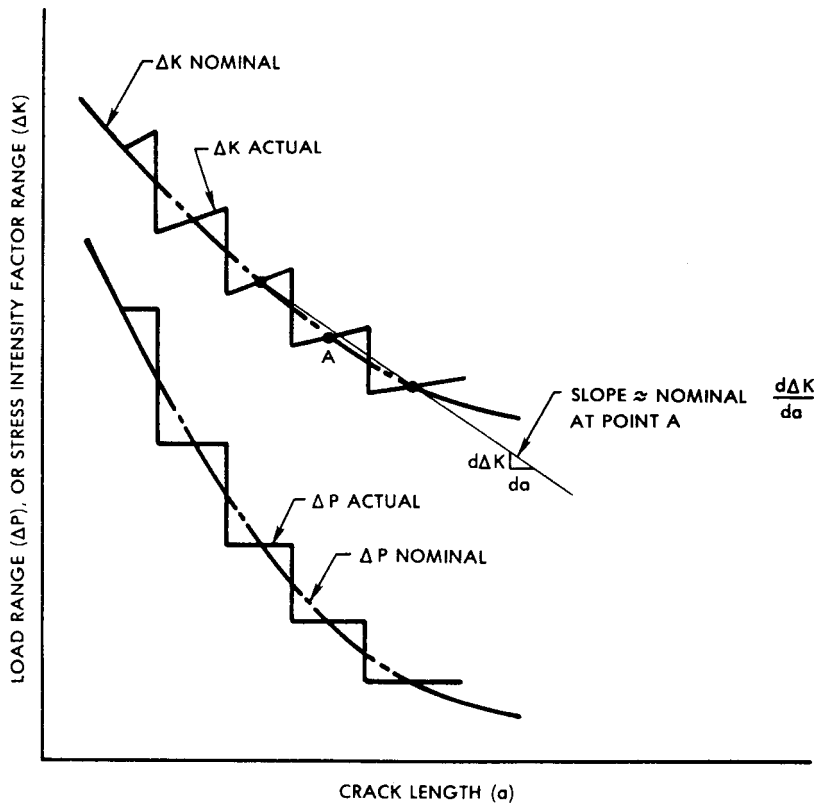
FIG. 6 Typical *K* Decreasing Test by Stepped Load Shedding

than that prescribed in 8.6.2, the procedure shall consist of decreasing *K* to the lowest growth rate of interest followed by a *K*-increasing test at a constant ΔP (conducted in accordance with 8.5). Upon demonstrating that data obtained using *K*-increasing and *K*-decreasing procedures are equivalent for a given set of test conditions, the *K*-increasing testing may be eliminated from all replicate testing under these same test conditions.

Note 9—It is good practice to have *K*-decreasing followed by *K*-increasing data for the first test of any single material regardless of the *C* value used.

8.6.4 It is recommended that the load ratio, *R*, and *C* be maintained constant during *K*-decreasing testing (see 8.7.1 for exceptions to this recommendation).

8.6.5 The relationships between *K* and crack length and between load and crack length for a constant-*C* test are given as follows:

8.6.5.1 $\Delta K = \Delta K_o \exp[C (a - a_o)]$, where ΔK_o is the initial ΔK at the start of the test, and a_o is the corresponding crack length. Because of the identity given in 3.2 (Note 1), the above relationship is also true for $K_{\max}$ and $K_{\min}$.

8.6.5.2 The load histories for the standard specimens of this test method are obtained by substituting the appropriate *K*-calibrations given in 9.3 into the above expression.

8.6.6 When employing step shedding of load, as in Fig. 6, the reduction in $P_{\max}$ of adjacent load steps shall not exceed 10 % of the previous $P_{\max}$. Upon adjustment of maximum load from $P_{\max 1}$ to a lower value, $P_{\max 2}$, a minimum crack extension of 0.50 mm (0.02 in.) is recommended.

8.6.7 When employing continuous shedding of load, the requirement of 8.6.6 is waived. Continuous load shedding is defined as $(P_{\max 1} - P_{\max 2})/P_{\max 1} \leq 0.02$.

8.7 *Alternative K-control test procedures*—Ideally, it is desirable to generate d*a*/d*N*, ΔK data at *K*-gradients independent of the specimen geometry **(22)**. Exercising control over this *K*-gradient allows much steeper gradients for small values of *a*/*W* without the undesirable feature of having too steep a *K*-gradient at the larger values of *a*/*W* associated with constant amplitude loading. Generating data at an appropriate *K*-gradient, using a constant and positive value of the *K*-gradient parameter, *C*, (see 8.6.2) provides numerous advantages: the test time is reduced; the d*a*/d*N*-ΔK data can be evenly distributed without using variable Δa increments; a wider range of data may be generated without incremental load increases; the *K*-gradient is independent of the specimen geometry.

8.7.1 Situations may arise where changing ΔK under conditions of constant $K_{\max}$ or constant $K_{\mean}$ may be more representative than under conditions of constant *R*. The application of the test data should be considered in choosing an appropriate mode of *K*-control. For example, a more conservative estimate of near-threshold behavior may be obtained by using this test method. This process effectively measures near-threshold data at a high stress ratio.

8.8 *Measurement of Crack Length*—Make fatigue crack length measurements as a function of elapsed cycles by means of a visual, or equivalent, technique capable of resolving crack extensions of 0.10 mm (0.004 in.), or 0.002*W*, whichever is greater. For visual measurements, polishing the test area of the specimen and using indirect lighting aid in the resolution of the

crack-tip. It is recommended that, prior to testing, reference marks be applied to the test specimen at predetermined locations along the direction of cracking. Crack length can then be measured using a low power (20 to 50×) traveling microscope. Using the reference marks eliminates potential errors due to accidental movement of the traveling microscope. If precision photographic grids or polyester scales are attached to the specimen, crack length can be determined directly with any magnifying device that gives the required resolution. It is preferred that measurements be made without interrupting the test.

NOTE 10—Interruption of cyclic loading for the purpose of crack length measurement can be permitted providing strict care is taken to avoid introducing any significant extraneous damage (for example, creep deformation) or transient crack extension (for example, growth under static load). The interruption time should be minimized (less than 10 min.) and if a static load is maintained for the purpose of enhanced crack tip resolution, it should be carefully controlled. A static load equal to the fatigue mean load is probably acceptable (with high temperatures and corrosive environments, even mean levels should be questioned) but in no case should the static load exceed the maximum load applied during the fatigue test.

8.8.1 Make crack length measurements at intervals such that da/dN data are nearly evenly distributed with respect to ΔK. The following measurement intervals are recommended according to specimen type:

8.8.1.1 C(T) *Specimen:*

$$\Delta a \leq 0.04W \text{ for } 0.25 \leq a/W \leq 0.40$$
$$\Delta a \leq 0.02W \text{ for } 0.40 \leq a/W \leq 0.60$$
$$\Delta a \leq 0.01 W \text{ for } a/W \geq 0.60$$

8.8.1.2 M(T) *Specimen:*

$$\Delta a \leq 0.03W \text{ for } 2a/W < 0.60$$
$$\Delta a \leq 0.02W \text{ for } 2a/W > 0.60$$

8.8.1.3 *ESE(T) Specimen*:

$$\Delta a \leq 0.04W \text{ for } a/W \leq 0.40$$
$$\Delta a \leq 0.02W \text{ for } 0.40 < a/W \leq 0.60$$
$$\Delta a \leq 0.01W \text{ for } a/W > 0.60$$

8.8.1.4 A minimum Δa of 0.25 mm (0.01 in.) is recommended. However, situations may arise where the Δa needs to be reduced below 0.25 mm (0.01 in.) in order to obtain at least five da/dN, ΔK data points in the near-threshold regime (see 9.4). In any case, the minimum Δa shall be ten times the crack length measurement precision.

NOTE 11—The crack length measurement precision is herein defined as the standard deviation on the mean value of crack length determined for a set of replicate measurements.

8.8.2 As a rule, crack length measurements should be made on both sides (front and back) of a specimen to ensure that the crack symmetry requirements of 8.8.3 are met. The average value of the measurements (two crack lengths for the C(T) specimen and four crack lengths for the M(T) specimen) should be used in all calculations of growth rate and K. If crack length measurements are not made on both sides at every crack length interval, the interval of both-side measurement must be reported. Measurement on only one side is permissible only if previous experience with a particular specimen configuration,

test material, testing apparatus, and growth rate regime has shown that the crack symmetry requirements are met consistently.

8.8.3 If at any point in the test the crack deviates more than ±20° from the plane of symmetry over a distance of 0.1W or greater, the data are invalid according to this test method. A deviation between ±10 and ±20° must be reported. (See Fig. 7) In addition, data are invalid if (1) crack lengths measured on front and back surfaces differ by more than 0.25B, or (2) for the M(T) specimen, measurements referenced from the specimen centerline to the two cracks (for each crack, use the average of measurements on front and back surfaces) differ by more than 0.025W.

NOTE 12—The requirements on out-of-plane cracking are commonly violated for large-grained or single-crystal materials. In these instances, results from anisotropic, mixed-mode stress analyses may be needed to compute K; (for example, see Ref. **(23)**).

NOTE 13—Crack tip branching has been noted to occur. This characteristic is not incorporated into the computation of ΔK. As a result, crack branching, or bifurcating, may be a source of variability in measured fatigue crack growth rate data. Data recorded during branching must be noted as being for a branching crack.

8.8.3.1 If nonvisual methods for crack length measurement are used and nonsymmetric or angled cracking occurs, the nonvisual measurements derived during these periods shall be verified with visual techniques to ensure the requirements of 8.8.3 are satisfied.

9. Calculation and Interpretation of Results

9.1 *Crack Curvature Correction*—After completion of testing, examine the fracture surfaces, preferably at two locations (for example, at the precrack and terminal fatigue crack lengths), to determine the extent of through-thickness crack curvature (commonly termed *crack tunneling*). If a crack contour is visible, calculate a three-point, through-thickness average crack length in accordance with Test Method E 399, sections on General Procedure related to Specimen Measurement; specifically the paragraph on crack length measurement. The difference between the average through-thickness crack length and the corresponding crack length recorded during the test (for example, if visual measurements were obtained this
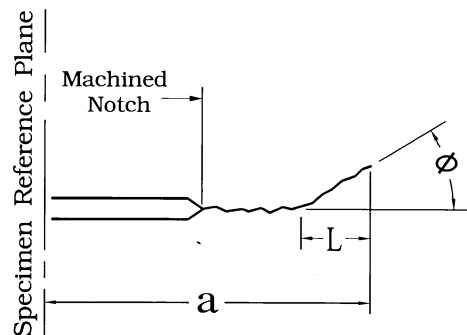
Valid if $\emptyset \leq 10°$
Report if $10° < \emptyset \leq 20°$
Invalid if $\emptyset > 20°$ for $L \geq 0.1W$

FIG. 7 Out-of-Plane Cracking Limits

might be the average of the surface crack length measurements) is the crack curvature correction.

9.1.1 If the crack curvature correction results in a greater than 5 % difference in calculated stress-intensity factor at any crack length, then employ this correction when analyzing the recorded test data.

9.1.2 If the magnitude of the crack curvature correction either increases or decreases with crack length, use a linear interpolation to correct intermediate data points. Determine this linear correction from two distinct crack contours separated by a minimum spacing of 0.25W or B, whichever is greater. When there is no systematic variation of crack curvature with crack length, employ a uniform correction determined from an average of the crack contour measurements.

9.1.3 When employing a crack length monitoring technique other than visual, a crack curvature correction is generally incorporated in the calibration of the technique. However, since the magnitude of the correction will probably depend on specimen thickness, the preceding correction procedures may also be necessary.

9.2 *Determination of Crack Growth Rate*—The rate of fatigue crack growth is to be determined from the crack length versus elapsed cycles data (*a* versus *N*). Recommended approaches which utilize the secant or incremental polynomial methods are given in Appendix X1. Either method is suitable for the *K*-increasing, constant ΔP test. For the *K*-decreasing tests where load is shed in decremental steps, as in Fig. 7, the secant method is recommended. Where shedding of *K* is performed continuously with each cycle by automation, the incremental polynomial technique is applicable. A crack growth rate determination shall not be made over any increment of crack extension which includes a load step.

NOTE 14—Both recommended methods for processing *a* versus *N* data are known to give the same average d*a*/d*N* response. However, the secant method often results in increased scatter in d*a*/d*N* relative to the incremental polynomial method, since the latter numerically" smooths" the data (**19, 24**). This apparent difference in variability introduced by the two methods needs to be considered, especially in utilizing d*a*/d*N* versus ΔK data in design.

9.3 *Determination of Stress-Intensity Factor Range, ΔK*— Use the crack length values of 9.1 and Appendix X1 to calculate the stress-intensity range corresponding to a given crack growth rate from the following expressions:

9.3.1 For the C(T) specimen calculate ΔK as follows:

$$\Delta K = \frac{\Delta P}{B\sqrt{W}} \frac{(2 + \alpha)}{(1 - \alpha)^{3/2}} (0.886 + 4.64\alpha \qquad (9)$$
$$- 13.32\alpha^2 + 14.72\alpha^3 - 5.6\alpha^4)$$

where $\alpha = a/W$; expression valid for $a/W \geq 0.2$ (**25, 26**).

9.3.2 For the M(T) specimen calculate ΔK consistent with the definitions of 3.2; that is:

$$\Delta P = P_{max} - P_{min} \text{ for } R > 0 \qquad (10)$$
$$\Delta P = P_{max} \text{ for } R \leq 0$$

in the following expression (**27**):

$$\Delta K = \frac{\Delta P}{B} \sqrt{\frac{\pi\alpha}{2W} \sec \frac{\pi\alpha}{2}} \qquad (11)$$

where $\alpha = 2a/W$; expression valid for $2a/W < 0.95$.

NOTE 15—Implicit in the above expressions are the assumptions that the test material is linear-elastic, isotropic, and homogeneous.

NOTE 16—The above operational definitions do not include potential effects of residual stress or crack closure on the computed ΔK value. Autographic load versus crack mouth opening displacement traces are useful for detecting and correcting residual stress/crack closure influences (**4**).

9.3.3 For the ESE(T) specimen calculate ΔK consistent with the definitions in Annex A4.

9.3.4 Check for compliance with the specimen size requirements of 7.2.

9.4 *Determination of a Fatigue Crack Growth Threshold*— The following procedure provides an operational definition of the threshold stress-intensity factor range for fatigue crack growth, ΔK_{th}, which is consistent with the general definition of 3.3.2:

9.4.1 Determine the best-fit straight line from a linear regression of log d*a*/d*N* versus log ΔK using a minimum of five d*a*/d*N*, ΔK data points of approximately equal spacing between growth rates of 10^{-9} and 10^{-10} m/cycle. Having specified the range of fit in terms of d*a*/d*N* requires that log ΔK be the dependent variable in establishing this straight line fit.

NOTE 17—Limitations of the linear regression approach of 9.4.1 are described in Ref (**28**). Alternative nonlinear approaches and their advantages are also given in Ref (**28**).

9.4.2 Calculate the ΔK-value that corresponds to a growth rate of 10^{-10} m/cycle using the above fitted line; this value of ΔK is defined as ΔK_{th} according to the operational definition of this test method.

NOTE 18—In the event that lower d*a*/d*N* data are generated, the above procedure can be used with the lowest decade of data. This alternative range of fit must then be specified according to 10.1.12.

10. Report

10.1 The report shall include the following information:

10.1.1 Specimen type, including thickness, B, and width, W. Figures of the specific M(T) specimen design and grips used, and a figure if a specimen type not described in this test method is used shall be provided.

10.1.2 Description of the test machine and equipment used to measure crack length and the precision with which crack length measurements were made.

10.1.3 Test material characterization in terms of heat treatment, chemical composition, and mechanical properties (include at least the 0.2 % offset yield strength and either elongation or reduction in area measured in accordance with Test Methods E 8). Product size and form (for example, sheet, plate, and forging) shall also be identified. Method of stress relief, if applicable, shall be reported. For thermal methods, details of time, temperature and atmosphere. For non-thermal methods, details of loads and frequencies.

10.1.4 The crack plane orientation according to the code given in Test Method E 399. In addition, if the specimen is removed from a large product form, its location with respect to the parent product shall be given.

10.1.5 The terminal values of ΔK, R and crack length from fatigue precracking. If precrack loads were stepped-down, the procedure employed shall be stated and the amount of crack extension at the final load level shall be given.

10.1.6 Test loading variables, including ΔP, R, cyclic frequency, and cyclic waveform.

10.1.7 Environmental variables, including temperature, chemical composition, pH (for liquids), and pressure (for gases and vacuum). For tests in air, the relative humidity as determined by Test Method E 337 shall be reported. For tests in inert reference environments, such as dry argon, estimates of residual levels of water and oxygen in the test environment (generally this differs from the analysis of residual impurities in the gas supply cylinder) shall be given. Nominal values for all of the above environmental variables, as well as maximum deviations throughout the duration of testing, shall be reported. Also, the material employed in the chamber used to contain the environment and steps taken to eliminate chemical/electrochemical reactions between the specimen-environment system and the chamber shall be described.

10.1.8 Analysis methods applied to the data, including the technique used to convert a versus N to da/dN, specific procedure used to correct for crack curvature, and magnitude of crack curvature correction.

10.1.9 The specimen K-calibration and size criterion to ensure predominantly elastic behavior (for specimens not described in this test method).

10.1.10 da/dN as a function of ΔK shall be plotted. (It is recommended that ΔK be plotted on the abscissa and da/dN on the ordinate. Log-log coordinates are commonly used. For optimum data comparisons, the size of the ΔK-log cycles should be two or three times larger than da/dN-log cycles.) All data that violate the size requirements of 7.2 shall be identified; state whether σ_{YS} or σ_{FS} was used to determine specimen size.

10.1.11 Description of any occurrences that appear to be related to anomalous data (for example, transience following test interruptions or changes in loading variables).

10.1.12 For K-decreasing tests, report C and initial values of K and a. Indicate whether or not the K-decreasing data were verified by K-increasing data. For near-threshold growth rates, report ΔK_{th}, the equation of the fitted line (see 9.4) used to establish ΔK_{th}, and any procedures used to establish ΔK_{th} which differ from the operational definition of 9.4. Also report the lowest growth rate used to establish ΔK_{th} using the operational definition of 9.4. It is recommended that these values be reported as ΔK_{th} (x) where x is the aforementioned lowest growth rate in m/cycle.

10.1.13 The following information shall be tabulated for each test: a, N, ΔK, da/dN, and, where applicable, the test variables of 10.1.3, 10.1.6, and 10.1.7. Also, all data determined from tests on specimens that violate the size requirements of 7.2 shall be identified; state whether σ_{YS} or σ_{FS} was used to determine specimen size.

11. Precision and Bias

11.1 *Precision*—The precision of da/dN versus ΔK is a function of inherent material variability, as well as errors in measuring crack length and applied load. The required loading precision of 8.4.1 can be readily obtained with modern closed-loop electrohydraulic test equipment and results in a ± 2 % variation in the applied ΔK; this translates to a ± 4 % to ± 10 % variation in da/dN, at a given ΔK, for growth rates above the near-threshold regime. However, in general, the

crack length measurement error makes a more significant contribution to the variation in da/dN, although this contribution is difficult to isolate since it is coupled to the analysis procedure for converting a versus N to da/dN, and to the inherent material variability. Nevertheless, it is clear that the overall variation in da/dN is dependent on the ratio of crack length measurement interval to measurement error (24, 29). Furthermore, an optimum crack length measurement interval exists due to the fact that the interval should be large compared to the measurement error (or precision), but small compared to the K-gradient of the test specimen. These considerations form the basis for the recommended measurement intervals of 8.8.2. Recommendations are specified relative to crack length measurement precision: a quantity that must be empirically established for the specific measurement technique being employed.

11.1.1 Although it is often impossible to separate the contributions from each of the above-mentioned sources of variability, an overall measure of variability in da/dN versus ΔK is available from results of an interlaboratory test program in which 14 laboratories participated (19).[9] These data, obtained on a highly homogeneous 10 Ni steel, showed the reproducibility in da/dN within a laboratory to average ± 27 % and range from ± 13 to ± 50 %, depending on laboratory; the repeatability between laboratories was ± 32 %. Values cited are standard errors based on ± 2 residual standard deviations about the mean response determined from regression analysis. In computing these statistics, abnormal results from two laboratories were not considered due to improper precracking and suspected errors in load calibration. Such problems would be avoided by complying with the current requirements of this test method as they have been upgraded since the interlaboratory test program was conducted. Because a highly homogeneous material was employed in this program, the cited variabilities in da/dN are believed to have arisen primarily from random crack length measurement errors.

11.1.2 For the near-threshold regime, a measure of the variability in ΔK_{th} is available from the results of an interlaboratory test program in which 15 laboratories participated (30).[8] These data, obtained on a homogeneous 2219 T851 aluminum alloy, show a reproducibility in ΔK_{th} within a laboratory to average $\pm$ 3 % with the repeatability between laboratories of ± 9 %. This observation is based on the 11 laboratories that provided valid near-threshold data. Because of the sensitivity of da/dN to small changes in ΔK, growth rates in this near threshold regime often vary by an order of magnitude, or more, at a given ΔK (30).[9]

11.1.3 It is important to recognize that for purposes of design or reliability assessment, inherent material variability often becomes the primary source of variability in da/dN. The variability associated with a given lot of material is caused by inhomogeneities in chemical composition, microstructure, or both. These same factors coupled with varying processing conditions give rise to further lot-to-lot variabilities. An assessment of inherent material variability, either within or between heats or lots, can only be determined by conducting a statistically planned test program on the material of interest. Thus,

---

results cited above from the interlaboratory test programs on 10 Ni steel and 2219 T851 aluminum, materials selected to minimize material variability and therefore allow an assessment of measurement precision, are not generally applicable to questions regarding inherent variability in other materials.

11.2 *Bias*—There is no accepted "standard" value for d*a*/d*N* versus ΔK for any material. In the absence of such a true value, no meaningful statement can be made concerning bias of data.

12. Keywords

12.1 constant amplitude; crack length; fatigue crack growth rate; stress intensity range

ANNEXES

(Mandatory Information)

A1. SPECIAL REQUIREMENTS FOR TESTING IN AQUEOUS ENVIRONMENTS

A1.1 Introduction

A1.1.1 Fatigue crack growth rates in metallic materials exposed to aqueous environments can vary widely as a function of mechanical, metallurgical, and electrochemical variables. Therefore, it is essential that test results accurately reflect the effects of specific variables under study. Test methods must be chosen to represent steady state fatigue crack growth behavior which neither accentuates nor suppresses the phenomena under investigation. Only then can data be compared from one laboratory investigation to another on a valid basis, or serve as valid basis for characterizing materials and assessing structural behavior.

A1.2 Scope

A1.2.1 This annex covers the determination of fatigue crack growth rates using either compact tension C(T) or middle-tension M(T) specimens under test conditions involving temperatures and pressures at, or near, ambient.

A1.3 Referenced Documents

A1.3.1 *ASTM Standards*:
D 1129 Terminology Relating to Water[10]
E 742 Definitions of Terms Relating to Fluid Aqueous and Chemical Environmentally Affected Fatigue Testing[3]
G 1 Practice for Preparing, Cleaning, and Evaluating Corrosion Test Specimens[11]
G 3 Practice for Conventions Applicable to Electrochemical Measurements in Corrosion Testing[11]
G 5 Reference Test Method for Making Potentiostatic and Potentiodynamic Anodic Polarization Measurements[11]
G 15 Terminology Relating to Corrosion and Corrosion Testing[11]

A1.4 Terminology

A1.4.1 The terms used in this annex are defined in the main body of this test method. Additional terms more specific to testing in aqueous environments can be found in Terminologies D 1129 and G 15 and Definitions E 742.

A1.5 Significance and Use

A1.5.1 In aqueous environments, fatigue crack growth rates are a complex function of many experimental variables. These include prior loading history, stress-intensity range, load ratio, cyclic frequency, load-versus-time wave-form, specimen thickness, crack geometry and size, electrolyte species and concentration, exposure time, flow rate, temperature, pH, dissolved oxygen content, and potential (free corrosion or applied). Background information on these effects can be found in Refs. **(31-38)**.

A1.5.2 Specimens which undergo fatigue crack growth rate testing in aqueous environments are subject to various corrosive effects which can either hasten or retard crack growth rates (see Refs. **(39)** and **(40)**). Generation of fatigue crack growth rate data on metallic materials in aqueous environments requires judicious selection, monitoring, and control of mechanical, chemical, and electrochemical test variables in order to ensure that the data are applicable to the intended use. For example, data generated in a laboratory test at a cyclic frequency of 10 Hz may not be applicable for predicting crack growth rates in a structure which is cycled at 0.1 Hz.

A1.5.3 Fatigue crack growth which occurs in the presence of an aqueous environment may be the product of both mechanical and chemical driving forces. The chemical driving force can vary with crack size, crack shape, and the degree of crack opening. Thus, fatigue crack growth rates in the presence of an aqueous environment may exhibit non-uniqueness when characterized in terms of d*a/*d*N* versus ΔK, Ref. **(38)**.

A1.6 Apparatus

A1.6.1 The environmental chamber shall enclose the entire portion of the test specimen over which crack extension occurs. A circulation system to provide replenishment and aeration of the test solution may be desirable. Nonmetallic materials are recommended for the entire environmental chamber and circulation system. The environmental chamber should be designed so as to prevent galvanic contact between dissimilar test specimen and grip assembly components. If a circulation system is employed, the environmental chamber should be of sufficient size, and inlet and outlet locations should be chosen, to ensure a flow of test solution around the portion of the test specimen where crack extension occurs. A circulation system should provide for continuous aeration and filtration of the test solution in order to remove corrosion products. Exceptions to the above may occur if a quiescent solution is specifically desired.

A1.7 Procedure

A1.7.1 *Specimen Preparation*—It is recommended that specimens be cleaned prior to precracking and testing in accordance with Practice G 1.

A1.7.2 *Specimen Precracking*—Preliminary precracking may be conducted in an ambient laboratory air environment using a cyclic frequency and waveform which differ from the test conditions. However, a final 1.0-mm increment (0.040-in. increment) of precracking shall be conducted in the aqueous environment under full test conditions.

A1.7.3 *General Test Procedure*—Fatigue crack growth rate testing in aqueous environments provides a means of detecting and assessing the effects of localized corrosion processes involving metal surfaces at crack tips. Thus, the corrosive environment must physically reach the crack-tip region and time-dependent corrosion processes must have sufficient opportunity to proceed. If test techniques fail to adequately promote and maintain localized corrosion in crack-tip regions throughout the full test duration, nonsteady-state conditions can affect the da/dN versus ΔK data. Therefore, testing shall be conducted in a manner which seeks to eliminate or minimize transient or nonsteady-state effects, or both, on da/dN versus ΔK data. Nonsteady-state or transient effects are defined as time-dependent fluctuations in da/dN values which do not directly correspond to any concomitant changes in mechanical crack driving force parameters, Ref. **(20)**.

A1.7.3.1 It is recommended that specimens be immersed in the full test environment for a suitable period of time immediately prior to precracking or gathering crack growth rate data, or both. A minimum period of 24 h is recommended.

A1.7.3.2 It is recommended that specimens undergoing fatigue testing remain immersed in the test solution during brief periods of test interruption. If specimens are removed from the test solution for more than a brief period, it is recommended that fatigue data gathering shall not resume until the crack has extended by a 1.0-mm increment (0.040-in. increment) under test conditions.

A1.7.3.3 It is recommended that specimens be visually examined periodically during the course of testing for evidence of corrosive attack. Corrosion product accumulation which may inhibit access of the test solution to the crack-tip region may be removed. The crack-tip region of the specimen surface may also be cleaned periodically to aid in visual observation of crack length or crack-tip morphology, or both. Upon completion of fatigue testing, it is recommended that the specimen be loaded to fracture and receive a thorough visual post-mortem examination.

A1.7.3.4 It is necessary to carefully monitor tests for evidence of environmentally-induced phenomena which may affect steady state da/dN versus ΔK data. The presence of an aqueous environment may cause numerous environmentally-induced phenomena to occur in the course of fatigue crack growth rate testing of metallic materials. Some common examples are transient changes in da/dN versus ΔK data in response to changes or interruptions in cyclic loading, crack growth acceleration or retardation, crack arrest, crack branching, crack-front curvature or irregularity, out-of-plane cracking, or corrosion product build-up within cracks.

A1.7.3.5 Steady state fatigue crack growth rates in aqueous environments can be strongly affected by cyclic waveform or cyclic frequency, or both. Knowledge of these effects can be an important consideration in selecting test parameters. It is especially important to note that certain frequencies or waveforms, or both, can act to suppress the influence of aqueous environments on fatigue crack growth in metallic materials. These effects generally relate to the rise time of the loading cycle, Refs. **(32)** and **(34)**. For steels and high-strength aluminum alloys, crack growth rates in aqueous environments tend to vary directly with the rise time. However, exceptions to this trend have been observed in high strength titanium alloys under cyclic loading conditions where $K_{max} < K_{Iscc}$, Ref. **(35)**.

A1.7.3.6 If significant transient behavior is apparent in da/dN versus ΔK data for a particular test, it is recommended that the test be repeated. However, in assessing apparent transient behavior, particular care should be taken to ensure that the crack length measurement intervals used in the data reduction are in accordance with those recommended in 8.6.2. Improper selection of Δa values for data reduction can greatly magnify apparent transients in da/dN versus ΔK data.

A1.7.4 *Crack Length Measurement*—Since the presence of an environmental chamber containing an aqueous solution may tend to obscure the crack, a nonvisual technique is recommended as the primary method, Refs. **(41-43)**. However, optical observation of the crack tip is recommended as an auxiliary method of crack length measurement and as a means of monitoring crack morphology, specifically crack branching or out-of-plane cracking which may render the test invalid. Fatigue crack surface features revealed in a post-mortem visual examination may provide useful reference marks for calibrating *in situ* crack length measurements. If the potential drop nonvisual technique is employed, it is recommended that care be taken to assure that electrochemical effects on the da/dN versus ΔK data are not introduced. Electrochemical effects, if sustained in duration, can either accelerate or retard crack growth rates in aqueous environments (see Refs. **(33)** and **(40)**).

A1.7.5 *Environmental Monitoring and Control*—Environmental parameters can strongly influence the results of fatigue crack growth rate tests conducted in aqueous environments. Therefore, environmental monitoring and control are recommended.

A1.7.5.1 It is recommended that tests be initiated using unused solution which has not previously been in contact with other metallic test specimens. It is further recommended that replenishment of evaporated solution be conducted once every 24 h testing period, or more frequently if required, and the entire test solution be emptied and replaced not less than once a week.

A1.7.5.2 It is recommended that measurements of solution temperature and specimen corrosion potential be made and recorded not less than once every 8 h testing period. Potential measurements should be made in accordance with conventions and procedures set forth in Practices G 3 and G 5. It is further recommended that measurements be made and recorded of pH, conductivity, and dissolved oxygen at similar intervals. Control of environment temperature is also recommended.

A1.8 Report

A1.8.1 The following information shall be reported in addition to the requirements stated in Section 11.

A1.8.2 Descriptions of the environmental chamber and all equipment used for environmental monitoring or control, or both, shall be reported.

A1.8.3 Environmental variables shall be reported as follows: the bulk solution chemical composition and details of its application shall be described; procedures for environmental monitoring and control shall be described; environmental monitoring data for such parameters as pH, potential, or temperature shall be expressed in terms of the normal daily range experienced throughout the duration of the test; relevant trends or transients in environmental parameters data shall be reported.

A1.8.4 It is important to maintain a test log which records all test interruptions or load changes in terms of elapsed cycles, crack length, and time. All data shall be scrutinized for transients and anomalies. All anomalous behavior shall be reported and described in relation to recorded test events.

A2. GUIDELINES FOR USE OF COMPLIANCE TO DETERMINE CRACK LENGTH

A2.1 The compliance method of crack length monitoring can be used during fatigue crack growth rate testing (21, 22). The optimum procedure employs the use of high speed digital data acquisition and processing systems, but low-speed autographic equipment can also be used to record the load and displacement signals. Depending on the data acquisition equipment and cyclic loading frequency, it may be necessary to lower the frequency during the period of data acquisition.

A2.2 The relationship between compliance (which is the reciprocal of the load-displacement slope normalized for elastic modulus and specimen thickness) and crack length has been analytically derived for a number of standard specimens (44). Such relationships are usually expressed in terms of the dimensionless quantities of compliance, $\frac{EvB}{P}$, and the normalized crack length, a/W, where E is the elastic modulus, v is the displacement between measurement points, B is specimen thickness, P is load, a is crack length, and W is the specimen width. All compliance-crack length relationships are applicable only for the measurement locations on the specimen for which they were developed. In lieu of an analytically derived compliance relationship, it is possible to empirically develop a compliance curve for any type of specimen used in fatigue crack growth rate testing. Such curves are not limited to displacement measurements alone and can involve strain related quantities.

A2.3 Specimens for fatigue crack growth rate testing covered in this standard are the compact tension, C(T), and the middle tension, M(T), specimens. Theoretical compliance expressions for specific measurement locations on the C(T) specimen are presented in Fig. A2.1 (44). Additional measurement locations are available through the use of rotation coefficients. An equation for the compliance measured on the center line of the M(T) specimen is shown in Fig. A2.2 (45). Both of these equations are for plane stress since this stress state is most applicable to measurements remote to the crack tip, regardless of the stress state local to the crack tip.

A2.4 Selection of displacement measurement gages, attachment points and methods of attachment are dependent on the test conditions such as frequency, environment, stress ratio, and temperature. Gages must be linear over the range of displacement measured, and must have sufficient resolution and frequency response. Insight into these issues can be obtained from Test Method E 813 and the relative Annex in Test Method E 399. Smaller specimens generally require higher resolution gages. Attachment points must be accurately and repetitively placed on the specimen, and must not be susceptible to wearing during the fatigue cycling.

NOTE A2.1—For a C(T) specimen of W = 40 mm, a gage located at any of the four locations shown in Fig. A2.1 and calibrated to 50 μm/V on a ± 10 V range will generally provide sufficient resolution. An M(T) specimen of W = 80 mm and $2y/W \leq 0.4$ will require a gage calibration of 15 μm/V on the same range. The increased resolution required for the M(T) specimen is caused by its greater stiffness which makes it less amenable to this form of nonvisual crack length monitoring. M(T) specimen compliance readings are also complicated by small, normally acceptable levels of bending.

A2.5 Gripping techniques for specimens that undergo bending, such as the C(T) specimen, have been observed to affect compliance readings. The C(T) specimen may be loaded with grips that have either flat bottom holes or needle bearings, as shown in Fig. A2.3, to circumvent such problems.

A2.6 The load-displacement plot of one complete cycle of fatigue loading is generally not linear. The lower portion is usually nonlinear and the upper portion is linear. Compliance is calculated by fitting a straight line to the upper linear part of a load-displacement curve.

NOTE A2.2—When using a digital data acquisition system it is permissible to obtain data from a few consecutive cycles provided the growth rate is relatively small. During multiple cycle sampling the normalized
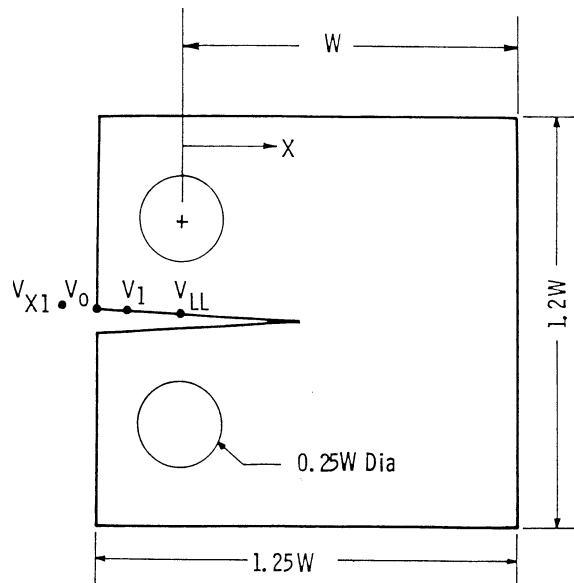
Meas. Location	X/W	C_0	C_1	C_2	C_3	C_4	C_5
				C(T) Specimen			
V_{X1}	−0.345	1.0012	−4.9165	23.057	−323.91	1798.3	−3513.2
V_0	−0.250	1.0010	−4.6695	18.460	−236.82	1214.9	−2143.6
V_1	−0.1576	1.0008	−4.4473	15.400	−180.55	870.92	−1411.3
V_{LL}	0	1.0002	−4.0632	11.242	−106.04	464.33	−650.68

$$\alpha = a/W = C_0 + C_1 u_x + C_2 u_x^2 + C_3 u_x^3 + C_4 u_x^4 + C_5 u_x^5$$

$$u_x = \left\{ \left[\frac{EvB}{P} \right]^{\frac{1}{2}} + 1 \right\}^{-1}$$

$$0.2 \le a/W \le 0.975$$

FIG. A2.1 Normalized Crack Length as a Function of Plane Stress Elastic Compliance for C(T) Specimens (44).

crack length, a/W, cannot change by more than 0.001 ($\Delta a/W \le 0.001$).

NOTE A2.3—There are indications that near the crack growth rate threshold, the upper linear portion of the curve may be very small making the compliance method unusable.

NOTE A2.4—It is usual practice to consistently fit to either the linear portion of the loading data or the unloading data.

NOTE A2.5—It is sometimes necessary to eliminate the data close to the top load reversal point because of rounding that occurs in this area. This is predominately true for data taken at low frequencies.

A2.7 At least one visual crack length reading must be taken either at the beginning or after the test. The visual reading must be adjusted for curvature to obtain the physical crack length using the procedures in the main section of this test method under Calculations and Interpretation of Results. Any difference between the physical and compliance crack length must be used to adjust all compliance crack lengths. Most often this is accomplished by calculating an effective modulus of elasticity, E', and using this in the compliance equation to adjust all crack length calculations. If the effective modulus of elasticity differs from the typical elastic modulus by more than 10 %, then the test equipment is improperly set-up and data generated from such records are to be considered invalid by this method.

NOTE A2.6—Usually $E \le E_M \le E/(1 - \mu^2)$, where μ is Poisson's ratio. E_M might be thought of as being proportional to E, that is, $E' = \gamma E$, where γ is an adjustment factor that accounts for parameters not controllable or measurable during a test.

NOTE A2.7—It is recommended that periodic optical readings be taken for comparison purposes during the first series of tests that use this or any other nonvisual method of crack length measurement.

16
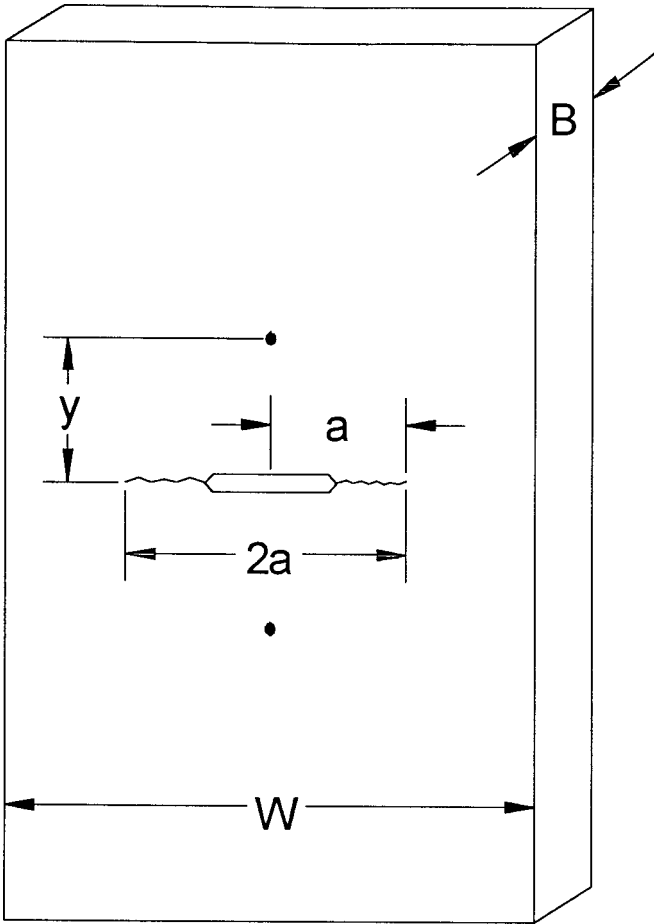
Middle-Tension, M(T) Specimen

a = crack length,
B = specimen thickness,
W = specimen width,
$C = v/P$ = compliance,
E = Young's modulus,
y = half gage length,
$\eta = 2y/W$ = nondimensional gage length

$$2a/W = 1.06905x + 0.588106x^2 - 1.01885x^3 + 0.361691x^4$$
where:

$$x = 1 - e^{\frac{-\sqrt{(EBC + \eta)(EBC - \eta + c_1\eta + c_2\eta^{c_3})}}{2.141}}$$

NOTE 1—This expression is valid for (1) $0 \leq 2y/W \leq 1.0$, and (2) $0 \leq 2a/W \leq 1.0$. Values of c_1, c_2, and c_3 are dependent on loading conditions and are shown below for three examples.

FIG. A2.2 Plane Stress Compliance Expression for the M(T) Specimen (45).
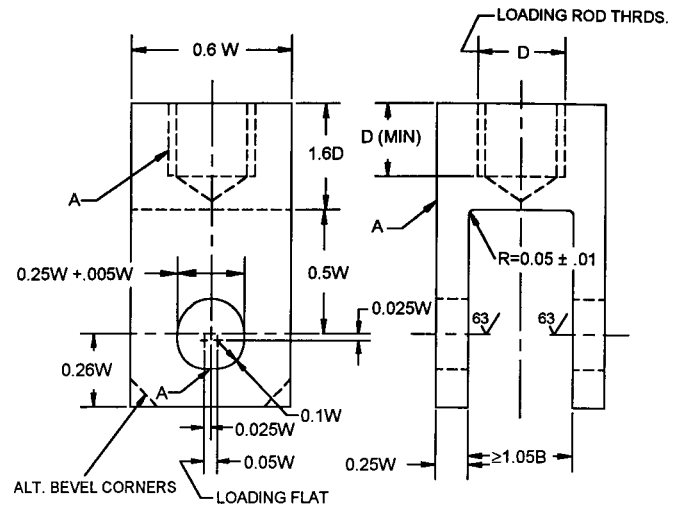
NOTE 1—Pin diameter = 0.24 W – 0.005 W.
NOTE 2—Flat bottom hole is a modified Test Method E 399 design.
NOTE 3—Corners of clevis may be removed if necessary to accommodate clip gage.
A—surfaces must be flat, in-line, and perpendicular, as applicable, to within 0.05 mm.

FIG. A2.3 Two Suggested Clevis Designs for C(T) Specimen Testing

Models of Laboratory Test Specimens
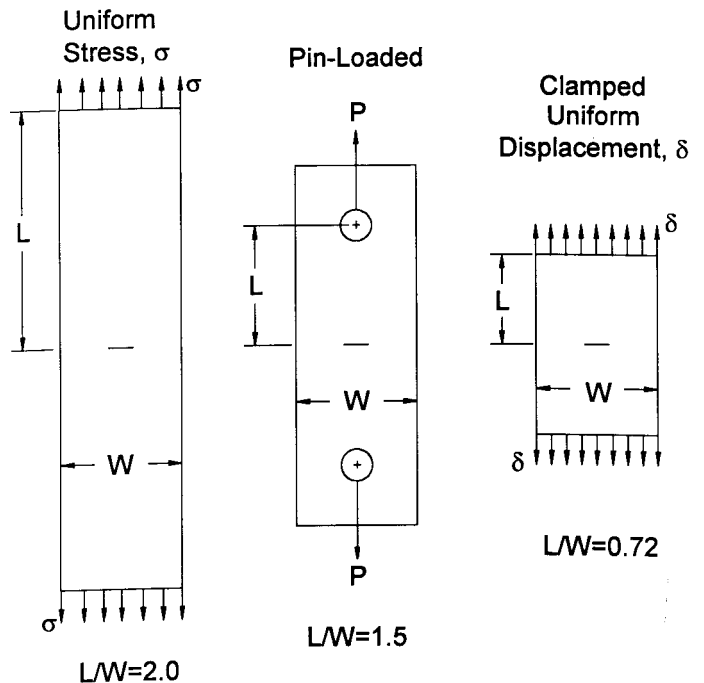
Modification to $x(EBC, 2y/W)$ for Different Loading Conditions

Uniform Stress	Pin-Loaded	Clamped Uniform Displacement
$c_1 = 0.0$	$c_1 = 0.005$	$c_1 = -0.03$
$c_2 = 0.0$	$c_2 = 0.0184$	$c_2 = 0.013$
$c_3 = 0.0$	$c_3 = 3.0$	$c_3 = 4.0$

FIG. A2.2 *(continued)*

17
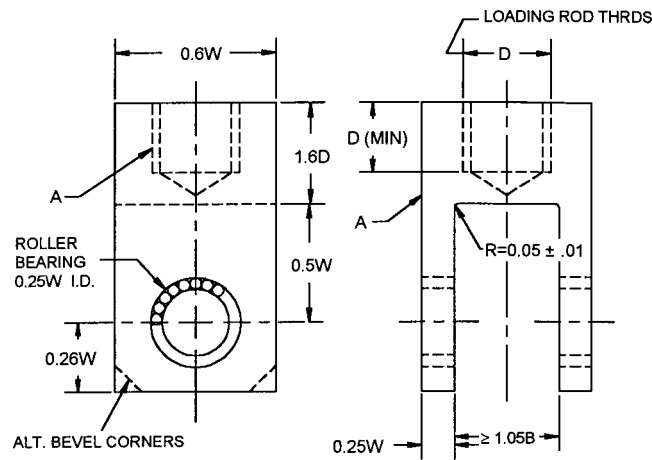
NOTE 1—Because of space requirements for the bearings, this grip is not practicable for small specimens.

A—surfaces must be flat, in-line, and perpendicular, as applicable, to within 0.05 mm.

FIG. A2.3 *(continued)*

A3. GUIDELINES FOR ELECTRIC POTENTIAL DIFFERENCE DETERMINATION OF CRACK SIZE

A3.1 *Applications*—Electric potential difference (EPD) procedures for crack size determination are applicable to virtually any electrically conducting material in a wide range of testing environments. Non-conducting materials may also be tested using the electric potential method by firmly attaching a conducting foil or film and treating it as a replicate specimen. This method is acceptable provided that cracking in the film duplicates cracking in the test specimen, and the film does not alter the fatigue crack growth rate properties of the test specimen. This replicate film method may also be used with conducting specimens as well.

A3.1.1 Procedures discussed herein are those for which two-dimensional models can be used both for the specimen configuration and for the electric potential.

A3.2 *Principle*—Determining crack size from electric potential measurements relies on the principle that the electrical field in a cracked specimen with a current flowing through it is a function of the specimen geometry, and in particular the crack size. For a constant current flow, the electric potential or voltage drop across the crack plane will increase with increasing crack size due to modification of the electrical field and associated perturbation of the current streamlines. The change in voltage can be related to crack size through analytical or experimental calibration relationships.

A3.3 *Basic Methods*—Both direct current (DC) and alternating current (AC) techniques have been used to measure crack size in test specimens (46-53). For the more common DC technique, a constant current is passed through the specimen resulting in a two-dimensional electrical field which is constant through the thickness at all points. For the AC technique, a constant amplitude (normally sinusoidal) current is passed through the specimen to generate the voltage drop across the crack tip. For relatively low frequencies (less than 100 Hz with

common materials), the field is approximately two-dimensional as in the DC current case. For higher frequencies, however, a non-uniform current distribution occurs through the thickness, the degree of which is dependent on the AC frequency and magnetic permeability of the specimen. This phenomenon is commonly termed the "skin effect" because the current tends to be carried only near the surface of the specimen. For some materials, particularly ferromagnetic specimens, this skin effect can be significant at frequencies as low as 100 Hz, and below (49, 50). The AC methods can thus be subdivided into two groups: lower frequency methods where the skin effect is negligible and higher frequency methods where the skin effect must be taken into account.

A3.3.1 For many materials under test in oxidizing environments an oxide layer forms immediately upon the creation of a "fresh" fracture face, thereby insulating the two specimen halves. Under these conditions, the voltage drop across the fatigue crack should remain constant throughout a complete load cycle (assuming no crack extension). An insulating surface may not be created in a non-oxidizing environment or where high fracture surface closure forces tend to compromise such an oxide layer. In these cases, fracture surface shorting may occur at load levels above the minimum test load leading to an under-estimation of the physical fatigue crack size (54, 55). This effect is of particular concern when testing at near threshold conditions, when the load at which shorting occurs approaches the peak test load level.

A3.3.2 Unless it can be shown that electrical shorting does not occur during the entire load cycle, the voltage measurements should be taken at or near the peak tensile load. Depending on the frequency response of the AC or DC voltage measuring equipment, it may be necessary to reduce testing frequency or, in some extreme instances, even to stop the test during a voltage measurement to ensure that the measurement

is taken only at peak load and without any signal attenuation. It should be noted that measurement of the electrical potential at maximum load does not always guarantee the absence of electrical shorting errors. Shorting errors can still be present at maximum load in cases where there is electrical contact between the fracture surfaces but no mechanical load is transferred. The fracture surface shorting effect can be accounted for after the test using post-test fracture surface crack size measurements. One approach is to compute offset and scaling factors to match the initial and final crack sizes from electric potential measurements and fracture surface measurements. A simple linear interpolation technique with the scaling factor as a function of *a/W* is then used to correct the intermediate electric potential values. This method may not be suitable for tests in which machine control parameters are derived from the crack size (such as a constant stress intensity test). In these cases, crack size measurement errors may cause unacceptable differences between the applied loads and the desired control load.

A3.3.3 Elastic and plastic deformation can in principle affect material resistivity and, for the case of AC potential difference measurement, magnetic permeability **(56)**. While unlikely to be an important source of error for the stress intensities typical of fatigue crack growth under small scale yielding and Test Method E 647, the user should document any load dependence of the potential for constant crack size without surface shorting and assess the importance of associated errors in calculated crack size. The correction method for shorting errors will generally account for deformation effects on the electrical and magnetic properties of the material.

A3.3.4 Changes in the specimen or instrumentation may result in proportional changes in the measured voltage. For example, a 1°C change in specimen temperature can result in a few μV change in EPD signal due to the change in the material's electrical resistivity. Also, some materials exhibit time-dependent conductivity changes while at elevated temperatures **(54)**. Variations in the gain of amplifiers or calibration of voltmeters may also result in a proportional scaling of the measured voltages. To compensate for these effects, voltage measurements can be normalized using additional voltage measurements taken at a reference location. The reference location may be either on the test specimen or on an alternate specimen in the same environment. If the reference measurements are made directly on the test specimen, the location must be chosen so that the reference voltage is not affected by crack size. Since all material and instrument variations are also included in the reference measurements, the normalization process should eliminate them. Use of reference voltage measurements can significantly increase crack size resolution.

A3.3.5 *DC Current Method*—The DC method is an established technique which can be applied using equipment commonly found in most testing laboratories as shown in Fig. A3.1. The output voltages are typically in the 0.1 to 50.0 mV range for common current magnitudes (5 to 50 A), specimen dimensions, and materials. Precise measurements (typically ±0.1 %) of these relatively small output voltages must be made to obtain accurate crack size values. To obtain sufficient voltage resolution usually requires special care in eliminating electrical
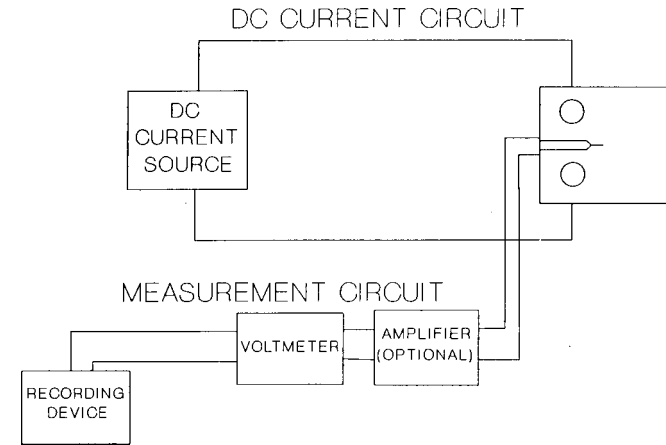

FIG. A3.1 Schematic Diagram of the DC Potential System

noise and drift (see A3.11). Generally, tradeoffs are made between measurement system response time and voltage resolution (see A3.5).

A3.3.5.1 The DC method is susceptible to thermoelectric effects **(57)** which produce DC potentials in addition to those due to the specimen electrical field. These thermoelectric voltages can be a substantial fraction of the total measured voltage. Since the thermoelectric effect is present even without the input current, it is possible to account for it by subtracting voltage measurements taken with the current off from the measurements made with the current on. An alternate method corrects for the thermoelectric effect by taking voltage measurements while reversing the direction of current flow. Corrected EPD measurements are then equal to one-half of the difference of the measured potential readings taken at each current polarity **(58)**.

A3.3.6 *AC Current Method*—Both the low and high frequency AC methods require equipment similar to that shown in Fig. A3.2 **(49)**. The AC equipment is more specialized than that for the DC approach (see A3.5.2). With the same specimen input current magnitude, this equipment can be used to obtain higher crack size resolution as compared to the DC method **(46)**. This is due in part to the different amplification and filtering techniques used in the two methods in addition to the skin effect previously noted. The AC method is not influenced by thermoelectric effects which produce a DC voltage offset.
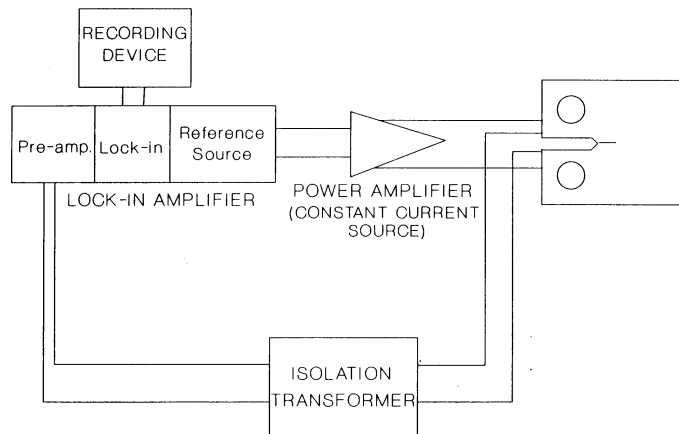

FIG. A3.2 Schematic Diagram of the AC Potential System (42)

A3.3.6.1 *Low Frequency AC Current Method*—The low frequency AC method is similar to the DC current method except that as previously noted, different equipment is required to produce the drive current and measure the output voltage. One possible problem with this type of system is that if the test loading frequency is an integral multiple of the AC potential frequency, fracture surface sorting (bridging) effects may produce unwanted signal components at the AC potential frequency.

A3.3.6.2 *High Frequency AC Current Method*—An advantage of this technique over the low frequency AC method is that better crack size resolution can typically be obtained using the same input current. This is due to the skin effect previously noted which effectively reduces the specimen thickness to the surface layers (51) and the fact that the output voltage is inversely proportional to the specimen thickness.

A3.3.6.3 At high frequencies where the skin effect becomes pronounced, only the near surface crack size will be obtained. This must be taken into account if through-the-thickness crack front curvature is significant. Other effects which may appear at high frequencies include induction and capacitance contributions from lead wires, specimen attachments, and the crack itself. These may be significant and may vary with crack size, causing difficulties in relating output voltage measurements to crack size unless precautions are taken (see A3.11.1).

A3.4 *Current Generating Equipment*—Any suitable constant current supply may be used which has sufficient short and long term stability. The required stability is a function of the resolution of the voltage measurement equipment (see A3.5) and the desired crack size resolution. For optimum conditions, the relative stability of the power supply should be equal to the effective resolution of the voltage measurements system; that is, if the voltage measurement system can effectively resolve one part in 10^3 of the output voltage from the specimen (including electrical noise, inherent inaccuracies such as non-linearity, and so forth), then the power supply should be stable to one part in 10^3.

A3.4.1 For AC systems, the current should be generated using an amplifier to produce an output current proportional to an input reference signal. The use of an amplifier instead of a stand-alone current generator allows the use of lock-in detection in the voltage measurement circuit (see A3.5.2). The amplifier should have suitably high input impedance (>10 kΩ) and should be capable of generating an output current which is stable as per the preceding discussion.

A3.5 *Voltage Measurement Equipment*—Voltage measurements may be made with any equipment which has sufficient resolution, accuracy, and stability characteristics. The following subsections deal with measurement equipment particular to the different potential drop methods.

A3.5.1 *DC Voltage Measurement Equipment*—The DC method requires equipment capable of measuring small changes in DC voltage (that is, 0.05 to 0.5 μV) with relatively low DC signal to AC RMS noise ratios. Although there are a variety of ways to implement the voltage measurement system, three commonly used systems are: amplifier/autographic recorder, amplifier/microcomputer analog to digital converter, and digital voltmeter/microcomputer.

A3.5.1.1 Autographic recorders are commonly available with suitable sensitivity and can be used to record the output voltage directly from the specimen. A preamplifier can be used to boost the direct voltage output from the specimen before recording. Another common technique uses a preamplifier to boost the direct output from the specimen to a level that can be digitized using a conventional analog to digital (A/D) converter and microcomputer. A third method makes use of a digital voltmeter with a digital output capability. The advantage of this type of system is that all of the sensitive analog circuits are contained within a single instrument. The response time of the voltage measurement system must be sufficient to resolve changes in EPD as a function of applied load if fracture surface shorting occurs.

A3.5.2 *AC Voltage Measurement Equipment*—Both low and high frequency AC systems make use of similar voltage measurement equipment as shown in Fig. A3.2. The voltage measurement circuit and the current amplifier (see A3.4) are interconnected through the lock-in amplifier. This specialized amplifier produces a reference output signal for the current amplifier and is able to discriminate against all input signals that are not at the reference signal frequency and phase. Thus, only signals produced as a result of the current amplifier output are amplified for measurement. This method is capable of amplifying only the desired AC voltage signal at very low signal-to-noise ratios and provides excellent noise rejection (49). Note that this type of system is insensitive to DC voltages which might be produced by thermoelectric effects.

A3.5.3 When selecting instrumentation for an AC system, care should be made to ensure proper impedance matching, since each component is designed for operation over a specific frequency domain. Input and output impedance should be matched. A check for frequency response to ensure operation in the "flat" region of the instruments' gain should also be performed.

A3.6 *Crack Length versus Potential Difference Relationships*—Closed form solutions for the relationship between potential difference versus crack size have been analytically derived for such specimen geometries as the M(T) specimen (59) and the part-through surface crack specimen (60, 61). Additional relationships are also available based on numerical solutions for a number of other specimen geometries (62-64). Such relationships are usually expressed in terms of the normalized voltage (V/V_r) and some reference crack size (a_r) as shown in Eq A3.1.

$$a = f(V/V_r, a_r) \tag{A3.1}$$

where:
V = the measured voltage,
V_r = a reference crack voltage,
a = crack size, and
a_r = a reference crack or notch size associated with V_r.

Alternative formulations are also used when the crack size is normalized by an in-plane characteristic dimension such as the specimen width W. When written in this form, the solutions can be made independent of specimen thickness, in-plane specimen size, applied current, and material.

A3.6.1 In lieu of an analytically derived expression, it is possible to empirically develop relationships for virtually any type of specimen geometry used in fatigue crack growth rate testing. Such empirical relationships can be advantageous in instances when specimen geometries are complex, or wire placement must be altered. In any event, analytical or empirical relationships should be experimentally verified using alternative measurements at various crack sizes in the range of interest (optical surface measurements, compliance measurements, or post-test fracture surface measurements). Such measurements should be reported and may be used for correcting crack lengths inferred from equations of the type in Eq A3.1.

A3.6.2 Voltage wire placements are usually a compromise between good sensitivity to crack size changes and freedom from errors caused by minor variations in lead location from specimen to specimen. Near crack tip lead locations (or notch tip locations for uncracked specimens) yield better sensitivity to changes in crack size. The difficulty with this type of arrangement is that the electrical field is, in general, highly nonuniform in the near tip region. Thus, minor variations in lead placement from one specimen to the next may produce significant differences in measured voltage for the same crack size **(63)**. In most cases those positions which give greatest sensitivity to crack size changes also have the greatest sensitivity to variations in lead wire positioning.

A3.7 *Specimen Geometries*—Specimen geometries for fatigue crack growth rate testing covered in this standard are the compact tension, C(T), and the middle cracked tension, M(T). The equations listed in the following sections are derived under DC conditions for sharp cracks in the respective specimen geometries. Errors in crack length measure-ments may arise if a blunt notch is used as the reference crack size **(59, 65)**.

A3.7.1 *C(T) Geometry Voltage versus Crack Size Relationships*—An example of a voltage versus crack size relationship for the C(T) specimen geometry is shown in Eq A3.2. The expression was developed by Hicks and Pickard from finite element analysis and was verified through both analogue and experimental techniques for a/W ranging from 0.24 to 0.7 **(62)**. This equation has been employed in two multi-laboratory, international co-operative testing efforts **(66, 67)**. Fig. A3.3 illustrates the C(T) geometry and specific wire placement locations for this solution. The relationship is valid only for the wire locations shown, which were determined by a compromise between sensitivity and reproducibility. If alter-

native wire placements (current or voltage) are used, the relationship shown is no longer valid and a new relationship must be developed.

$$V/V_r = A_o + A_1(a/W) + A_2(a/W)^2 + A_3(a/W)^3 \qquad \text{(A3.2)}$$
$$\text{for } 0.24 \leq a/W \leq 0.7$$

where:
V = the measured EPD voltage,
V_r = the reference crack voltage corresponding to $a/W = 0.241$,
a = the crack size (as defined in Test Method E 647),
W = the specimen width,
A_o = 0.5766,
A_1 = 1.9169,
A_2 = −1.0712, and
A_3 = 1.6898
  or in reverse notation

$$a/W = B_o + B_1(V/V_r) + B_2(V/V_r)^2 + B_3(V/V_r)^3 \qquad \text{(A3.3)}$$
$$\text{for } 0.24 \leq a/W \leq 0.7$$

where:
B_o = −0.5051,
B_1 = 0.8857,
B_2 = −0.1398,
B_3 = 0.0002398.

Note that the first form of the equation can be used to compute the constant V_r from any reference a/W and corresponding voltage measurement V. Computing V_r in this way accounts linearly for small changes in applied current, measured specimen dimensions, and slight errors in wire placement from specimen to specimen. The computed reference voltage can then be used with the second form of the equation to determine the crack size for all voltage values V.

A3.7.2 *M(T) Geometry Voltage versus Crack Size Relationship*—A closed form analytical voltage versus crack size relationship for an infinitely long M(T) specimen **(59)** is shown in Eq A3.4. This relationship is valid only in cases where the current density is uniform at some cross section of the specimen remote from the crack plane and the voltage is measured on the centerline of the specimen across the crack plane. Fig. A3.4 illustrates the M(T) geometry and wire placement locations for this solution.
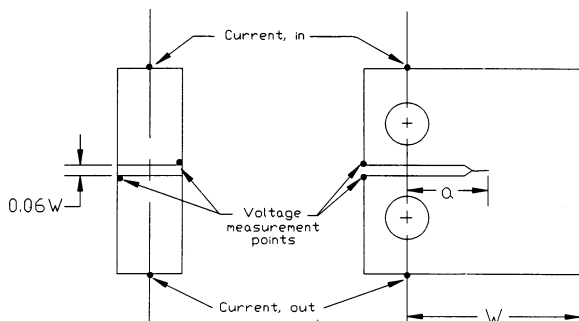

FIG. A3.3 C(T) Geometry and Electric Potential Wire Placement Locations for Fig. A3.2 (52)
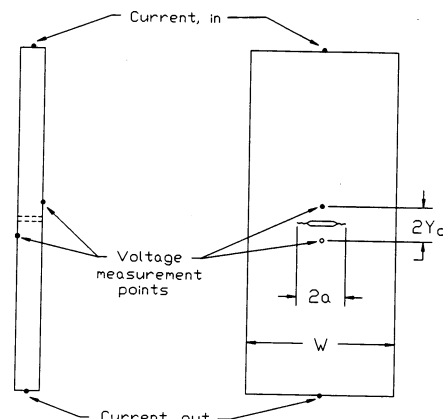

FIG. A3.4 M(T) Geometry and Electric Potential Wire Placement Locations for Eq A3.3 (5)

$$a = \frac{W}{\pi} COS^{-1}$$

$$\left[\frac{COSH\left(\frac{\pi}{W} \times Y_o\right)}{COSH\left[\frac{V}{V_r} \times COSH^{-1} \cdot \left[\frac{COSH\left(\frac{\pi}{W} \times Y_o\right)}{COS\left(\frac{\pi}{W} \times a_r\right)}\right]\right]} \right]$$

(A3.4)

for $0 \leq {}^{2a}\!/w \leq 1$

where:
a = the crack size (as defined in Test Method E 647),
a_r = the reference crack size from some other method,
W = the specimen width,
V = the measured EPD voltage,
V_r = the measured voltage corresponding to a_r, and
Y_o = the voltage measurement lead spacing from the crack plane.

The requirement that current density be uniform at some cross section remote from the crack plane can be easily met by introducing the current through the standard M(T) specimen ends, with a distance between current input locations of approximately three times the width. Shorter current lead spacing may also be used provided that the uniform current density requirement be demonstrated. The calibration constants a_o and V_o may be any crack size and corresponding voltage measurement where the crack size has been determined using an alternate method. Optical surface measurements may be used to determine a_o provided crack front curvature is not significant or is accounted for. If real time crack size measurements are not required during the test, post-test fracture surface measurements may be used to determine a_o.

NOTE A3.1—One or more measurements of the crack size should be made during the test using an alternative technique such as optical measurements on the specimen surface. These values should be used for comparison to evaluate the progress of each test. This is particularly important where a parameter derived from the crack length (stress intensity, and so forth) is being controlled. If optical measurements cannot be made during the test, the final crack size, along with the initial starter crack size, should be compared to the crack sizes determined from electric potential measurements. If a difference is observed between the optical and EPD crack sizes, a linear correction factor, similar to that described for crack curvature correction in the main section (Calculation and Interpretation of Results), must be employed to "post-correct" the EPD crack size values (see also A3.3).

NOTE A3.2—Regardless of which EPD versus crack size expression is used, the use of a reference probe is encouraged (see A3.3). This reference probe should be located on the test specimen (or another specimen at the identical test conditions) in a region unaffected by crack growth and should be equal to or greater in magnitude to the expected voltage levels measured across the crack. When employing such a reference probe, the EPD measurements made for crack size determination (V in Eq A3.3 and Eq A3.4) are divided by the ratio V_{ref}/V_{ref_0},

where:
V_{ref} = the reference probe voltage measured at the same time as the EPD crack voltage is measured, and
V_{ref^0} = the initial reference probe voltage.

NOTE A3.3—For AC potential systems, caution should be applied when using either of the referenced equations for crack length determination (Eqs. Eq A3.3 and Eq A3.4), which were developed under the assumption that the measured potentials reflect only a resistive voltage component.

With an AC potential system the measured EPD voltage across the crack contains both a resistive and a reactive voltage component. For materials with high conductivity at high AC frequencies the reactive component can be a substantial fraction of the measured voltage and can lead to significant errors if used with the equations cited above. If conditions are such that the reactive component is significant then a new relationship must be empirically developed for the particular test/specimen conditions.

A3.8 *Gripping Considerations*—The electric potential difference method of crack size determination relies on a current of constant magnitude passing through the specimen when the potential voltage is measured. During such potential measurements it is essential that no portion of the applied current be shunted in a parallel circuit through the test machine. For most commercially available test machines and grip assemblies the resistance through the test frame is considerably greater than that of the test specimen. However, in some situations an alternative path for the applied current may exist through the test frame. In such cases, additional steps to provide isolation between the specimen and load frame may be necessary. Users of the potential difference method should ensure that the electrical resistance measured between the grips (with no specimen in place) is several orders of magnitude higher than the resistance of the specimen between the current input locations. The specimen resistance should be determined for the range of crack sizes encountered during the test. A resistance ratio (test frame resistance divided by the specimen resistance) of 10^4 or greater is sufficient for most practical applications. Isolation of the specimen from the load frame is particularly important when using power supplies with non-isolated (ground referenced) outputs. Use of this type of power supply may require isolating both ends of the test specimen from the test frame to avoid ground loop problems.

A3.8.1 For specimens in which the current is introduced through the loading pins, care must be taken to ensure that good electrical contact is maintained between the pin and the specimen. Constant current power supplies can usually correct for small changes in the pin/specimen/grip resistance, however, abrupt or large changes in resistance due to oxidation or other effects may cause varying or erratic current levels, or both, during the loading cycle. Poor loading pin contact may increase the percentage of an alternate current path and shunting errors.

A3.9 *Wire Selection and Attachment*—Careful selection and attachment of current input and voltage measurement wires can avoid many problems associated with the electric potential method. This is particularly important in aggressive test environments such as elevated temperature where the strength, melting point, and oxidation resistance of the wires must be taken into account. Aggressive test environments may require special lead wire materials or coatings, or both, to avoid loss of electrical continuity caused by corrosive attack.

A3.9.1 *Current Input Wires*—Selection of current input wire should be based on current carrying ability, and ease of attachment (weldability, connector compatibility). Wires must be of sufficient gage to carry the required current under test conditions and may be mechanically fastened or welded to the specimen or gripping apparatus.

A3.9.2 *Voltage Measurement Wires*—Voltage wires should

be as fine as possible to allow precise location on the specimen and minimize stress on the wire during fatigue loading which could cause detachment. Ideally, the voltage sensing wires should be resistance welded to the specimen to ensure a reliable, consistent joint. Lead wires may be fastened using mechanical fasteners for materials of low weldability (for example, certain aluminum alloys), provided that the size of the fastener is accounted for when determining location of voltage sensing leads. Voltage sensing wire should be located diagonally across the starter notch or crack tip as shown in Fig. A3.3 and Fig. A3.4 to average measurements of non-uniform crack fronts.

A3.10 *Resolution of Electric Potential Systems*—The effective resolution of EPD measurements depends on a number of factors including voltmeter resolution (or amplifier gain, or both), current magnitude, specimen geometry, voltage measurement and current input wire locations, and electrical conductivity of the specimen material. Herein, effective resolution is defined as the smallest change in crack size which can be distinguished in actual test operation, not simply the best resolution of the recording equipment. For common laboratory specimens, a direct current in the range of 5 to 50 A and voltage resolution of about ± 0.1 µV or ± 0.1 % of V_r will yield a resolution in crack size of better than 0.1 % of the specimen width (crack size resolution must be in accordance with 8.8). For highly conductive materials (that is, aluminum, copper) or lower current levels, or both, the resolution would decrease, while for materials with a lower conductivity (that is, titanium, nickel) resolutions of better than 0.01 % of the specimen width have been achieved. For a given specimen geometry, material, and instrumentation, crack size resolution shall be analyzed and reported.

NOTE A3.4—The following is an example of the magnitude of voltages as measured on a standard C(T) specimen for a direct current of 10 A:

Material	Approximate EPD Measured at 10A	Approximate Change in Crack Length for 1 µV Change in EPD (Based on Eq A3.2)
Aluminum	0.1 mV	300 µm
Steel	0.6 mV	50 µm
Titanium	3.5 mV	9 µm

Based on a/W = 0.22, B = 7.7 mm, and W = 50 mm.

A3.11 *Techniques to Reduce Voltage Measurement Scatter*—Because of the low level signals which must be measured with either the DC or AC current methods, a number of procedures should be followed to improve voltage measurement precision.

A3.11.1 *Induced EMF*—Voltage measurement lead wires should be as short as possible and should be twisted to reduce stray voltages induced by changing magnetic fields. Holding them rigid also helps reduce the stray voltages which can be generated by moving the wires through any static magnetic fields that may exist near the test frame. In addition, routing the voltage measurement leads away from the motors, transformers, or other devices which produce strong magnetic fields is recommended.

A3.11.1.1 For AC systems, care should be taken to keep the current wires away from the potential leads. If shielded voltage lead wire is used, the shield should be properly grounded at one end.

A3.11.2 *Electrical Groundings*—Proper grounding of all devices (current source, voltmeters, and so forth) should be made, avoiding ground loops. This is particularly important when DC procedures are used in conjunction with electrochemical polarization equipment relevant to corrosion fatigue.

A3.11.3 *Thermal Effects*—For DC systems thermal emf measurement and correction is critically important. A minimum number of connections should be used and maintained at a constant temperature to minimize thermoelectric effects (see A3.3.1).

A3.11.3.1 All measuring devices (amplifiers/preamplifiers, voltmeters, analog-to-digital converters) and the specimen itself should be maintained at a constant temperature. Enclosures to ensure constant temperatures throughout the test are generally beneficial.

A3.11.3.2 Some voltmeters for DC systems have built-in automatic correction for internal thermoelectric effects. These units may be of benefit in cases where it is not possible to control the laboratory environment.

A3.11.4 *Selection of Input Current Magnitude*—The choice of current magnitude is an important parameter: too low a value may not produce measurable output voltages; too high a value may cause excessive specimen heating or arcing **(51)**.

A3.11.4.1 To minimize these problems, current densities should be kept to the minimum value which can be used to produce the required crack size resolution. The maximum current that can be used with a particular specimen can be determined by monitoring the specimen temperature while increasing the current in steps, allowing sufficient time for the specimen to thermally stabilize. Particular care should be exercised when testing in vacuum, as convection currents are not available to help maintain the specimen at ambient temperature.

A3.11.5 *DC Current Stabilization Period*—Allow a sufficient stabilization period after turning the DC electric potential current either on or off before making a voltage measurement. Most solid-state power sources can stabilize the output current within a period of 1 or 2 s for a step change in output, however, this should be verified for each particular specimen and experimental setup.

A3.12 *Precautions*—Care must be taken to demonstrate that the applied current does not affect crack tip damage processes and crack growth rates. For example, in corrosion fatigue, current leakage into the crack solution could alter electrochemical reaction rates and affect cracking. Results to date indicate that this is not a practical problem, presumably because of the high metal conductivity compared to even the most conductive of electrolytes (for example, NaCl). Current flow in the solution is not affected by the current in the specimen **(68)**.

A3.12.1 Large-scale crack tip plasticity can increase measured electrical potentials due to resistivity increases without crack extension **(50)**. Experience indicates that this potential source of error is not significant even when plastic deformation is greater than the small-scale yielding criteria of Test Method E 647 **(47)**.

A4. THE ECCENTRICALLY-LOADED SINGLE EDGE CRACK TENSION SPECIMEN

A4.1 Introduction

A4.1.1 The eccentrically-loaded single edge crack tension specimen ESE(T) can exhibit advantages over other specimen types. The following paragraphs lists possible advantages.

A4.1.2 The elongated (extended) design gives the experimenter additional working space compared to the standard compact tension C(T) specimen configuration. This configuration lends itself to attaching complex displacement or strain gage measurement systems and environmental cells (69).

A4.1.3 The specimen configuration requires lower applied forces for equivalent crack tip stress-intensity factor compared to other specimen configurations, such as the middle-crack tension M(T) specimen. This results in lower net section stress and reduces the likelihood of premature fracture of sheet materials tested in highly corrosive environments.

A4.1.4 The specimen design reduces the T-stress (stress parallel to crack surface) and crack fracture paths are more self-similar than in the standard C(T) specimen (70).

A4.1.5 The specimen design is compatible with common automated techniques for the measurement of through-the-thickness crack lengths.

A4.2 Specimen

A4.2.1 The standard ESE(T) specimen is a single edge-cracked specimen similar to the C(T) specimen loaded in tension - tension (71-73). The general proportions of this specimen configuration are given in Fig. A4.1.

A4.2.2 It is recommended that the ESE(T) specimen thickness be in the range $W/20 \leq B \leq W/4$.

A4.3 Apparatus

A4.3.1 Tension testing clevis and displacement gage apparatus are to be identical to that used by the C(T) specimen.

NOTE A4.1—The clevis pin is to be sized to 0.175W (+0.000, −0.025W).

A4.4 Procedure

A4.4.1 *Measurement*—Measure the width, *W*, and the crack length, *a*, from the specimen front face as shown in Fig. A4.1.

A4.4.2 ESE(T) *Specimen Testing*—All testing procedures are similar to the C(T) specimen.

A4.5 Calculations

A4.5.1 *Determination of Stress-Intensity Factor Range, ΔK*—For the ESE(T) specimen, calculate ΔK as follows (72).

$$\Delta K = [\Delta P/(B\sqrt{W})]\,F \qquad (A4.1)$$

and
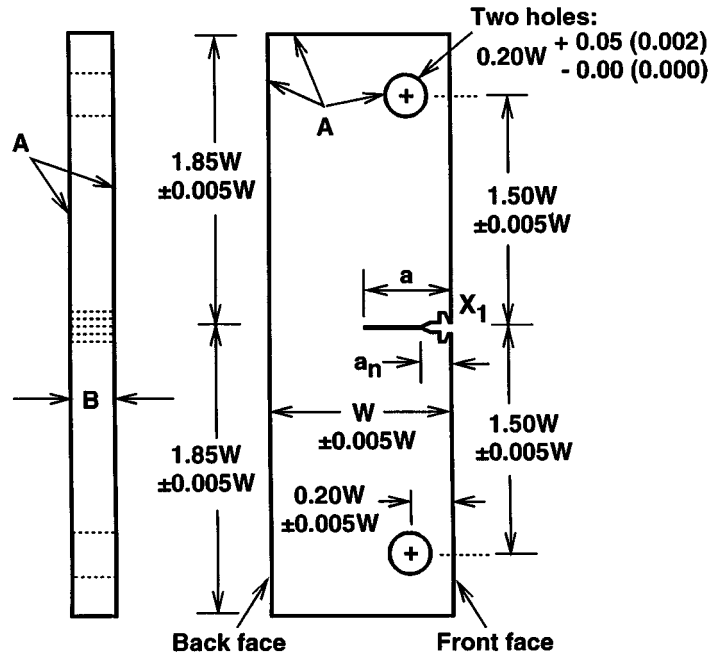
$$F = \alpha^{1/2}[1.4+\alpha][1-\alpha]^{-3/2}G \qquad (A4.2)$$

where

$$G = 3.97-10.88\alpha+26.25\alpha^2-38.9\alpha^3+30.15\alpha^4-9.27\alpha^5 \qquad (A4.3)$$

$$\alpha = a/W$$

for $0 < \alpha < 1$.

NOTE 1—Dimensions are in millimeters (inches).
NOTE 2—A-surfaces perpendicular and parallel (as applicable) to within ±0.002W, TIR.
NOTE 3—Intersection of the machined notch with the specimen face shall be equi-distant from top and bottom of the specimen to within 0.005W.
NOTE 4—Surface finish, including holes, shall be 0.8(32) or better.
FIG. A4.1 Standard Eccentrically-Loaded Single Edge Crack Tension Specimen.

A4.5.2 *Determination of Crack Length by Compliance*—The determination of crack length by the compliance method can be conducted at the ESE(T) front-face and back-face.

A4.5.2.1 *Front-face compliance*—The following expressions were derived for monitoring crack length by measuring the displacement (*v*) at the front face. The term v_0 is the displacement at location X_1 as shown in Fig. A4.1 (72, 74).

$$a/W = M_0 + M_1 U + M_2 U^2 + M_3 U^3 + M_4 U^4 + M_5 U^5 \quad (A4.4)$$

where:
$U \quad = \quad [(EBv_0/P)^{1/2}+ 1]^{-1}$
$M_0 \quad = \quad 1.00132$
$M_1 \quad = \quad -3.58451$
$M_2 \quad = \quad 6.599541$
$M_3 \quad = \quad -19.22577$
$M_4 \quad = \quad 41.54678$
$M_5 \quad = \quad -31.75871$
   for $0.1 \leq a/W \leq 0.84$.
   Normalized compliance in terms of crack length is given by

$$EBv_0/P = [15.52a/W - 26.38(a/W)^2 + 49.7(a/W)^3 - 40.74(a/W)^4 + \qquad (A4.5)$$

$$14.44(a/W)^5]/[1-a/W]^2$$

for $0 < a/W < 1$.
A4.5.2.2 *Back-face compliance*—The following expression

was derived for monitoring crack length by measuring strains at the back-face. Here, back-face strain, ϵ, is measured at a location along the crack plane similar to the C(T) specimen, shown in Fig. X2.1 of the standard.

$$a/W = N_0 + N_1 (\log A) + N_2(\log A)^2 +$$
$$N_3 (\log A)^3 + N_4 (\log A)^4 \qquad \text{(A4.6)}$$

where:
$A = -(\epsilon/P)BWE$
$N_0 = 0.09889$
$N_1 = 0.41967$
$N_2 = 0.06751$
$N_3 = -0.07018$

$N_4 = 0.01082$

for $0.1 \leq a/W \leq 0.84$.

A4.5.3 *Determination of Crack Length by Electrical Potential Difference*—Refer to Annex A3. Crack length determinations may be performed using the Johnson's equation **(59, 75)**. Typical electrical potential wire placement locations are similar to the C(T) specimen, refer to Fig. A3.3 of the standard.

NOTE A4.2—The Johnson equation, based on the electrostatic analysis of a finite width plate with an infinitesimally thin central slot, has been shown to give accurate results for M(T) specimens. Its use with the ESE(T) specimen configuration, however, must be experimentally verified.

APPENDIXES

(Nonmandatory Information)

X1. RECOMMENDED DATA REDUCTION TECHNIQUES

X1.1 Secant Method

X1.1.1 The secant or point-to-point technique for computing the crack growth rate simply involves calculating the slope of the straight line connecting two adjacent data points on the *a* versus *N* curve. It is more formally expressed as follows:

$$(da/dN)_{\bar{a}} = (a_{i+1} - a_i)/(N_{i+1} - N_i) \qquad \text{(X1.1)}$$

Since the computed da/dN is an average rate over the $(a_{i+1} - a_i)$ increment, the average crack length, $\bar{a} = \frac{1}{2}(a_{i+1} + a_i)$, is normally used to calculate ΔK.

X1.2 Incremental Polynomial Method

X1.2.1 This method for computing da/dN involves fitting a second-order polynomial (parabola) to sets of $(2n + 1)$ successive data points, where n is usually 1, 2, 3, or 4. The form of the equation for the local fit is as follows:

$$\hat{a}_i = b_0 + b_1\left(\frac{N_i - C_1}{C_2}\right) + b_2\left(\frac{N_i - C_1}{C_2}\right)^2 \qquad \text{(X1.2)}$$

where:

$$-1 \leq \left(\frac{N_i - C_1}{C_2}\right) \leq +1 \qquad \text{(X1.3)}$$

and b_0, b_1, and b_2 are the regression parameters that are determined by the least squares method (that is, minimization of the square of the deviations between observed and fitted values of crack length) over the range $a_{i-n} \leq a \leq a_{i+n}$. The value $\hat{a}_i$ is the fitted value of crack length at N_i. The parameters $C_1 = \frac{1}{2}(N_{i-n} + N_{i+n})$ and $C_2 = \frac{1}{2}(N_{i+n} - N_{i-n})$ are used to scale the input data, thus avoiding numerical difficulties in determining the regression parameters. The rate of crack growth at N_i is obtained from the derivative of the above

parabola, which is given by the following expression:

$$(da/dN)_{\hat{a}_i} = (b_1)/(C_2) + 2b_2(N_i - C_1)/C_2^2 \qquad \text{(X1.4)}$$

The value of ΔK associated with this da/dN value is computed using the fitted crack length, $\hat{a}_i$, corresponding to N_i.

X1.2.2 A Fortran computer program that utilizes the above scheme for $n = 3$, that is, 7 successive data points, is given in Table X1.1 (see Eq X1.1). This program uses the specimen *K*-calibrations given in 9.3 and also checks the data against the size requirements given in 7.2.

NOTE X1.1—It should be noted that the basic regression equations that are used to calculate da/dN can also be solved on a programmable calculator; thus large electronic computer facilities are not required to use this technique.

X1.2.3 An example of the output from the program is given in Table X1.3. Information on the specimen, loading variables, and environment are listed in the output along with tabulated values of the raw data and processed data. A(MEAS.) and A(REG.) are values of total crack length obtained from measurement and from the regression equation (Eq X1.2), respectively. The goodness of fit of this equation is given by the multiple correlation coefficient, MCC (note that MCC = 1 represents a perfect fit). Values of DELK (ΔK) and DA/DN (da/dN) are given in the same units as the input variables (for the example problem these are ksi $\sqrt{in.}$ and in./cycle, respectively). Values of da/dN that violate the specimen size requirement appear with an asterisk and note as shown in Table X1.3 for the final nine data points.

X1.2.4 The definition of input variables for the program and formats for these inputs are given in Table X1.4.

TABLE X1.1 Fortran Computer Program for Data Reduction by the Seven Point Incremental Polynomial Technique

```
  1*          DIMENSION A(200),N(200),EB(3),DADN(200),DELK(200),ID(7)
  2*          DIMENSION AA(10),NN(10)
  3*          REAL N
  4*          REAL NN
  5*          INTEGER GQ
  6*          INTEGER TYPE
  7*       10 FORMAT(/A6, 9H SPECIMEN,5X,2HB=,F6.3,5H IN. ,5X,2HW=,F6.3,5H IN.
  8*          * ,5X,3HAN=,F6.3,5H IN. )
  9*       15 FORMAT(1H1,' SEVEN POINT INCREMENTAL POLYNOMIAL METHOD FOR DETERMI
 10*          *NING DA/DN ')
 11*       17 FORMAT(/)
 12*       20 FORMAT(/6H PMIN=,F6.3,4HKIPS,5X,5HPMAX=,F6.3,4HKIPS,5X,2HR=,F6.3,5
 13*          *X,10HTEST FREQ=,F6.3,3HHZ.)
 14*       22 FORMAT(/7H TEMP.=,F4.0,1HF,5X,12HENVIRONMENT=,A15)
 15*       25 FORMAT (A6,9X,F5.1,F8.3,A6,9X)
 16*       30 FORMAT(6A6,A4,2I6)
 17*       35 FORMAT (////11H SPEC. NO.    , 6A6,A4,10X,14H NO.POINTS  = ,I3)
 18*       40 FORMAT(4 (F6.4, F9.0))
 19*       55 FORMAT(/8H CES.NO..  5X,6HCYCLES,11X,8HA(MEAS.),8X,7HA(REG.),9X,6HM
 20*          *.C.C.,14X,4HDELK,14X,5HDA/DN)
 21*       92 FORMAT(I4,9X,F8.0,7X,F8.3,8X,F8.3,8X,F8.6,11X,F8.2,12X,E8.3)
 22*       95 FORMAT(I4,9X,F8.0,7X,F6.3)
 23*       98 FORMAT(I4,9X,F8.0,7X,F8.3,8X,F8.3,8X,F8.6,11X,F8.2,12X,E8.3,2H *)
 24*       99 FORMAT(F6.3,F6.3,F6.1,F6.3,F6.3,F6.3)
 25*      200 FORMAT(////10H          )
 26*      300 FORMAT(/45H * - DATA VIOLATE SPECIMEN SIZE REQUIREMENTS )
 27*    C     TYPE=1 FOR CT AND 2 FOR A CCP
 28*      500 READ(5,30,END=1000) (ID(I),I=1,7),NPTS,TYPE
 29*          READ(5,99) PMIN,PMAX,F,Q,W,AM
 30*    C     KIND=CT,CCP,ETC.
 31*          READ (5,25) ENV,TEM,YS,KIND
 32*          READ(5,40)(A(I),N(I),I=1,NPTS)
 33*          PRINT 15
 34*          PRINT 35,(ID(II),II=1,7),NPTS
 35*          PRINT 10,KIND,B,W,AM
 36*          R=PMIN/PMAX
 37*          PRINT 20 ,PMIN,PMAX,R,F
 38*          PRINT 22 , TEM , ENV
 39*          PRINT 55
 40*          PRINT 200
 41*          DO 31 I=1,NPTS
 42*          A(I)=A(I) + AM
 43*       31 CONTINUE
 44*          K=0
 45*          PI=3.1416
 46*          PP=PMAX-PMIN
 47*          DO 110 I=1,3
 48*          PRINT 95,I,N(I),A(I)
 49*      110 CONTINUE
 50*          NPTS=NPTS-6
 51*          DO 100 I=1,NPTS
 52*          L=0
 53*          K=K+1
 54*          K1=K+6
 55*          DO 60 J= K,K1
 56*          L=L+1
 57*          AA(L) = A(J)
 58*          NN(L) = N(J)
 59*       60 CONTINUE
 60*          C1 = 0.5*(NN(1)+NN(7))
 61*          C2 = 0.5*(NN(7)-NN(1))
 62*          SX=0
 63*          SX2=0
 64*          SX3=0
 65*          SX4=0
 66*          SY=0
 67*          SYX=0
 68*          SYX2=0
 69*          DO 70 J=1,7
 70*          X = (NN(J)-C1)/C2
 71*          YY = AA(J)
 72*          SX = SX + X
 73*          SX2 = SX2 + X**2
 74*          SX3 = SX3 + X**3
 75*          SX4 = SX4 + X**4
 76*          SY = SY + YY
 77*          SYX = SYX + X*YY
 78*          SYX2 = SYX2 + YY*X**2
 79*       70 CONTINUE
 80*          DEN=7.0*(SX2*SX4-SX3**2)-SX*(SX*SX4-SX2*SX3)+SX2*(SX*SX3-SX2**2)
 81*          T2=SY*(SX2*SX4-SX3**2)-SYX*(SX*SX4-SX2*SX3)+SYX2*(SX*SX3-SX2**2)
 82*          EB(1) = T2/DEN
 83*          T3=7.0*(SYX*SX4-SYX2*SX3)-SX*(SY*SX4-SYX2*SX2)+SX2*(SY*SX3-SYX*SX2
 84*          *)
 85*          BB(2) = T3/DEN
 86*          T4=7.0*(SX2*SYX2-SX3*SYX)-SX*(SX*SYX2-SX3*SY)+SX2*(SX*SY)-SX2*SY)
 87*          B3(3) = T4/DEN
 88*          YB = SY/7.0
 89*          RSS = 0
 90*          TSS = 0
 91*          DO 75 J=1,7
 92*          X = (NN(J)-C1)/C2
 93*          YHAT = BB(1)+BB(2)*X+BB(3)*X**2
 94*          RSS = RSS+(AA(J)-YHAT)**2
 95*          TSS = TSS+(AA(J)-YB)**2
 96*       75 CONTINUE
 97*          R2 = 1.0-RSS/TSS
 98*          DADN(I) = BB(2)/C2 + 2.0*EB(3)*(NN(4)-C1)/C2**2
 99*          X=(NN(4)-C1)/C2
100*          AR=EB(1)+EB(2)*X+EB(3)*X**2
101*          S=1E+10
102*          SNET=0
103*          QQ=I+3
104*          GO TO(1,2) ,TYPE
105*        1 CONTINUE
106*          T = AR/W
107*          FT=((2+T)*(0.886+4.64*T-13.32*T**2+14.72*T**3-5.6*T**4))/(1-T)**1.
108*          *5
109*          S = YS*SQRT(PI*W*(1-T))/2
110*          GO TO 190
111*        2 CONTINUE
112*          T= 2*AR/W
```

26

TABLE X1.1 *Continued*

```
113*          SEC = 1.0/(COS(PI*T/2))
114*          FT = SQRT((PI*T*SEC)/2.0)
115*          SNET=PMAX/(D*W*(1-T))
116*    190   DELK(I)=(FT*FF)/(B*SQRT(W))
117*          AX=DELK(I)/(1-R)
118*          IF(AX.GE.S) GO TO 97
119*          IF(SNET.GE.YS)GO TO 97
120*     91   PRINT 92,QQ,N(QQ),A(QQ),AR,R2,DELK(I),DADN(I)
121*          GO TO 100
122*     97   PRINT 98,QQ,N(QQ),A(QQ),AR,R2,DELK(I),DADN(I)
123*    100   CONTINUE
124*          J=NPTS+4
125*          K=NPTS+6
126*          DO 120 I=J,K
127*          PRINT 95,I,N(I),A(I)
128*    120   CONTINUE
129*          PRINT 17
130*          PRINT 17
131*          PRINT 300
132*          GO TO 500
133*   1000   CALL EXIT
134*          END
```

TABLE X1.2 Example Output from Incremental Polynomial Computer Program

SEVEN POINT INCREMENTAL POLYNOMIAL METHOD FOR DETERMINING DA/DN

SPEC. NO. 1DN-9   NO. POINTS = 37

C(T) SPECIMEN   B= .250 IN.   W= 2.000 IN.   AN= .500 IN.

PMIN= 4.000KIPS   PMAX= 5.000KIPS   R= .800   TEST FREQ= .100HZ.

TEMP.= 75.F   ENVIRONMENT=   AIR

OBS.NO.	CYCLES	A(MEAS.)	A(RES.)	M.C.C.	DELK	DA/DN
1	0.	.539				
2	15480.	.631				
3	22070.	.656				
4	30240.	.674	.677	.996911	17.56	.323-05
5	36090.	.693	.698	.996347	18.03	.337-05
6	41370.	.718	.715	.995268	18.44	.337-05
7	46850.	.735	.736	.998739	18.83	.344-05
8	50090.	.746	.746	.998733	19.17	.345-05
9	54380.	.753	.760	.999740	19.53	.350-05
10	60320.	.781	.781	.999713	20.08	.382-05
11	65160.	.801	.801	.999411	20.60	.403-05
12	70240.	.821	.822	.999473	21.19	.433-05
13	74690.	.843	.842	.999461	21.76	.453-05
14	80070.	.865	.866	.999436	22.51	.480-05
15	83860.	.886	.885	.999299	23.11	.493-05
16	88080.	.906	.906	.999176	23.75	.517-05
17	91460.	.925	.924	.999120	24.41	.545-05
18	95620.	.945	.946	.999483	25.21	.583-05
19	99000.	.967	.967	.999173	25.99	.611-05
20	102360.	.988	.988	.998500	26.84	.623-05
21	105110.	1.008	1.006	.997105	27.58	.668-05
22	108440.	1.028	1.028	.997266	28.55	.693-05
23	111660.	1.047	1.051	.997266	29.60	.741-05
24	113410.	1.067	1.064	.997552	30.23	.759-05
25	116810.	1.090	1.091	.996303	31.65	.843-05
26	118730.	1.108	1.108	.995912	32.55	.898-05 *
27	121220.	1.128	1.130	.998627	33.91	.105-04 *
28	121880.	1.138	1.137	.998593	34.32	.111-04 *
29	122830.	1.148	1.148	.998087	35.00	.114-04 *
30	124280.	1.166	1.166	.999287	36.20	.127-04 *
31	125820.	1.187	1.185	.999156	37.54	.134-04 *
32	127460.	1.207	1.208	.992990	39.20	.165-04 *
33	128700.	1.226	1.227	.994644	40.79	.201-04 *
34	129760.	1.245	1.249	.977629	42.69	.279-04 *
35	130790.	1.277				
36	131480.	1.298				
37	131550.	1.323				

* - DATA VIOLATE SPECIMEN SIZE REQUIREMENTS

TABLE X1.4 Definition of Input Variables for Fortran Program

Input Card	Program Line	Fortran Code	Variable Definition	Card Columns	
1	28	ID(I)	Specimen identification, for example Specimen number, heat number, material	1–40+	
	28	NPTS	Number of paired (a, N) data points	40–46*	
	26	TYPE	TYPE = 1 for C(T) specimen TYPE = 2 for M(T) specimen	47–52*	
2	29	PMIN	Minimum load, P_{min}, in kips	1–6°	
	29	PMAX	Maximum load, P_{max}, in kips	7–12°	
	29	F	Test frequency	13–18°	
	29	B	Specimen thickness, B	19–24°	
	29	W	Specimen width, W	25–30°	
	29	AM	Machine notch length, a_n	31–36°	
3	31	ENV	Test environment	1–6+	
	31	TEM	Test temperature, F	7–11°	
	31	YS	0.2 % yield stress of specimen	12–19°	
	31	KIND	Specimen type, that is C(T) or M(T)	20–25+	
4,5,6,etc.	32	A(I)	Crack length, a, measured from machine notch, a_n	A(1) 1–6°	
	32	N(I)	Elapsed cycles, N	A(2) 16–21°	
				N(2) 22–30°	
				A(3) 31–36°	4 paired (a, N) data
				N(3) 37–45°	points per card
				A(4) 46–51°	
				N(4) 52–60°	
				A(5) 1–6°	
				N(5) 7–15°	next card
				etc.	

Key
+ alphanumeric
* integer, entered to far right of available columns
° use decimal point

X2. RECOMMENDED PRACTICE FOR DETERMINATION OF FATIGUE CRACK OPENING LOAD FROM COMPLIANCE

X2.1 Introduction

X2.1.1 The term *crack closure* refers to the phenomenon whereby the fracture surfaces of a fatigue crack come into contact during the unloading portion of a load cycle and load is transferred across the crack. In many materials, crack closure can occur while the load is above the minimum load in the cycle even when the minimum load is tensile. Upon reloading from minimum load, some increment of tensile loading must be applied before the crack is again fully open. Thus, crack closure provides a mechanism whereby the effective cyclic stress intensity factor range near the crack tip (ΔK_{eff}) differs from the nominally applied value (ΔK). Therefore, information on the magnitude of the crack closure effect is essential to understand and interpret observed crack growth behavior. An estimate of ΔK_{eff} can be obtained experimentally by determining the minimum load at which the crack is open (opening load, P_o) and, if $P_o > P_{min}$, using the effective load range ($\Delta P_{eff} = P_{max} - P_o$) in expressions for the stress intensity factor range instead of load range ($\Delta P = P_{max} - P_{min}$).

X2.1.2 Many experimental techniques have been used to determine the opening load. These techniques have included the use of ultrasonics, potential drop, eddy current, acoustic emission, high magnification photography, and strain or displacement versus load (compliance) measurements. Due mainly to its experimental simplicity, the compliance technique has become the most widely used approach.

X2.2 Scope

X2.2.1 This appendix covers the experimental determina-tion of fatigue crack opening load in tests of the compact tension, C(T), or middle tension, M(T), specimens subjected to constant amplitude or slowly changing (similar to load shedding rates recommended in this test method for threshold tests at constant load ratio) loading.

X2.3 Terminology

X2.3.1 Definitions of terms specific to this appendix are given in this section. Other terms used in this appendix are defined in the main body of this test method.

X2.3.2 *Definitions*:

X2.3.2.1 *crack closure*—in fatigue, the phenomenon whereby the fracture surfaces of a fatigue crack come into contact during the unloading portion of a load cycle and load is transferred across the crack.

X2.3.2.2 *effective load range*, ΔP_{eff} [F]—in fatigue, that part of the increasing-load range of the cycle during which the crack is open. The effective load range is expressed as:

$$\Delta P_{eff} = P_{max} - P_o \quad \text{if} \quad P_o > P_{min}, \text{and} \quad (X2.1)$$

$$\Delta P_{eff} = \Delta P = P_{max} - P_{min} \quad \text{if} \quad P_o < \text{or} = P_{min} \quad (X2.2)$$

X2.3.2.3 *effective stress intensity factor range*, ΔK_{eff} [$FL^{-3/2}$]—in fatigue, the stress intensity factor range computed using the effective load range, ΔP_{eff}.

X2.3.2.4 *opening load, P_o* [F]—in fatigue, the minimum load at which the fatigue crack is open at the tip during the increasing-load part of a cycle.

X2.4 Significance and Use

X2.4.1 The method of determining crack opening load, and

therefore of estimating ΔK_{eff}, presented in this appendix should be useful in assessing and comparing the effects of crack closure on the crack growth behavior of various materials. The method does not define the exact portion of the applied ΔK that is effective in growing the crack nor the exact values of the opening load at all points along the crack front, but does provide a well-defined operational approach that can be used to estimate the first-order effects of closure.

X2.4.2 Measurements of opening load made using this procedure can serve as reference or benchmark values that can be used in evaluating crack closure information from different sources and from other experimental techniques.

X2.5 Basis for Determination of Opening Load From Compliance

X2.5.1 The determination of opening load from compliance is based on the observation that when a cracked specimen is loaded up to the load at which the crack becomes fully open, the compliance (slope of the strain or displacement against load curve) attains a characteristic value and remains essentially constant upon further load increase until the load is increased enough to cause large-scale yielding near the crack tip. Upon unloading from the maximum load in a cycle, the compliance again has the characteristic value for the fully-open crack regardless of whether large-scale yielding occurred before maximum load was achieved. Conceptually, the experimental task is very simple—determine the load at which the strain or displacement against load curve becomes linear (analogous to the determination of proportional limit in a tensile test). However, in practice, this task is very difficult due to the gradual change in compliance as it approaches the open-crack value and to the nonlinearity and variability, or *noise*, in the compliance data. Nonlinearity and noise in the measurement system can cause significant variation in the estimates of opening load.

X2.5.2 One way to reduce scatter in opening load results due to noise and nonlinearity in the measurement system is to define opening load as the load corresponding to a compliance that is offset from (lower than) the fully-open-crack value rather than the load at which the compliance attains the fully-open value (that is, the point where the curve becomes linear). The scatter will be reduced because the offset compliance value corresponds to a position on the loading curve where a change in compliance is associated with a smaller change in load than would be the case for a position very near the start of the linear part of the curve. Of course, with the offset compliance approach, the opening loads determined will be somewhat lower than the load at which the crack becomes fully open. Selection of an appropriate compliance offset criterion then becomes a trade-off between achieving a reduction in scatter and minimizing the deviation of the compliance-offset opening load from the load at which the crack becomes fully open. Some information on this trade-off is given in Ref **(76)**.

X2.6 Apparatus

X2.6.1 The procedure requires a strain or displacement transducer which can be mounted on the specimen and a digital data acquisition and processing system capable of acquiring data from the testing machine load cell and the strain/displacement transducer.

X2.6.2 The requirements for the strain/displacement transducers and other experimental apparatus are, in general, the same as that specified in Annex A2 for using compliance to determine crack length. However, the requirement for high quality (good linearity and low noise) strain/displacement data is especially critical in measuring opening load using the compliance procedure. Accordingly, an accept/reject criterion for data quality is described in X2.8.

X2.6.3 The location of the strain or displacement measurement may be near the crack tip or remote from the tip. However, for tests within the scope of this appendix, remote measurements are recommended because they are experimentally simpler and are likely to be more repeatable than near-tip measurements. For the C(T) specimen, the recommended measurements are: (*1*) displacement across the crack mouth, and (*2*) strain at the mid-height location on the back face. For the M(T) specimen, the recommended measurement is displacement across the crack on the longitudinal centerline (see Fig. X2.1).

X2.7 Recommended Procedure—Determination of Opening Load by the Compliance Offset Method

X2.7.1 Background information on the rationale for using this method can be found in Refs **(76)** and **(77)**. The step-by-step procedure for determining opening load from strain or displacement against load data is as follows:

X2.7.1.1 Collect digitized strain/displacement and load data for a complete load cycle. The data sampling rate should be high enough to ensure that at least one data pair (displacement and load) is taken in every 2 % interval of the cyclic load range for the entire cycle. (Different loading waveforms require different minimum sampling rates to ensure that one point is taken in every 2 % interval.)

X2.7.1.2 Starting just below maximum load (not less than 0.90 maximum load) on the unloading curve, fit a least-squares straight line to a segment of the curve that spans a range of approximately 25 % of the cyclic load range. The slope of this line is assumed to be the compliance value that corresponds to the fully-open crack configuration.

NOTE X2.1—**Caution:** For some materials and loading conditions that produce high opening loads, this assumption may not be correct. The opening load may actually lie within the fitted load range, and in that case,
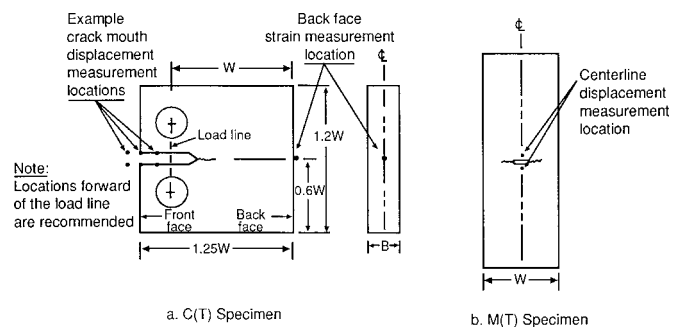

a. C(T) Specimen

b. M(T) Specimen

FIG. X2.1 Recommended Displacement and Strain Measurement Locations for Determination of Fatigue Crack Opening Load on C(T) and M(T) Specimens

X2.7.1. Using the compliance offset values for the increasing load portion of the load cycle, compute the mean of the compliance offset values and the standard deviation of the offset values about the mean. For a perfectly linear noise-free measurement system, the mean and standard deviation of the offsets should be zero. If the absolute value of the mean of the measured offsets (expressed as percentages of the open-crack compliance) is greater than 1 % or the standard deviation of the offsets is greater than 2 %, the quality of the data is considered unacceptable for the determination of opening load using the compliance offset method. If data quality is not acceptable, the user should check for problems with transducer linearity (see A2.4), specimen flatness, load train alignment (see 6.3), gripping arrangement (see 6.1, 6.2, and A2.5), and noise on the transducer signals (see X2.7.1.5).

X2.9 Report

X2.9.1 The following information should be reported along with all reported measurements of opening load:

X2.9.1.1 The location of the strain or displacement measurement on the specimen and the transducer used to make the measurement.

X2.9.1.2 The value of the compliance offset criterion used in defining opening loads.

X2.9.1.3 The values of the mean and standard deviation of compliance offsets measured on the uncracked specimens.

X2.9.1.4 Typical plots of load against compliance offset for an uncracked specimen and a cracked specimen.

X2.9.1.5 Specimen thickness.

X2.9.1.6 A summary of the fatigue loading conditions prior to the opening load measurements.

X3. GUIDELINES FOR MEASURING THE GROWTH RATES OF SMALL FATIGUE CRACKS

X3.1 Introduction

X3.1.1 Fatigue cracks of relevance to many structural applications are often small or short for a significant fraction of the structural life. The growth rates of such cracks usually cannot be measured with the standard procedures described in the main body of Test Method E 647, which emphasizes the use of large, traditional fracture mechanics specimen geometries. Of greater importance, the growth behavior of these small cracks is sometimes significantly different from what would be expected based on large-crack growth rate data and standard fatigue crack growth analysis techniques. Direct measurement of small-crack growth rates may be desirable in these situations.

X3.1.2 This appendix provides general guidelines for test methods and related data analysis techniques to measure the growth rates of small fatigue cracks. Complete, detailed test procedures are not prescribed. Instead, the appendix provides general guidance on the selection of appropriate experimental and analytical techniques and identifies aspects of the testing process that are of particular importance when fatigue cracks are small.

X3.1.3 Many of the principles and procedures described in the main body of Test Method E 647 are applicable to small fatigue cracks, and their use is encouraged unless otherwise noted here. Several aspects of Test Method E 647 that should be modified for small cracks are highlighted in this appendix.

X3.2 Scope

X3.2.1 This appendix describes the determination of fatigue crack growth rates in metallic materials for crack sizes that are too small to permit application of the standard methods described in the main body of Test Method E 647. A variety of possible specimen geometries and crack length measurement techniques are introduced.

X3.3 Referenced Documents

E 4 Practices for Force Verification of Testing Machines[3]

E 466 Practice for Conducting Constant Amplitude Axial Fatigue Tests of Metallic Materials[3]

E 467 Practice for Verification of Constant Amplitude Dynamic Loads on Displacements in an Axial Load Fatigue Testing System[3]

E 606 Practice for Strain-Controlled Fatigue Testing[3]

E 616 Terminology Relating to Fracture Testing[3]

E 1351 Practice for Production and Evaluation of Field Metallographic Replicas[3]

X3.4 Terminology

X3.4.1 The terms used in this appendix are given in the main body of Test Method E 647 and in the other terminology documents referenced in X3.3.

X3.4.2 *Descriptions of Terms Specific to This Standard*:

X3.4.2.1 *small crack*—a crack is defined as being small when all physical dimensions (in particular, both length and depth of a surface crack) are small in comparison to a relevant microstructural scale, continuum mechanics scale, or physical size scale. The specific physical dimensions that define *small* vary with the particular material, geometric configuration, and loadings of interest.

X3.4.2.2 *short crack*—a crack is defined as being short when only one physical dimension (typically, the length of a through-crack) is small according to the description of X3.4.2.1.

NOTE X3.1—Historically, the distinction between *small* and *short* cracks delineated here has not always been observed. The two terms have sometimes been used interchangeably in the literature, and some authors (especially in Europe) employ the term *short crack* to denote the meaning given here to *small crack*.

X3.4.2.3 *surface-crack length*—see Terminology E 616. In this appendix, physical surface-crack length is represented as 2c.

X3.4.2.4 *surface-crack depth*—see **crack depth** in Terminology E 616. In this appendix, the physical surface-crack

31

TABLE X3.1 Classification and Size Guidelines for Small Fatigue Cracks (adapted from 84)

NOTE 1—a here denotes a characteristic crack dimension (length or depth).
r_y is plastic zone size or plastic field of notch.
d_g is characteristic microstructural dimension, often grain size.

Type of Small Crack	Dimension
Mechanically-small	$a \sim\, \leq r_y$
Microstructurally-small	$a \sim\, \leq$ 5–10 d_g
Physically-small	$a \sim\, \leq$ 1 mm
Chemically-small	a up to ~10 mm

depth is represented as a.

X3.5 Significance and Use

X3.5.1 *The Small-Crack Effect*:

X3.5.1.1 Small fatigue cracks can be particularly important in structural reliability because of the so-called *small-crack effect*, the observation that small cracks sometimes grow at rates that are faster than long fatigue cracks at the same nominal crack driving force (typically expressed as ΔK). The reasons for this effect, the circumstances under which it will occur, and the proper means of rationalizing it analytically have been studied and discussed extensively (**78-84**), although full consensus has not been reached on all major issues.

X3.5.1.2 The effect is most often observed when the crack size is on the order of a characteristic microstructural dimension, such as the grain size, or a characteristic continuum mechanics dimension, such as the crack-tip or notch plastic zone size. In the former case, enhanced or reduced crack growth rates arise from interactions with the local microstructure that do not occur when total crack sizes and crack-tip process zones are relatively large. In the latter case, the variation in growth rates may arise from a fundamental change (that is, an increase) in the crack driving force due to enhanced plastic deformation that is not reflected in the usual small-scale-yielding parameter ΔK. Small-crack effects can also arise from other phenomena, such as alterations in localized crack chemistry and the associated kinetics of environmentally-assisted fatigue crack growth.

X3.5.1.3 It is often of practical importance to estimate the crack size below which data from small- and large-crack tests tend to differ. Different criteria (**85**) have been proposed for this dimension depending on the particular type of small crack, as summarized in Table X3.1. A crack which satisfies any one (or more) of these dimensional criteria may exhibit small-crack behavior.

X3.5.1.4 Another approach to identification of the small-crack regime follows from the original work of Kitagawa and Takahashi (**86**) which showed that threshold crack growth rate data display a dependence on crack size that is related to the material's fatigue limit (ΔS_e) and ΔK_{th}. This idea, which combines fatigue crack initiation and propagation concepts, is illustrated schematically in Fig. X3.1. Considering crack initiation, and disregarding the possibility of a pre-existing crack, specimen failure should occur only if

$$\Delta S_{applied} > \Delta S_e \qquad (X3.1)$$

Alternatively, considering a fracture mechanics approach, crack growth should occur only if

$$\Delta K_{applied} > \Delta K_{th} = F\Delta S\sqrt{\pi a} \qquad (X3.2)$$

where F is a function of crack and specimen geometry and a is the crack length. Solving this equation for ΔS gives

$$\Delta S = \frac{\Delta K_{th}}{F\sqrt{\pi a}} \qquad (X3.3)$$

indicating that crack propagation should only occur in the region above the line of slope equal to $-1/2$. Thus, the utility of ΔK_{th} as a *material property* appears to be limited to cracks of length greater than that given by the intersection of the two lines (a_0). For many materials, a_0 appears to give a rough approximation of the crack size below which microstructural small-crack effects become potentially significant (**87**). Note, however, that a_0 may underestimate the importance of small-crack effects when crack wake closure or localized chemistry dominates the geometry effect on crack growth rates. Further discussion of this construction and its limitations is available in (**88**).

X3.5.1.5 An important manifestation of the small-crack effect is that physically small cracks may grow at ΔK values below the measured large-crack threshold stress-intensity factor range, ΔK_{th}, even when the small cracks are large compared to the microstructure and small-scale-yielding parameters appear to adequately describe the crack driving force. It is not entirely clear if this phenomenon indicates anomalous small-crack behavior or anomalous large-crack behavior. These small-crack growth data are often consistent with the large-crack data if the near-threshold large-crack data are neglected and if large-crack data are determined so as to minimize the effects of crack closure. In any case, the phenomenon is significant because predictions of small-crack growth in engineering structures based on laboratory large-crack (near-threshold) data may be extremely nonconservative. It is not clear if a measurable threshold exists for the growth of small fatigue cracks, although small cracks are sometimes observed to become nonpropagating.

X3.5.1.6 Structural applications in which small fatigue cracks are significant may involve applied stresses that approach or exceed the yield strength of the material. Characterization of the material resistance to stable cyclic crack growth under these conditions may require laboratory testing at similar applied stresses. These tests are not valid by the criteria of the main body of Test Method E 647 (see Specimen Configuration, Size, and Preparation), since the specimen is not predominantly elastic at all values of applied load. The basic techniques described in this appendix for performing the test, measuring crack length, and computing the crack growth rate are largely applicable, although a modified specimen design may be
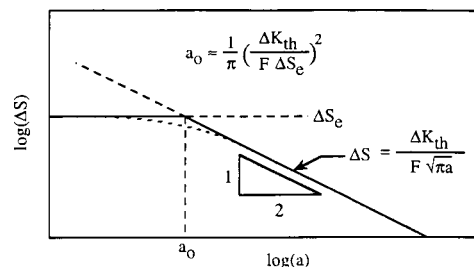

FIG. X3.1 Diagram for Estimating a_o

required. Alternative elastic-plastic formulations of the correlating parameter for fatigue crack growth rates, such as the range of the *J*-integral (ΔJ), may be required under these conditions **(89)**. Changes in crack closure behavior, which may further influence the crack driving force, may also be significant at larger applied stresses.

X3.5.2 *Choice of a Test Method*:

X3.5.2.1 Several well-established experimental techniques are available for measuring the growth rates of small fatigue cracks and for characterizing other important aspects of small-crack behavior. Some are more amenable than others for routine use, and some require significant expertise. Some require almost no financial investment, while others may require substantial expenditures. All are useful for measuring the growth of fatigue cracks sized on the order of 50 µm or greater, and some are applicable to even smaller cracks.

X3.5.2.2 It is not the purpose of this appendix to recommend one particular measurement technique to the exclusion of the others. Each technique has unique strengths and limitations, and different techniques are optimum for different circumstances. This appendix introduces the various methods available, highlights relative advantages and disadvantages, and discusses in more detail the procedural issues that are common to all methods.

X3.5.2.3 These techniques are described in detail in an ASTM Special Technical Publication, STP 1149 **(80)**. That publication and related references should be consulted for further information before a specific testing program is devised. Descriptions of other small fatigue crack experimental and analytical investigations are available in **(81-84)**.

X3.5.3 *Specific Test Methods Available*:

X3.5.3.1 *Replication* **(90)**—While fatigue cycling is interrupted and a static load is applied to the specimen, a small piece of thin cellulose acetate sheet is softened with acetone, gently applied to the specimen surface, and allowed to dry for a few minutes. The acetate replica forms a permanent record of the surface topography, including the crack mouth, and is subsequently viewed in an optical or (with appropriate replica processing) scanning electron microscope to measure surface crack length. See also Practice E 1351.

X3.5.3.2 *Photomicroscopy* **(91)**—To implement photomicroscopy (PM), a 35-mm camera with bulk film capability is linked to a standard metallurgical microscope and interfaced with the fatigue test frame via a microcomputer. An extensive series of high magnification photographs of the small fatigue crack is obtained during brief interruptions of cycling. Following the test, the crack photographs are projected on a computer digitizing tablet for crack length measurement.

X3.5.3.3 *Potential Difference* **(92)**—The direct current electric potential difference (dcEPD) method for continuous in-situ monitoring of crack growth (see Annex A3 to Test Method E 647) can be extended to small fatigue cracks. Closed-form analytical models are available to relate crack size to measured potential, as a function of crack shape and probe position locally spanning the crack mouth.

X3.5.3.4 *Ultrasonic* **(93)**—A surface acoustic wave (SAW) technique involves excitation of Rayleigh waves on the surface of a specimen and the automated data acquisition of the reflected echo from a small surface crack. A simple analytical model relates the echo amplitude to crack size.

X3.5.3.5 *Laser Interferometry* **(94)**—A computerized, laser-based, interferometric strain/displacement gage (ISDG) is used to monitor the relative displacement between two tiny indentations placed across small surface cracks. Estimates of crack sizes are obtained from measurements of elastic compliance.

X3.5.3.6 *Scanning Electron Microscopy* **(95)**—A small specimen is cycled on a specialized fatigue loading stage located inside the scanning electron microscope (SEM), and appropriate photographs or videotapes are taken as desired. Stereoimaging can be used to obtain high resolution displacement measurements on the specimen surface.

X3.5.3.7 *Constant K_{max}-Decreasing ΔK Method* **(96)**—The application of a constant K_{max}-decreasing ΔK load history to a standard (large-crack) FCG specimen has been proposed as a relatively rapid, simple means of minimizing the effects of crack closure. Based on the assumption that small cracks are distinguished from large cracks primarily in terms of reduced closure levels, it has been argued that the method generates an upper bound estimate to small-crack growth rates. This technique cannot address other aspects of the small-crack effect, such as microstructural interactions, extensive crack-tip plasticity, or near-surface residual stresses. This technique is addressed by the main body of Test Method E 647.

X3.5.4 *Comparative Remarks about Test Methods*:

X3.5.4.1 *Crack Location*—The replica technique is preferable when the location of crack initiation cannot be predicted with certainty. A chronological series of replicas can be used to track crack growth in reverse time from a large, easily found crack to its origins as a tiny, difficult-to-find microcrack. All other methods generally require a small crack to be located at an early stage of growth (perhaps by replication), or require the location of the crack to be fixed in advance with a micronotch.

X3.5.4.2 *Specimen and Crack Geometries*—The direct optical or imaging (PM, ISDG, SEM) and SAW techniques require specimen surfaces that are either flat or gently curved. The replica and dcEPD methods can be used on a wider variety of specimens, including cylindrical or notched geometries. Replica, PM, and SEM methods provide information on surface crack length only, while the ISDG, SAW, and dcEPD measurements give information about crack depth or cracked area. All methods require independent confirmation of crack shape to complete a crack growth analysis. The ISDG, SAW, and dcEPD information can be corrupted by the presence of multiple cracks.

X3.5.4.3 *Test Environments*—Replication is difficult to apply in any environment other than room temperature lab air unless the test is interrupted and the specimen is temporarily separated from the environment. Crack growth in high temperature or aggressive environments is probably best addressed by dcEPD. SEM, ISDG, PM, and SAW can be used, in principle, at elevated temperatures, although additional specialized equipment may be required, and some limitations may remain. The replication process has been shown to influence crack growth rates artificially in some materials, perhaps related to environmental effects. Small-crack tests in the SEM must be performed in vacuum, which may influence crack

behavior if ambient environmental effects are significant.

X3.5.4.4 *Resolution*—The SEM technique gives the highest resolution of surface crack length, followed by replication with a resolution on the order of 0.1 μm. The PM and ISDG methods both claim resolutions on the order of 1 μm. The average crack depth resolution of dcEPD is slightly lower, and the SAW technique perhaps the lowest (on the order of several microns). These are only general, comparative guidelines. The specific resolution attained can be influenced by the quality of the equipment, the experience of the investigators, and the material under investigation. The values given above are based on the work of specialists for each technique. Also note that "resolution" can have different meanings in different applications: for example, direct resolution of surface crack length vs. average resolution of crack depth from model calculations of some measured quantity.

X3.5.4.5 *Cost*—The replica technique involves minimal equipment cost but is extremely labor-intensive and time-consuming. The SEM and ISDG approaches require expensive and highly specialized equipment and relatively highly trained operators. PM, dcEPD, and SAW techniques require some specialized but relatively inexpensive equipment and may be automated to reduce labor and clock time.

X3.6 Apparatus

X3.6.1 Specimens used to measure the growth rates of small fatigue cracks (X3.7.1) are usually different from standard geometries established for long fatigue crack testing or other fatigue and fracture studies addressed by ASTM standard practices. Because nonstandard specimens and test practices are employed, it is especially important to ensure that basic concerns about specimen fixturing and load frame preparation are given appropriate attention. Specimen fixtures should grip the ends securely, minimize backlash if negative stress ratios are imposed, transmit load to the specimen uniformly, and prevent crack formation at the grips. The test frame should be properly aligned and the load cell properly calibrated. Specific recommendations on some of these issues are contained in the main body of Test Method E 647 and in Practices E 4, E 466, E 467, and E 606.

X3.6.2 Some small-crack specimen geometries become asymmetric as the crack grows (for example, the corner crack specimen in X3.7.1.4), and the resulting bending moment imposed on the specimen depends on the nature and rigidity of the fixturing. Special caution should be taken to minimize and/or characterize the rotation of the fixturing.

X3.6.3 Nearly all small-crack length measurement techniques (X3.5.3) require additional specialized apparatus such as advanced electronic instrumentation, microscopes, or other devices. This apparatus must be recognized as the source of potential measurement error or artificial influence on crack growth rates. Careful attention must be given to appropriate equipment calibration and verification of proper operation before commencing small-crack testing. The sensitivity or precision of any equipment that directly influences the quantitative measurement of crack length should be determined and reported.

X3.7 Specimen Configuration and Preparation

X3.7.1 *Specimen Design*:

X3.7.1.1 The study of small fatigue cracks requires detection of crack initiation and growth while physical crack sizes are extremely small, and this requirement influences specimen design. Several different small- or short-crack test specimens have been developed to obtain fatigue crack growth rate data. Some of the early specimens were prepared by growing large cracks, interrupting the test, and machining away some of the specimen material to obtain a physically short crack. However, the preferred (and most widely used) specimens promote the initiation of naturally small surface or corner cracks. The early detection of these cracks can be facilitated by using specimens with very small machined starter notches or specimens with mild stress concentrations. Some recommended small-crack specimens are shown schematically in Fig. X3.2.

X3.7.1.2 The rectangular surface-crack specimen, Fig. X3.2(a), is subjected to either remote tension or bending loads. To localize the crack initiation site(s) for the convenience of crack monitoring, three-point bending can be used to confine the maximum outer fiber stress to a small region. Alternatively, a reduced section with a mild radius can be used to localize initiation sites under remote tension (**91**). Note that although localization by either means is convenient, it may also influence the behavior of naturally initiated cracks due to sampling effects (for example, worst-case effects may not be observed due to biasing of the initiation location).

X3.7.1.3 The cylindrical surface-crack specimen, Fig. X3.2(b), may be identical to a traditional axial fatigue specimen. This geometry may be particularly useful to avoid crack formation at specimen corners or for testing at large stress ranges. Cracks may be initiated naturally or from a small notch machined on the surface.

X3.7.1.4 The corner-crack specimen, Fig. X3.2(c), was developed to simulate geometries encountered in critical locations in engine discs (**97, 98**). The small corner crack is introduced into the specimen by electrical-discharge machining a small corner notch into one edge. This specimen has the advantage that both crack length (*c*) and crack depth (*a*) can be monitored by either visual or photographic means.

X3.7.1.5 The specimen with a surface or corner crack at a semi-circular edge notch, Fig. X3.2(d), was developed to produce naturally-occurring cracks at material defects and to propagate cracks through a three-dimensional stress field
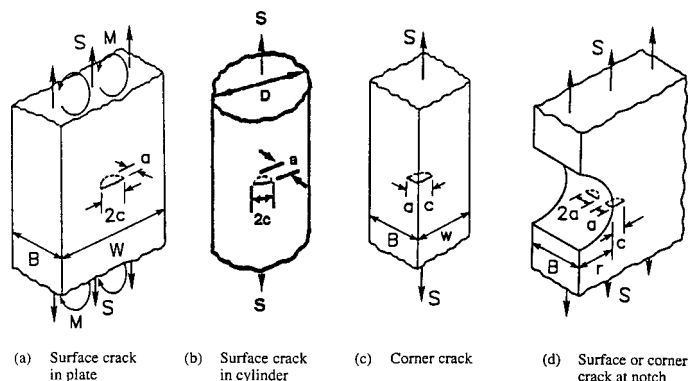

(a) Surface crack in plate   (b) Surface crack in cylinder   (c) Corner crack   (d) Surface or corner crack at notch

FIG. X3.2 Schematic of Commonly Used Small Crack Specimens

similar to that encountered at bolt holes in structures (99).

X3.7.2 *Crack Initiation Sites*:

X3.7.2.1 Small artificial flaws can be introduced into a specimen through methods such as electrical discharge machining or thin wafer cutoff wheels. These methods may disturb the material ahead of the resulting notch, and require precracking past the distressed zone before the onset of data acquisition. In order to eliminate mechanical notch effects, the length of the precrack region should be at least twice that of the notch tip radius.

X3.7.2.2 The specimen geometries used for naturally-occurring small fatigue cracks (X3.7.1.2) are designed to localize the crack initiation region within a small area, which allows for crack monitoring methods such as replication or microphotography to be used. These natural small cracks will typically initiate at inclusion particles, voids, scratches, or deformation bands. To ensure that cracks initiate in these intended regions, it is recommended that the corners of the specimens be deburred to suppress corner initiation. This type of specimen permits the acquisition of meaningful fatigue crack growth data immediately after first crack detection.

X3.7.3 *Surface Preparation*:

X3.7.3.1 Near-surface residual stresses and surface roughness induced by specimen machining can artificially influence small-crack growth behavior and should be eliminated prior to testing. However, it should be recognized that the growth rates of small surface cracks in engineering components may be influenced by residual stress fields arising from fabrication of the component, and this may have implications for the application of the laboratory small-crack data.

X3.7.3.2 Electrical discharge machining and low stress grinding are the preferred machining methods since they have been found to produce significantly lower residual stresses than mechanical milling (91). If mechanical milling is employed, it should be followed by a low stress grinding operation.

X3.7.3.3 Surface polishing techniques are used to remove the residual stresses and surface roughness induced by the machining process, and to provide a reflective finish adequate for accurate crack length measurements if visual techniques are employed. The two recommended techniques for surface polishing are electropolishing and chemical polishing (90, 91). Both methods typically require a surface finish equivalent to 500 grit SiC or better before polishing is initiated. Hand polishing with abrasive media until a desired surface finish is achieved may also be used, but this procedure produces residual stresses and should be followed by either a chemical etching or electro-etching procedure to remove the affected material.

X3.7.3.4 Chemical or ion etching of the specimen surface prior to testing may facilitate identification of microstructural influences on crack behavior when optical or imaging methods are employed to measure crack length. In some materials, however, an etch may confound clear identification of the crack tip location or even remove key microstructural features from which small cracks naturally initiate. Etching after a naturally-initiated crack has been located may be preferable in some cases, although chemical etching in this case may influence subsequent crack growth.

X3.8 Procedure

X3.8.1 The detailed procedure for conducting small-crack experiments is test method-specific, and extended discussion of suggested practices for the methods discussed in X3.5.3 is found in (80). Procedural issues of general applicability are outlined below.

X3.8.2 *Crack Size and Geometry*—Because the initiation and growth of small fatigue cracks are often dominated by local microstructural and geometric features, it is important that small-crack test specimens simulate actual applications in terms of microstructure, heat treatment, surface finish, and residual stress state, as well as crack size and geometry. The range of crack sizes to be investigated and the crack geometry of interest may have a significant impact on the selection of a test method. For example, the smallest of cracks must be naturally initiated, which precludes the use of artificial crack starters that predetermine the point of crack initiation. Although the absolute minimum detectable crack size may be of scientific interest, data to be used in life predictions of engineering structures may have a practical minimum crack size that is dictated by the limits of available, or foreseeable, methods of nondestructive inspection. Crack sizes in this range tend to be more amenable to study by a variety of experimental techniques.

X3.8.3 *Stress Level and Stress Ratio*—Selection of the stress level and stress ratio for testing are important considerations, and have numerous ramifications, both experimentally and analytically. For many materials, nominal maximum stresses of the order of 0.6 times the material yield strength (σ_{YS}) will facilitate natural initiation of a small number of cracks in a relatively short time, and the nominally elastic stress state permits a traditional fracture mechanics analysis to be used. Maximum stress levels approaching or exceeding σ_{YS} tend to produce multiple cracks, and the associated analysis must deal with the accompanying extended plastic deformation. Moreover, the stress ratio chosen may dramatically influence the time required to naturally initiate cracks. Ultimately, decisions regarding stress level and stress ratio may be dictated by the intended application for the data.

X3.8.4 *Crack Length Measurements*:

X3.8.4.1 To document crack growth events adequately at the smallest crack sizes, it is desirable to measure crack length at frequent intervals. In addition, real-time assessment of crack length may not be practical using some techniques, requiring that frequent measurements be made to capture unexpected events. This is particularly true for the smallest crack sizes. Recommended analysis procedures for dealing with such data are discussed in X3.9.2.

X3.8.4.2 In addition to measurement of surface crack length (2*c*), calculations of crack driving force require knowledge of crack shape. Normally a semielliptical crack shape is assumed, but some measurement of crack depth (*a*) must be made. Given a knowledge of surface crack length, some measurement techniques provide approaches for deducing crack depth, but direct, nondestructive measurement of crack shape is not currently possible. For some materials, it is possible to use fractographic measurements to develop a relationship of crack aspect ratio as a function of crack size that is representative of

all small cracks in the material (90). This relationship may then be used in crack driving force calculations.

X3.8.5 *Controlled-ΔK Testing*—It may be useful to monitor small-crack growth under computer-automated applied ΔK-control. The major requirement for such experiments is continuous input of small-crack length and aspect ratio for calculation of ΔK (or other correlating parameter), along with computer control of load (and therefore ΔK). The dcEPD and ISDG methods are well suited for ΔK-controlled small-crack growth from artificial initiation sites (92, 100). Other methods such as SAW could be similarly automated. ΔK-controlled experiments are particularly useful for characterizing growth rate changes at constant ΔK in response to crack wake morphology evolution, crack tip-microstructure interactions, and crack size-sensitive occluded chemistry changes. The application of ΔK-decreasing methods with small or short cracks provides an expeditious means of characterizing low growth rate cracking, often at low loading frequencies where large-crack methods are not feasible.

X3.9 Calculation and Interpretation

X3.9.1 *Calculation of ΔK:*

X3.9.1.1 Many of the available small-crack test methods address cracks that are assumed to be approximately semielliptical in shape. Accepted stress intensity factor solutions for a variety of embedded, surface, and corner crack geometries in plates and rods are given in (101-103). The general form of these solutions is

$$\Delta K = F_j \Delta S_i \sqrt{\pi a/Q} \qquad (X3.4)$$

where ΔS_i is the remote uniform tensile stress range ($i = t$) or outer fiber bending stress range ($i = b$), Q is the elliptical crack shape factor, and F_j is the boundary-correction factor which accounts for the influence of the various free-boundary conditions. Note that F_j changes around the perimeter of the crack, and this dependence may influence the crack growth process. It is customary to characterize fatigue crack growth for a stable, semicircular crack shape on the basis of ΔK calculated at the deepest point of the crack. Note also that some K solutions in the literature are presented using notations that differ from the notations in Fig. X3.2 (for example, plate half-width w versus full plate width $W = 2w$).

X3.9.1.2 For fine-grain, isotropic materials the assumption of a semielliptical shape appears reasonable. Although the shapes of very small cracks may be dramatically affected by local microstructural features, as the cracks grow they tend to assume a semielliptical shape and, in many instances, become nearly semicircular. Cracks in materials having coarse microstructures and/or exhibiting crystallographic texture and anisotropy may never assume a semielliptical shape. As stated in X3.8.4.2, crack shape must be documented for accurate calculation of ΔK. Simple approximation techniques have been presented to estimate the stress intensity factor for surface or corner cracks of non-elliptical shape (104). Typically, non-elliptical crack shapes depend on local microstructural features and, as such, their shapes tend to be inherently variable. Recognizing the stochastic nature of these cracks, it is often reasonable, or necessary, to approximate their shapes as semielliptical.

X3.9.1.3 Another problem involves the initiation of multiple cracks within a small region. These cracks may coalesce to form a single long, shallow surface crack. Criteria have been proposed (90) for defining the point at which the stress fields of closely spaced crack tips begin to interact.

X3.9.1.4 Under tension-compression loading, $R \leq 0$, it is conventional to use only the positive portion of the stress range to calculate the crack driving force; that is, $\Delta K = K_{max}$ (see Terminology in the main body of Test Method E 647). When crack closure is considered, however, the issue becomes significantly more complex, and the conventional definition of $\Delta K = K_{max}$ may be inappropriate. Numerous investigators have demonstrated that the level of crack closure depends on many factors, including crack size (for example, see (105)). In particular, crack opening stresses are thought to be lower for small cracks, even opening at nominally compressive stresses under some conditions. This factor raises important questions regarding the applicability of large-crack data, particularly in the near-ΔK_{th} region, to the prediction of the growth of small cracks. Some of the crack length measurement techniques described in X3.5.3 also may be used to measure crack closure levels, particularly ISDG and SEM.

X3.9.2 *Calculation of Crack Growth Rate*:

X3.9.2.1 Analysis of crack-length data to determine crack growth rates requires special consideration. The minimum interval between successive crack length measurements for large-crack tests (see Procedure in the main body of Test Method E 647) is stipulated as ten times the measurement precision. This may require that crack growth data be acquired at specified intervals of crack length, or that the a–N data be edited to remove data to achieve the desired interval, Δa. The inherent difficulty in this process is selecting the data points for removal. Small-crack measurement techniques often have measurement precision that is of the order of microstructural dimensions. As a result, discontinuities in the a–N (or $2c$–N) data arise due to crack interactions with microstructure, as well as from inherent errors in the measurements. If a minimum level of Δa is used as a criterion for editing the data, then the selected data points will often be the first point after the crack has broken through a local microstructural obstacle, and the data exhibiting the crack retardation in the microstructure will be lost. While the large-crack measurement intervals are recommended where possible, some uses of small-crack data may require smaller measurement intervals in order to capture key microstructural effects.

X3.9.2.2 Much of the small-crack growth rate data in the literature has not been reduced following the above guidance, and in many cases the *da/dN* calculations appear to demonstrate variability that is significantly influenced by measurement error. The basic problem may be outlined as follows. As the crack length interval, Δa, between successive measurements decreases, the relative contribution of the measurement error to the calculated value of *da/dN* increases. For example, assume that a single crack length measurement is given by $\hat{a} = a + \epsilon$, where $\hat{a}$ is the measured crack length, a is the true crack length, and ϵ is the error inherent in the crack length measurement, normally distributed about zero. A direct-secant calculation of crack growth rate between two successive crack

length measurements (a_1 and a_2) is given by

$$\frac{\Delta \hat{a}}{\Delta N} = \frac{(a_2 + \epsilon_2) - (a_1 + \epsilon_1)}{\Delta N} = \frac{\Delta a}{\Delta N} + \frac{\Delta \epsilon}{\Delta N} \qquad \text{(X3.5)}$$

Thus, as $\Delta a/\Delta N$ approaches zero, the error term $\Delta \epsilon/\Delta N$ dominates the calculated value of $\Delta \hat{a}/\Delta N$. Since small-crack data are often acquired at low growth rates, the crack extension between successive measurements tends to be small, and the growth rate data may exhibit an unusually large variability due to measurement error. It is recommended that the small-crack data be edited to remove this variability, or one may use a modified version (for example, **(91)**) of the standard incremental polynomial regression used for large cracks. The reader is cautioned that different data analysis procedures can also significantly influence the apparent scatter in growth rate **(106)**.

X3.10 Reporting

X3.10.1 The reporting guidelines prescribed in the main body of Test Method E 647 apply to the suggested procedure for small-crack tests. In addition, it is often useful to provide a record of the degree of crack deflection and tortuosity, the degree of asymmetric crack growth, and the crack shape for use in calculations of crack driving force. It is customary to report crack length in terms of its projection on a plane normal to the axis of loading, but significant deviations of the crack path from this plane should be noted in the report. Since the method of crack initiation can have a significant influence on subsequent crack growth, the test conditions and number of cycles required for crack initiation should be reported, along with the measured size of the crack at this number of cycles. The estimated resolution of the crack size measurement technique, the specific data analysis method used to calculate crack growth rates, and the specific K solution employed should also be recorded.

X3.11 Precision and Bias

X3.11.1 The general guidelines in the main body of Test Method E 647 apply. Specific emphasis should be given to the concerns described in X3.9.2 of this appendix, as a significant component of the variability exhibited by small-crack data can often be attributed to errors inherent in the crack length measurements.

REFERENCES

(**1**) Hudak, Jr., S. J., and Bucci, R. J., *Fatigue Crack Growth Measurement and Data Analysis, ASTM STP 738*, ASTM, 1981.

(**2**) Paris, P. C., "The Fracture Mechanics Approach to Fatigue," *Proceedings of the Tenth Sagamore Army Materials Research Conference*, Syracuse University Press, 1964, pp. 107–132.

(**3**) Beevers, C. J., *The Measurement of Crack Length and Shape During Fracture and Fatigue*, Engineering Materials Advisory Services LTD, West Middlelands, U.K., 1981.

(**4**) Bucci, R. J., "Effect of Residual Stress on Fatigue Crack Growth Rate Measurement," *Fracture Mechanics (13th Conference), ASTM STP 743*, 1981, pp. 28–47.

(**5**) Suresh, S., and Ritchie, R. O.," Propagation of Short Fatigue Cracks," *International Metals Review*, Vol 29, #6, December 1984, pp. 445–476.

(**6**) Hudak, Jr., S. J., "Small Crack Behavior and the Prediction of Fatigue Life," *Journal of Engineering Materials and Technology*, Vol 103, Jan. 1981, pp. 26–35.

(**7**) Herman, W. A., Hertzberg, R. W., and Jaccard, R., "A Simplified Laboratory Approach for the Prediction of Short Crack Behavior in Engineering Structures," Fatigue and Fracture of Engineering Materials and Structures, Vol II, No. 4, 1988.

(**8**) Suresh, S., and Ritchie, R. O., "Near-Threshold Fatigue Crack Propagation: A Perspective on the Role of Crack Closure," *Fatigue Crack Growth Threshold Concepts* TMS-AIME D. L. Davidson, S. Suresh, editors; Warrendale, PA, 1984, pp. 227–261.

(**9**) Clark, Jr., W. G., "Fracture Mechanics in Fatigue," *Experimental Mechanics*, September 1971, pp. 1–8.

(**10**) Hoeppner, D. W., and Krupp, W. E., "Prediction of Component Life by Application of Fatigue Crack Growth Knowledge," *Engineering Fracture Mechanics*, Vol 6, 1974, pp. 47–70.

(**11**) *Fatigue Crack Growth Under Spectrum Loads, ASTM STP 595*, ASTM, 1976.

(**12**) Hartman, G. A., and Ashbaugh, N. E., "Load Pin Size Effects in the C(T) Geometry," ASTM Research Report RR: E24-1016, Oct 1991.

(**13**) Scarone, D. W., "Development of an Instrumented Device to Measure Fixture-Induced Bending in Pin-Loaded Specimen Trains," *Factors That Affect the Precision of Mechanical Test, ASTM STP 1025*,

Papirno, R. and Weiss, H. C. Eds., ASTM, 1989, pp. 160–173.

(**14**) Hudak, Jr., S. J., Saxena, A., Bucci, R. J., and Malcolm, R. C., "Development of Standard Methods of Testing and Analyzing Fatigue Crack Growth Rate Data—Final Report," *AFML TR 78-40*, Air Force Materials Laboratory, Wright Patterson Air Force Base, OH, 1978.

(**15**) Brose, W. R., and Dowling, N. E., "Size Effects on the Fatigue Crack Growth Rate of Type 304 Stainless Steel," *Elastic-Plastic Fracture, ASTM STP 668*, 1979, pp. 720–735.

(**16**) Hudak, Jr., S. J., "Defining the Limits of Linear Elastic Fracture Mechanics in Fatigue Crack Growth," *Fatigue Crack Growth Measurement and Data Analysis, ASTM STP 738*, ASTM, Oct. 29–30, 1980.

(**17**) Dowling, N. E., "Fatigue Crack Growth Rate Testing at High Stress Intensities," *Flaw Growth and Fracture, ASTM STP 631*, ASTM, 1977, pp. 139–158.

(**18**) James, L. A., "Specimen Size Considerations in Fatigue-Crack Growth Rate Testing," *Fatigue Crack Growth Measurement and Data Analysis, ASTM STP 738*, ASTM, 1981, pp. 45–57.

(**19**) Clark, Jr., W. G., and Hudak, Jr., S. J., "Variability in Fatigue Crack Growth Rate Testing," *Journal of Testing and Evaluation*, Vol 3, No. 6, 1975, pp. 454–476.

(**20**) Hudak, Jr., S. J., and Wei, R. P., "Consideration of Nonsteady State Crack Growth in Materials Evaluation and Design," *International Journal of Pressure Vessels and Piping*, Vol 9, 1981, pp. 63–74.

(**21**) Saxena, A., Hudak, Jr., S. J., Donald, J. K., and Schmidt, D. W., "Computer-Controlled Decreasing Stress Intensity Technique for Low Rate Fatigue Crack Growth Testing," *Journal of Testing and Evaluation*, Vol 6, No. 3, 1978, pp. 167–174.

(**22**) Donald, J. K., and Schmidt, D. W., "Computer-Controlled Stress Intensity Gradient Technique for High Rate Fatigue Crack Growth Testing," *Journal of Testing and Evaluation*, Vol 8, No. 1, Jan. 1980, pp. 19–24.

(**23**) Chan, K. S., and Cruse, T. A., "Stress Intensity Factors for Anisotropic Compact Tension Specimens With Inclined Cracks," Engineering Fracture Mechanics, Vol 23, No. 5, pp. 863–874.

(**24**) Clark, Jr., W. G., and Hudak, Jr., S. J., "The Analysis of Fatigue Crack

Growth Rate Data," *Application of Fracture Mechanics to Design*, Burke, J. J. and Weiss, V., Eds, Vol 22, Plenum, 1979, pp. 67–81.

(25) Newman, Jr., J. C.," Stress Analysis of the Compact Specimen Including the Effects of Pin Loading" *Fracture Analysis (8th Conference), ASTM STP 560*, ASTM, 1974, pp. 105–121.

(26) Srawley, J. E., "Wide Range Stress Intensity Factor Expressions for ASTM Method E 399 Standard Fracture Toughness Specimens," *International Journal of Fracture*, Vol 12, June 1976, pp. 475–476.

(27) Feddersen, C. E., "Discussion of Plane-Strain Crack Toughness Testing of Metallic Materials," *Current Status of Plane Strain Crack Toughness Testing of High-Strength Metallic Materials, ASTM STP 410*, 1967, pp. 77–79.

(28) Bucci, R. J., in *Fatigue Crack Growth Measurement and Data Analysis, ASTM STP 738*, ASTM, 1981, pp. 5–28.

(29) Wei, R. P., Wei, W., and Miller, G. A., "Effect of Measurement Precision and Data-Processing Procedure on Variability in Fatigue Crack Growth-Rate Data," *Journal of Testing and Evaluation*, Vol 7, No. 2, March 1979, pp. 90–95.

(30) Donald, J. K.," Preliminary Results of the ASTM E24.04.03 Round-Robin Test Program on Low Delta-*K* Fatigue Crack Growth Rates," ASTM E24.04.03 Task Group Document, December 1982.

(31) Wei, R. P., and Shim, G., "Fracture Mechanics and Corrosion Fatigue," *Corrosion Fatigue: Mechanics, Metallurgy, Electrochemistry and Engineering, ASTM STP 801*, ASTM, 1983, pp. 5–25.

(32) Barsom, J. M., "Effects of Cyclic Stress Form on Corrosion Fatigue Crack Propagation Below K_{Iscc} in a High Yield Strength Steel," *Corrosion Fatigue: Chemistry, Mechanics and Microstructure*, NACE-2, National Association of Corrosion Engineers, 1972, pp. 424–433.

(33) Vosikovsky, O., "Effects of Mechanical and Environmental Variables on Fatigue Crack Growth Rates in Steel. A Summary of Work Done At CANMET," *Canadian Metallurgical Quarterly*, Vol 19, 1980, pp. 87–97.

(34) Selines, R. J., and Pelloux, R. M., "Effect of Cyclic Stress Wave Form on Corrosion Fatigue Crack Propagation in Al-Zn-Mg Alloys," *Metallurgical Transactions*, Vol 3, 1972, pp. 2525–2531.

(35) Dawson, D. B., and Pelloux, R. M., "Corrosion Fatigue Crack Growth in Titanium Alloys in Aqueous Environments." *Metallurgical Transactions*, Vol 5, 1974, pp. 723–731.

(36) Bogar, F. D., and Crooker, T. W., "The Influence of Bulk-Solution-Chemistry Conditions on Marine Corrosion Fatigue Crack Growth Rate," *Journal of Testing and Evaluation*, Vol 7, 1979, pp. 155–159.

(37) Vosikovsky, O., Neill, W. R., Carlyle, D. A., and Rivard, A., "The Effect of Sea Water Temperature on Corrosion Fatigue Crack Growth in Structural Steels," *CANMET Physical Metallurgy Research Laboratories Report* ERP/PMRL 83-27 (OP-J), Ottawa, Canada, April 1983.

(38) Gangloff, R. P., "The Criticality of Crack Size in Aqueous Corrosion Fatigue," *Res Mechanica Letters*, Vol 1, 1981, pp. 299–306.

(39) van der Velden, R., Ewalds, H. L., Schultze, W. A., and Punter, A., "Anomalous Fatigue Crack Growth Retardation in Steels for Offshore Applications," *Corrosion Fatigue: Mechanics, Metallurgy, Electrochemistry and Engineering, ASTM STP 180*, ASTM, 1983, pp. 64–80.

(40) Bogar, F. D., and Crooker, T. W., "Effects of Natural Seawater and Electrochemical Potential on Fatigue-Crack Growth in 5086 and 5456 Aluminum Alloys," *NRL Report 8153*, Naval Research Laboratory, Washington, DC, October 7, 1977.

(41) Yoder, G. R., Cooley, L. A., and Crooker, T. W., "Procedures for Precision Measurement of Fatigue Crack Growth Rate Using Crack-Opening Displacement Techniques," *Fatigue Crack Growth Measurements and Data Analysis, ASTM STP 738*, ASTM, 1981, pp. 85–102.

(42) Wei, R. P., and Brazill, R. L., "An Assessment of A-C and D-C Potential Systems for Monitoring Fatigue Crack Growth," *Fatigue Crack Growth Measurement and Data Analysis, ASTM STP 738*, ASTM, 1981, pp. 103–119.

(43) Liaw, P. K., Hartmann, H. R., and Helm, E. J., "Corrosion Fatigue Crack Propagation Testing with the KRAK-GAGE® in Salt Water," *Engineering Fracture Mechanics*, Vol 18, 1983, pp. 121–131.

(44) Saxena, A., and Hudak, Jr., S. J., "Review and Extension of Compliance Information for Common Crack Growth Specimens," International Journal of Fracture, Vol 14, No. 5, Oct 1978.

(45) Ashbaugh, N. E., and Johnson, D. A.," Determination of Crack Length as a Function of Compliance and Gage Length for an M(T) Specimen," ASTM Research Report (RR: E24–1017, April 1992).

(46) Watt, K. R., "Consideration of an a.c. Potential Drop Method for Crack Length Measurement," from *The Measurement of Crack Length and Shape During Fracture and Fatigue*, Beevers, C. J., Ed., EMAS, Cradley Heath, UK, 1980, pp. 202–201.

(47) Bakker, A., "A DC Drop Procedure for Crack Initiation and R-Curve Measurements During Fracture Tests," *Elastic-Plastic Fracture Test Methods: The User Experience, ASTM STP 856*, Wessel, E. T. and Loss, F. J., Eds., ASTM, 1985, pp. 394–410.

(48) Richards, C. E., "Some Guidelines to the Selection of Techniques," *The Measurement of Crack Length and Shape During Fracture and Fatigue*, Beevers, C. J., Ed., EMAS, Cradley Heath, UK, 1980, pp. 461–468.

(49) Wei, R. P., and Brazill, R. L., "An a.c. Potential System for Crack Length Measurement" from *The Measurement of Crack Length and Shape During Fracture and Fatigue*, Beevers, C. J., Ed., EMAS, Cradley Heath, UK, 1980, pp. 190–201.

(50) Wilkowski, G. M., and Maxey, W. A.," Review and Applications of the Electric Potential Method for Measuring Crack Growth in Specimens, Flawed Pipes, and Pressure Vessels," *Fracture Mechanics: Fourteenth Symposium-Volume II: Testing and Applications, ASTM STP 791*, Lewis, J. C. and Sines, G., Eds., ASTM, 1983, pp. II-266–II-294.

(51) Dover, W. D., et al.," a.c. Field Measurement—Theory and Practice," from *The Measurement of Crack Length and Shape During Fracture and Fatigue*, Beevers, C. J., Ed., EMAS, Cradley Heath, UK, 1980, pp. 222–260.

(52) Metals Handbook, Vol 8, Published under the direction of the American Society for Metals, 9th Edition, Metals Park, OH, 1987, pp. 386–391.

(53) Gangloff, R. P., "Electrical Potential Monitoring of the Formation and Growth of Small Fatigue Cracks in Embrittling Environments," from *Advances in Crack Length Measurement*, Beevers, C. J., Ed., EMAS, Cradley Heath, UK, 1982, pp. 175–229.

(54) Hartman, G. A., and Johnson, D. A.," D-C Electric Potential Method Applied to Thermal/Mechanical Fatigue Crack Growth," *Experimental Mechanics*, March 1987, pp. 106–112.

(55) Bachman, V., and Munz, D., "Fatigue Crack Closure Evaluation with the Potential Method," *Engineering Fracture Mechanics*, Vol 11, No. 1, 1979, pp. 61–71.

(56) Okumra, N., Venkatasubramanian, T. V., Unvala, B. A., and Baker, T. J., "Application of the AC Potential Drop Technique to the Determination of R-Curves of Tough Ferritic Steels," *Engineering Fracture Mechanics*, Vol 14, 1981, pp. 617–625.

(57) Pollock, D. D., "Thermoelectricity, Theory, Thermometry, Tool," *ASTM STP 852*, ASTM, 1985.

(58) Catlin, W. R., Lord, D. C., Prater, T. A., and Coffin, L. F., "The Reversing D-C Electrical Potential Method," *Automated Test Methods for Fracture and Fatigue Crack Growth, ASTM STP 877*, Cullen, W. H., Landgraf, R. W., Kaisand, L. R., and Underwood, J. H., Eds., ASTM, 1985, pp. 67–85.

(59) Johnson, H. H., "Calibrating the Electric Potential Method for Studying Slow Crack Growth," *Materials Research and Standards*, Vol 5, No. 9, Sept. 1965, pp. 442–445.

(60) Van Stone, R. H., and Richardson, T. L., "Potential Drop Monitoring of Cracks in Surface Flawed Specimens," *Automated Test Methods for Fracture and Fatigue Crack Growth, ASTM STP 877*, W. H. Cullen, R. W. Landgraf, L. R. Kaisand, and J. H. Underwood, Eds., ASTM, 1985, pp. 148–166.

(61) Gangloff, R. P., "Electrical Potential Monitoring of Crack Formation and Subcritical Growth from Small Defects," *Fatigue of Engineering Materials and Structures*, Vol 4, 1981, pp. 15–33.

(62) Hicks, M. A., and Pickard, A. C., "A Comparison of Theoretical and Experimental Methods of Calibrating the Electrical Potential Drop Technique for Crack Length Determination," *Int. Journal of Fracture*, No. 20, 1982, pp. 91–101.

(63) Aronson, G. H., and Ritchie, R. O., "Optimization of the Electrical Potential Technique for Crack Monitoring in Compact Test Pieces Using Finite Element Analysis," *Journal of Testing and Evaluation, JTEVA*, Vol 7, No. 4, July 1979, pp. 208–215.

(64) Ritchie, R. O., and Bathe, K. J., "On the Calibration of the Electrical Potential Technique for Monitoring Crack Growth Using Finite Element Methods," *International Journal of Fracture*, Vol 15, No. 1, February 1979, pp. 47–55.

(65) Li, Che-Yu, and Wei, R. P., "Calibrating the Electrical Potential Method for Studying Slow Crack Growth," *Materials Research & Standards*, Vol 6, No. 8, August 1966, pp. 392–394.

(66) Mom, A., and Raizenne, M. D.," AGARD Engine Disk Cooperative Test Programme," AGARD report number 766, Aug., 1988.

(67) Raizenne, M. D., "AGARD TX114 Test Procedures for Supplemental Engine Disc Test Programme," National Research Council Canada, LTR-ST-1671, June 1988.

(68) Piascik, R. S.," Mechanisms of Intrinsic Damage Localization During Corrosion Fatigue: Al-Li-Cu System," Ph.D. Dissertation, University of Virginia, 1989.

(69) Piascik, R. S. and Willard, S. A, "The Growth of Small Corrosion Fatigue Cracks in Alloy 2024," *Fatigue Fract. Engng. Mater. Struct.*, Vol. 17, No. 11, 1994, pp. 1247–1259.

(70) Richardson, D. E. and Goree, J. G., "Experimental Verification of a New Two-Parameter Fracture Model," *ASTM STP 1189*, R. Chona, ed., 1993, pp. 738–750.

(71) Sullivan, A.M., "New Specimen Design for Plane-Strain Fracture Toughness Tests," *Materials Research and Standard*, Vol. 4, No. 1, 1964, pp. 20–24.

(72) Piascik, R.S., Newman, J.C., Jr., and Underwood, J.H., "The Extended Compact Tension Specimen," *Fatigue and Fract. Engng. Mater. Struct.*, Vol. 20, No. 4, 1997, pp. 559–563.

(73) John, R., "Stress Intensity Factor and Compliance Solutions for an Eccentrically Loaded Single Edge Cracked Geometry," *Engineering Fracture Mechanics*, Vol. 58, No. 1/2, 1997, pp. 87–96.

(74) Piascik, R.S. and Newman, J.C., Jr., "An Extended Compact Tension Specimen for Fatigue Crack Growth and Fracture Testing," *International Journal of Fracture*, Vol. 76, No. 3, 1995, pp. R43-R48.

(75) Schwalbe, K. H. and Hellmann, "Applications of the Electrical Potential Method to Crack Length Measurements Using Johnson's Formula," *Journal of Testing and Evaluation*, Vol. 9, No. 3, 1981, pp. 218–221.

(76) Phillips, Edward P., "Results of the Second Round Robin on Opening-Load Measurement Conducted by ASTM Task Group E24.04.04 on Crack Closure Measurement and Analysis," NASA Technical Memorandum 109032, November 1993.

(77) Donald, J. Keith," A Procedure for Standardizing Crack Closure Levels," *Mechanics of Fatigue Crack Closure, ASTM STP 982*, ASTM, 1988, pp. 222–229.

(78) Suresh, S., and Ritchie, R. O., "Propagation of Short Fatigue Cracks," *International Metals Review*, Vol 29, 1984, pp. 445–476.

(79) Hudak, S. J., Jr., "Small Crack Behavior and the Prediction of Fatigue Life," *ASME Journal of Engineering Materials and Technology*, Vol 103, 1981, pp. 26–35.

(80) *Small-Crack Test Methods, ASTM STP 1149*, Larsen, J. M., and Allison, J. E., Eds., ASTM, 1992.

(81) *Current Research on Fatigue Cracks*, Tanaka, T., Jono, M., and Komai, K., Eds., The Society of Materials Science, Japan, 1985.

(82) *Small Fatigue Cracks*, Ritchie, R. O., and Lankford, J., Eds., The Metallurgical Society, Warrendale, PA, 1986.

(83) *The Behaviour of Short Fatigue Cracks, EGF 1*, Miller, K. J., and de los Rios, E. R., Eds., Mechanical Engineering Publications, London, 1986.

(84) *Short Fatigue Cracks, ESIS 13*, Miller, K. J., and de los Rios, E. R., Eds., Mechanical Engineering Publications, London, 1992.

(85) Ritchie, R. O., and Lankford, J., "Overview of the Small Crack Problem," *Small Fatigue Cracks*, Ritchie, R. O., and Lankford, J., Eds., The Metallurgical Society, Warrendale, PA, 1986, pp. 1–5.

(86) Kitagawa, H., and Takahashi, S.," Applicability of Fracture Mechanics to Very Small Cracks or the Cracks in the Early Stage," Proc. Second International Conference on Mechanical Behavior of Materials, Boston, MA, 1976, pp. 627–631.

(87) Tanaka, K., Nakai, Y., and Yamashita, M., "Fatigue Growth Threshold of Small Cracks," *International Journal of Fracture*, Vol 17, 1981, pp. 519–533.

(88) Miller, K. J., "Materials Science Perspective of Metal Fatigue Resistance," *Materials Science and Technology*, Vol 9, 1993, pp. 453–462.

(89) McClung, R. C., and Sehitoglu, H., "Characterization of Fatigue Crack Growth in Intermediate and Large Scale Yielding," *ASME Journal of Engineering Materials and Technology*, Vol 113, 1991, pp. 15–22.

(90) Swain, M. H., "Monitoring Small-Crack Growth by the Replication Method," *ASTM STP 1149*, ASTM, pp. 34–56.

(91) Larsen, J. M., Jira, J. R., and Ravichandran, K. S., "Measurement of Small Cracks by Photomicroscopy: Experiments and Analysis," *ASTM STP 1149*, ASTM, pp. 57–80.

(92) Gangloff, R. P., Slavik, D. C., Piascik, R. S., and Van Stone, R. H., "Direct Current Electrical Potential Measurement of the Growth of Small Cracks," *ASTM STP 1149*, ASTM, pp. 116–168.

(93) Resch, M. T., and Nelson, D. V., "An Ultrasonic Method for Measurement of Size and Opening Behavior of Small Fatigue Cracks," *ASTM STP 1149*, ASTM, pp. 169–196.

(94) Sharpe, W. N., Jr., Jira, J. R., and Larsen, J. M., "Real-Time Measurement of Small-Crack Opening Behavior Using an Interferometric Strain/Displacement Gage," *ASTM STP 1149*, ASTM, pp. 92–115.

(95) Davidson, D. L., "The Experimental Mechanics of Microcracks," *ASTM STP 1149*, ASTM, pp. 81–91.

(96) Hertzberg, R., Herman, W. A., Clark, T., and Jaccard, R., "Simulation of Short Crack and Other Low Closure Loading Conditions Utilizing Constant K_{max} ΔK-Decreasing Fatigue Crack Growth Procedures," *ASTM STP 1149*, ASTM, pp. 197–220.

(97) Mom, A. J. A., and Raizenne, M. D., "AGARD Engine Disc Cooperative Test Programme," AGARD Report No. 766, 1988 (available NTIS).

(98) Pickard, A. C., Brown, C. W., and Hicks, M. A., "The Development of Advanced Specimen Testing and Analysis Techniques Applied to Fracture Mechanics Lifting of Gas Turbine Components," *Advances in Life Prediction Methods*, Woodford, D. A. and Whitehead, J. R., Eds., ASME, New York, 1983, pp. 173–178.

(99) Newman, J. C., Jr., and Edwards, P. R., "Short-Crack Growth Behaviour in an Aluminum Alloy—an AGARD Cooperative Test Programme," AGARD Report No. 732, 1988 (available NTIS).

(100) Jira, J. R., Nagy, D., and Nicholas, T., "Influences of Crack Closure and Load History on Near-Threshold Crack Growth Behavior in Surface Flaws," *Surface-Crack Growth: Models, Experiments, and Structures, ASTM STP 1060*, Reuter, W. G., Underwood, J. H., and Newman, J. C., Jr., Eds., ASTM, 1990, pp. 303–314.

(101) Newman, J. C., Jr., and Raju, I. S., "Stress-Intensity Factor Equations for Cracks in Three-Dimensional Finite Bodies," *Fracture Mechanics: Fourteenth Symposium—Volume I: Theory and Analysis, ASTM STP 791*, Lewis, J. C. and Sines, G., Eds., ASTM, 1983, pp. I-238–I-265.

(102) Raju, I. S., and Newman, J. C., Jr., "Stress-Intensity Factors for Circumferential Surface Cracks in Pipes and Rods under Tension and Bending Loads," *Fracture Mechanics: Seventeenth Volume, ASTM STP 905*, Underwood, J. H., Chait, R., Smith, C. W., Wilhem,

D. P., Andrews, W. A., and Newman, J. C., Jr., Eds., ASTM, 1986, pp. 789–805.

(**103**) Newman, J. C., Jr., "Fracture Mechanics Parameters for Small Fatigue Cracks," *ASTM STP 1149*, ASTM, pp. 6–33.

(**104**) Tada, H., and Paris, P., "Discussion on Stress-Intensity Factors for Cracks," *Part-Through Crack Fatigue Life Prediction, ASTM STP 687*, Chang, J. B., Ed., ASTM, 1979, pp. 43–46.

(**105**) *Mechanics of Fatigue Crack Closure, ASTM STP 982*, Newman, J. C., Jr., and Elber, W., Eds., ASTM, 1988.

(**106**) Kendall, J. M., and King, J. E.," Short Fatigue Crack Growth Behaviour: Data Analysis Effects," *International Journal of Fatigue*, Vol 10, 1988, pp. 163–170.